dc_5_10

The Hungarian Academy of Sciences
Doctor of Sciences Dissertation

THE ROLE OF MOLECULAR GENETICS IN EXPLORING THE PATHOGENESIS OF MULTIPLE SCLEROSIS

BERNADETTE KALMAN, M.D. PH.D.

2010

CONTENT

Preface

I would like to acknowledge those extraordinary people who cannot be all named in the Acknowledgement section, but whose knowledge, support and kindness shaped my life during early development, training and works. I was very fortunate receiving my education from the pre-school level to the residency training and even beyond in their environment. Education in both natural and human sciences was very comprehensive and thorough in Hungary. However, what I recognize now even with a greater appreciation is the ubiquitous expression of an exceptional quality: the academic spirit of many of my teachers, senior colleagues and my parents, who possessed the intrinsic drive for delivering and expecting much more than that set in the regular curriculum, the trait of novelty seeking, and the ability of generating in their mysterious ways the conditions for the “beyond of average” without ample resources. My parents not only supported my ordinary education for over two decades, but generously also provided the opportunity of a long lasting music training, language courses and early trips within Europe. In my medical school, we were encouraged to become “physician-scientists” long before the term was introduced. We got the opportunity of experimenting in fields where a discovery had just happened, and translation of scientific results into practice was exemplified. During residency, we regularly heard about the works of world famous neurologists, and on a smaller scale, we were expected to try something similar. I feel greatly privileged being raised in this remarkable spirit generated by these exceptional people. It was this spirit that made possible for me to proceed later on my own in a competitive international environment. I most gratefully also recognize that everything was provided with the only expectation that I will use this generous investment well in my life.

1. INTRODUCTION

While specific causes of multiple sclerosis (MS) remain uncertain, an interaction between environmental and genetic factors has been implicated in pathogenesis leading to inflammation, demyelination and neurodegeneration in the central nervous system (CNS). Genetic determination of this process is supported by epidemiological studies in ethnic groups, families, twins, half sibs and conjugate pairs (1). The risk for monozygotic twins is 300-times, and for first-degree relatives 20-50-times higher than for an individual in the general population of Northern-European origin with a prevalence rate of 0.1. The observed transmission patterns are not compatible with an autosomal dominant, recessive or X-linked inheritance. MS is a complex trait disorder, defined by several genes, each exerting small effect, and in an interaction with the environment (2-14). Phenotypic expressions of MS suggest the involvement of complex mechanisms with features of autoimmunity and neurodegeneration (15-22). The currently approved disease modifying drugs primarily target the inflammatory components, while exert limited effect on neurodegeneration in MS. We chose using molecular and genetic approaches to better understand disease pathogenesis and to identify new targets for therapy.

1.1 THE MS PHENOTYPE

1.1.1 Terminology and definition

The definitions of clinical, pathological and molecular phenotypes and ascertainment of patients are the foundation of conducting translational studies. Relapsing-remitting (RR), secondary progressive (SP), primary progressive (PP) and progressive-relapsing courses (PR) of MS have been clinically distinguished (23). While this empirical classification is currently under revision to include additional subtypes, the existence of the four courses is supported by natural history studies. The majority, 80-85% of patients have a RR onset with a substantial proportion converting into SP-MS over time. The remaining patients present with PP-MS characterized by a later onset, less female predominance and a more rapid deterioration (24). The median times from disease onset to reaching an extended disability status scale score (EDSS) 4, 6 and 7 are longer in RR than in PP disease, but the time to reaching EDSS 6 from EDSS 4 is similar in the SP and PP-MS groups (25). These observations suggest that the rates of accumulating irreversible tissue pathology are different in RR and PP-MS, but the progressive phases of SP and PP-MS are similar (25-26). Comparisons of long term outcomes suggest that patients with relapsing-progressive (RP)-course can be reassigned either to SP or PP-MS, and patients with PR-course can be reassigned to PP-MS (27). Therefore, our studies distinguish RR, SP and PP forms of clinically definite MS, and use the diagnostic criteria of Poser et al (28), McDonald et al (29) and Thompson et al (30).

1.1.2 Features of autoimmunity in MS

Common features of MS and other autoimmune conditions include a higher incidence in women, a peak of onset in the third and fourth decades of life, a common relapsing-remitting initial presentation with subsequent progressive deterioration, and a beneficial influence of pregnancy but a transiently adverse effect of puerperium (16,31). Corticosteroids and immunosuppressive drugs are at least partially effective. The presence of immune cells and immunoglobulins against autoantigens in the target organ can be demonstrated. Distinct alleles of the Human Leukocyte Antigen (HLA) genes and an overlapping set of non-HLA genes define a genetic constitution called autoimmune trait (16,32). The existence of this autoimmune trait is supported by the increased occurrence of autoimmunity (8.4%), MS (6.2%) or both (0.8%) in first degree relatives of MS patients (31,33-36). An intra-individual recurrence of autoimmunity is also noted in MS, but it is even more prominently in neuromyelitis optica (NMO) or Devic's disease (37-40). The risk of non-specific autoimmunity for siblings of MS probands is estimated to be λ_s=1.65 and the risk of MS is estimated to be λ_s=2 (31,41) (λ_s is the relative risk score for siblings and is defined as the ratio of recurrence risk of the disease in siblings of probands to the prevalence of that disease in the general population).

Comparative analyses of genome scans reveal that 65% of the positive non-HLA linkage data fall into 18 clusters of overlapping autoimmune diseases (18). Both linkage and candidate gene studies confirm the existence of shared regions of susceptibility in MS and Insulin Dependent Diabetes Mellitus, rheumatoid arthritis, systemic lupus erythematosus (SLE), inflammatory bowel disease and ankylosing spondylitis (42-44). Chromosome 17q11 including the β-chemokine region represents one of the susceptibility loci identified in more than one autoimmune disease (45,46). To further define inflammatory regulators of MS pathogenesis, our studies investigate the β-chemokine cluster in 17q11 (Section 2).

1.1.3 Neurodegeneration in MS

Although neurodegeneration accumulates from the earliest stages and dominates pathological features of some forms of MS, its mechanism and relationship with autoimmunity, inflammation and demyelination is only partially understood. The temporal sequence of inflammation, demyelination and tissue degeneration has been described by magnetic resonance imaging (MRI) and pathological studies (17,47). The breakdown of blood brain barrier (BBB), reflected by the extravasation of gadolinium, represents an early event in lesion development (48). Serial magnetization transfer ratio (MTR) and imaging (MTI) studies, however, detect subtle structural changes reflecting edema, inflammation and degeneration even prior to the occurrence of lesions on contrast enhanced T1 and

T2-weighed MRI in the normal appearing white matter (NAWM) (49-51). Magnetic resonance spectroscopy (MRS) shows decreased values of N-acetyl aspartate (NAA) suggestive of axonal and neuronal degeneration in chronic plaques, but to some degrees also in the NAWM and normal appearing gray matter (NAGM) (52-53). Evaluations of clinical measures, MRI and MRS data establish that axonal degeneration and CNS atrophy are the major pathological correlate of disability (53-54).

Histological determinants of plaques include perivenular and parenchymal inflammation, demyelination, axonal loss and astrogliosis (52). Four patterns of demyelinating lesions with intra-individual homogeneity and inter-individual heterogeneity were proposed (19), although not universally accepted (55). Pattern I is characterized by T cell and macrophage infiltration, whereas pattern II has an additional IgG plus complement contribution to myelin destruction. Both patterns III and IV appear to be oligodendrocytopathy rather than autoimmunity. In pattern III, oligodendrocyte apoptosis occurs at the active plaque border with a paucity of oligodendrocytes in the inactive center. These lesions share histological (“dying back” oligodendrocytopathy) and molecular (expression of HIF1α and Hsp70) similarities with those of ischemic brain injury. In pattern IV, a non-apoptotic oligodendrocyte death is seen adjacent to the zone of demyelination associated with a lack of remyelination. While the distinction among the four patterns may be debated, the existence of a histopathological heterogeneity modulated by individually distinct genetic constellations is uniformly accepted by pathologists (19,55).

In addition to oligodendrocyte depletion, axonal loss develops in and outside of plaques (56). While activated inflammatory cells consistently co-localize with axonal impairment (56), this degenerative process does not always correlate with the demyelinating activity, suggesting that inflammatory cell products can directly impair axons (57). Immune mediated cytotoxicity, apoptosis and necrosis, glutamate-induced neurotoxicity and insufficient trophic support are only partially responsible for the observed loss of oligodendrocytes and neurons (47-59,60-62). Our works add to existing data a mitochondrial component of neurodegeneration associated with immune activation and inflammation (Section 3).

1.1.4 Current concepts of immune mediated demyelination and neurodegeneration

The pathogenesis of MS is generally (although not unambiguously) attributed to the activation of mononuclear cells (MNCs) in the peripheral immune system and their migration via the BBB (55,63). If MNCs (T and B lymphocytes, monocytes, macrophages) encounter further activation signals in the CNS, they may contribute to demyelination and tissue degeneration either by direct cell-cell interactions or by their soluble inflammatory products. Blood-derived CSF and

CNS immune cells include CD8+ and CD4+ T lymphocytes, memory B lymphocytes and plasma blasts, monocytes / macrophages and dendritic cells in MS. There is an abnormal proportion of both regulatory (e.g. CD4+ CD25+ FOXP3+ nTreg, CD4+ TH-2) and effector (e.g. CD4+ TH-1 / TH-17, CD8+CD45RA+CD27-) T cell populations. CD4 and CD8 T lymphocytes and B lymphocytes specific for a broad range of CNS antigens have increased frequency and clonal expansion in the CSF and CNS, and have been implicated in the disease development (63).

The main part of Figure 1 shows in a simplified manner those cellular and molecular elements of the immune and neurodegenerative MS pathways, which are relevant to the present study. Some molecular details are depicted in the inserts. When the antigen specific receptor of a CD4 or CD8 T lymphocyte (TCR) recognizes its antigenic determinant presented by the major histocompatibility (MHC) Class II or Class I molecule, respectively, on an antigen presenting cell (APC), and this interaction is complemented by an engagement between a necessary set of costimulatory molecules and their receptors, the T cell will undergo activation (Insert 1: Events in the peripheral immune system). We comprehensively studied elements of the trimolecular complex (MHC II – antigenic peptide – TCR) in both MS and its animal model (Ph.D. thesis). Activated T cells express adhesion molecules facilitating their rolling, adherence and transmigration via the endothelial (E) cell, basal membrane (BM) and matrix layers of the BBB. Chemokines produced in the CNS exert chemotactic signals and facilitate cell trafficking. In addition, the binding of chemokine ligands to their receptors on T lymphocytes triggers intracellular signaling that increases the adhesion between VLA4 - VCAM1 at the BBB. The LFA1 – ICAM1 interaction is also essential for lymphocytes traversing the BBB. The break-down of the BM is facilitated by the production of matrix metalloproteases (MMPs) by activated T lymphocytes (Insert 2: Interactions at the BBB). If a T cell recognizes its specific antigenic determinant, then it will further be activated and retained in the CNS. T cells with pathogenic potential predominantly express T helper (TH)-1 (characterized by interferon-γ, interleukin-2 and tumor necrosis factor α/β production) and TH-17 phenotypes (characterized by IL-17 production; the involvement of this subset is established in EAE but still being investigated in MS) which may exert cytotoxic activity on myelin and oligodendrocytes. Inflammatory products of these lymphocytes and the co-migrating macrophages in concert with the activated residential microglia and astroglia release cytotoxic cytokines, reactive oxygen species (ROS) and nitric oxide (NO). Immunoglobulins and complement as well as glutamate may also contribute to the cytotoxic process leading to myelin loss, oligodendrocyte apoptosis, axonal transection and neuronal degeneration (Insert 3: Cytotoxicity in the CNS) (15-16,60-64).

Figure 1. Immune mediated demyelination and neurodegeneration

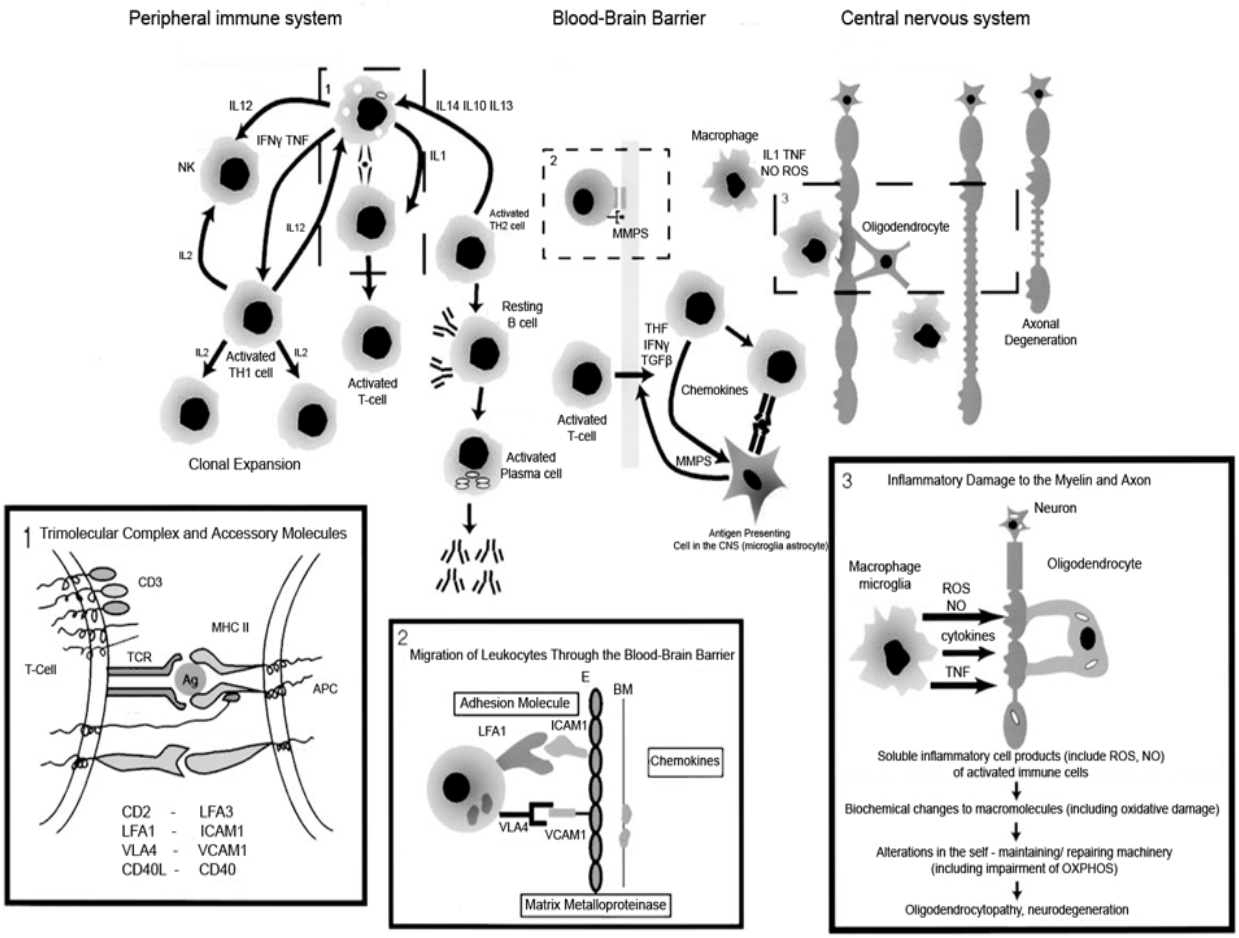

See explanation for Figure 1 in section 1.1.4.

1.2 GENETICS OF MS

Different approaches have been used to study genetic susceptibility in MS. In classical case-control designs, candidate genes are selected based on a perceived concept of disease pathogenesis (Figure 1), and the frequency of alleles in these polymorphic candidate genes are compared in the groups of patients and matched controls. Despite the hypothesis driven nature (e.g. genes of immune regulation and myelin production are involved) and the technical pitfalls (e.g. the selection of proper controls), case – control studies have greatly contributed to the current state of MS genetics and established that the MHC DR15, DQ6, Dw2, or in current sequence based terminology the DRB1*1501, DQA1*0102, DQB1*0602 haplotype, has the strongest and most consistent association with MS in Caucasians (1,37,65,66). The importance of the DR15 subtype was underscored in our own study of DR2 positive Hungarian and Gypsy patients and controls (37,66,67).

The method of linkage is free of preconceived assumptions regarding disease pathogenesis, and investigates segregation of susceptibility markers with the disease in a cohort of families. Four comprehensive genome scans in sibpair and multiplex families show linkage to multiple susceptibility loci, each with a minor effect (λ_s=/<2) compatible with a complex trait of MS (41,68-70). Among several reported provisional sites, the 6p21, 5p15 - 5q13, 17q22 and 19q13 loci are consistently identified (41,68-71). Our follow up linkage studies replicates these findings and further refine loci of interest in large numbers of families (72, my studies in Oxford, not detailed here). A meta-analysis of combined, raw genotype data of three genome scans confirms the importance of 17q11 and 6p21 (73). Within the identified susceptibility regions, candidate genes involved in immune regulation (e.g. 6p21 – MHC cluster; 17q11 – β-chemokine cluster; 17q22 - PRKCA) or neurodegeneration are located (e.g. the ApoE4 allele of ApoE gene at 19q13) (74-78). Consistent with the case-control data, microsatellite based linkage studies detect the highest lod scores in the MHC region on 6p21 (41,69). MHC is estimated to account for 15-65% of genetic susceptibility in MS (77,78). There are more uncertainties regarding the identity of non-MHC genetic determinants.

While the method of linkage successfully identified major susceptibility loci, it does not have the power to further confine these large (often ranging 2-20 cM, approximately 2-20 MB) susceptibility loci to single genes in MS. Theoretical considerations and experimental data suggest that methods of association are more suitable for the identification of genes with small effects and the restriction of large susceptibility loci to small chromosomal segments (41,68-71,79). Observations from the Human Genome and HapMap projects made possible the identification of the means of association studies in families used by the author of this dissertation (Figure 2). The Human Genome Project reveals that

there is a sequence variation, so called single nucleotide polymorphism (SNP), at approximately every 1000 nucleotide. SNPs align in haplotypes that tend to be inherited together as chromosomal blocks in the population. SNP variants and haplotypes define not only inter-individual phenotypic differences but also differences in susceptibility to common diseases. The term linkage disequilibrium (LD) describes the correlation of marker alleles in haplotypes more often than expected by chance in a population. LD depends on many factors including inter-marker distances, marker allele frequency, local structure and sequence composition of a chromosome and most importantly, the history of a given population (80). The theoretical background to LD mapping (used in this study) is schematically illustrated in Figure 2. In brief, this method is basen on the concept that any SNP marker or haplotype found in association with the disease could be an indicator of a disease-relevant mutation in the proximity due to LD between that SNP marker or the disease-relevant mutation (80).

Therefore, the search for candidate genes in susceptibility loci previously identified by linkage studies may involve a three-phase strategy using LD mapping. In the first and second phases, we identify and then confirm in the selected region the disease-associated SNPs and haplotypes on which, or close to which, disease relevant mutations likely arose. In the third phase, we seek for the disease-relavant mutations or variants by sequencing these particular haplotypes and their flanking regions. General information regarding the distribution and population characteristics of SNPs, haplotypes and LD maps are publicly available (http://www.ncbi.nlm.nih.gov/SNP/index.html and http://www.hapmap.org). The necessary density of SNP markers in an association study based on LD scanning is discussed in Figure 2. The HapMap data base also assists us selecting tagging SNP markers for an initial determination of disease associated haplotypes, which then may be followed by a more restricted search for disease specific variants.

Figure 2. Theoretical considerations to linkage disequilibrium mapping

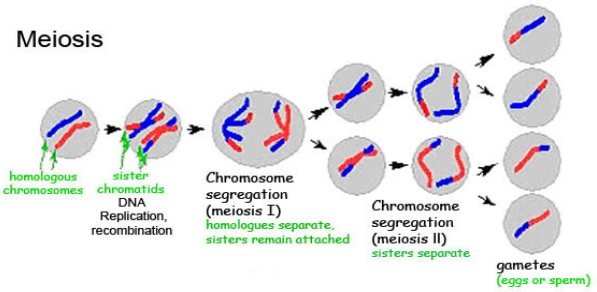

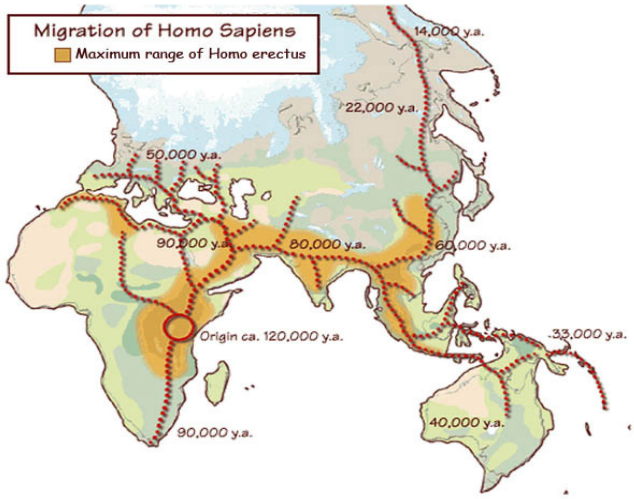

HAPLOTYPES ARE PARTICULAR COMBITATIONS OF ALLELES IN A POPULATION

WHEN A NEW MUTATION ARISES, IT DOES SO IN A SPECIFIC CHROMOSOMAL HAPLOTYPE

EACH VARIANT ALLELE CAN BE TRACKED IN THE POPULATION BY IDENTIFYING THE CORRESPONDING ANCESTRAL SEGMENT ON WHICH IT AROSE

A fertilized oocyte undergoes divisions called meiosis (left upper part of Figure 2). During meiosis, an exchange between the maternal and paternal chromosomal materials occurs, called recombination. The longer the meiotic history (or the higher the number of subsequent generations), the more recombinations occurred in a given population. The more recombinations lead to smaller chromosomal blocks (haplotypes) inherited together in that population. In other words, older populations generally have shorted LD blocks than younger populations. Homo Sapiens arose approximately 120,000 years ago in East – Central Africa (left lower part of Figure 2). Over time, small subgroups continuously migrated out of Africa (evolutionary bottle neck) and populated the Middle East, Asia, Australia and Europe. The ancestors of today Europeans settled 50,000 years ago. Giving 25 years to each generation, East-Central Africans had approximately 4800 subsequent generations, while Europeans had approximately 2000 generations. Thus, the number of recombination events in the African chromosomal population was much higher than that in the European chromosomal population resulting in shorter haplotypes (LD) in Africans than in Europeans. The out-of-Africa hypothesis of the Homo Sapiens history was initially suggested by anthropological and linguistic studies, and is recently confirmed by molecular DNA analyses. These genetic studies define that half of the bi-marker haplotypes are 22 kb or larger in African (Yoruban) and African-American populations, while half of the bi-marker haplotype blocks are 44 kb or larger in Asian and European populations, in correlation with the corresponding meiotic history of each population (80). This information guide us defining the density of SNP markers required for LD mapping in our studies identifying the disease associated haplotype(s) in MS families.

Here we present our studies on candidate genes involved in autoimmunity and neurodegeneration in MS. In addition to functional considerations, the selection of genes was guided by the results of linkage analyses. From the previously defined susceptibility loci, we chose to study genetic variants of CC chemokine ligands (mediators of inflammation, Section 2) and of Complex I (a likely player in neurodegeneration, Section 3). In the conclusion of studies (Section 4), we propose a role for mitochondrial molecules in contributing to neurodegeneration associated with inflammation. The integration of our genetic and functional data into a mechanistic concept extends existing observations on MS pathogenesis and reveals new potential targets for therapy (1,16,17,37,81-84).

1.3 OBJECTIVES OF THE STUDIES

Curing or preventing MS remains elusive until its etiology and pathogenesis are better understood. We hypothesize that 1) genetic variants in key determinants of inflammation and neurodegeneration confer susceptibility to MS; 2) CCLs play important roles in controlling inflammation; and 3) mitochondrial mechanisms are involved in the final pathway of neurodegeneration associated with inflammation. We apply genetic, molecular and biochemical methods to identify and characterize novel candidate molecules that may play important roles in the pathogenesis of MS.

The main goals of our studies are to identify genetic determinants of CCLs that may be important in inflammation, and to define mitochondrial molecules and mechanisms that are involved in neurodegeneration developing secondary to inflammation.

Specifically, we

1. Search for new candidate genes within susceptibility loci defined by linkage analyses. Even though the function of these candidate genes has been taken into consideration (inflammatory candidates including CCLs and neurodegenerative candidates including Complex I), a selection of genes from linkage defined susceptibility loci is less prone to biases (as linkage is *a priori* free of preconceived assumptions regarding the disease pathogenesis) than a mere selection of candidate molecules based on existing hypotheses of pathogenesis.
2. Apply methods more powerful than linkage in complex traits. The method of linkage has been successful in identifying disease causing genes in Mendelian disorders and in defining susceptibility loci in complex trait disorders. However, in the latter case, linkage as a method reached its limits and has no power to further confine the large susceptibility loci to specific

genes. For identifying candidate genes within linkage defined susceptibility loci of MS, we used the method of LD mapping and sequencing.

3. Define the expression distribution and function of genes identified in our genetic studies. A differential expression distribution and functional involvement of gene products in plaques, NAWM and NAGM may further confirm the relevance of these molecules in the disease development.

4. Form a new mechanistic view based on our observations and expand previously developed concepts of MS. The outcomes of our studies in two major groups of candidate genes and their products (CCL and Complex I) contribute to a concept linking at molecular level the immune inflammatory process to neurodegeneration in MS.

5. Reveal potentially new targets for therapy. Both the upstream part of our studies concerning a group of small inflammatory mediators (β-chemokines), and the downstream part concerning mitochondrial molecules and mechanisms involved in neurodegeneration, present new targets for the treatment of MS.

2. THE ROLE OF CC CHEMOKINES IN INFLAMMATORY DEMYELINATION (62,82-84)

2.1 BACKGROUND

As the interactions between β-chemokine ligands and their receptors play central roles in the recruitment and retention of inflammatory cells in the CNS, both these ligands and their receptors represent potential therapeutic targets in MS. Chemokines are small, evolutionarily related chemoattractant molecules regulating cell trafficking through interactions with their receptors (85). The approximately 50 known human chemokine genes are divided into four subfamilies based on distinct patterns of cysteine residues close to the N-terminal end of the products. The CC chemokine ligand family (CCL) (also called β-chemokines or Small Cytokine Group A-SCYA) is characterized by two adjacent cysteines, while the CXC (SCYB) and CX_3C (SCYD or fractalkine) chemokine families have one or three intervening amino acids, respectively, between the two cysteines. In the XC family (SCYC or lymphotactin), only one cysteine is present (85). Fourteen of the 27 human CC chemokines including CCL2, CCL7, CCL11, CCL8, CCL13, CCL1, CCL5, CCL16, CCL14, CCL15, CCL23, CCL18, CCL3 and CCL4, respectively, are encoded within 17q11 (Figure 3).

Figure 3. Chromosome 17q11

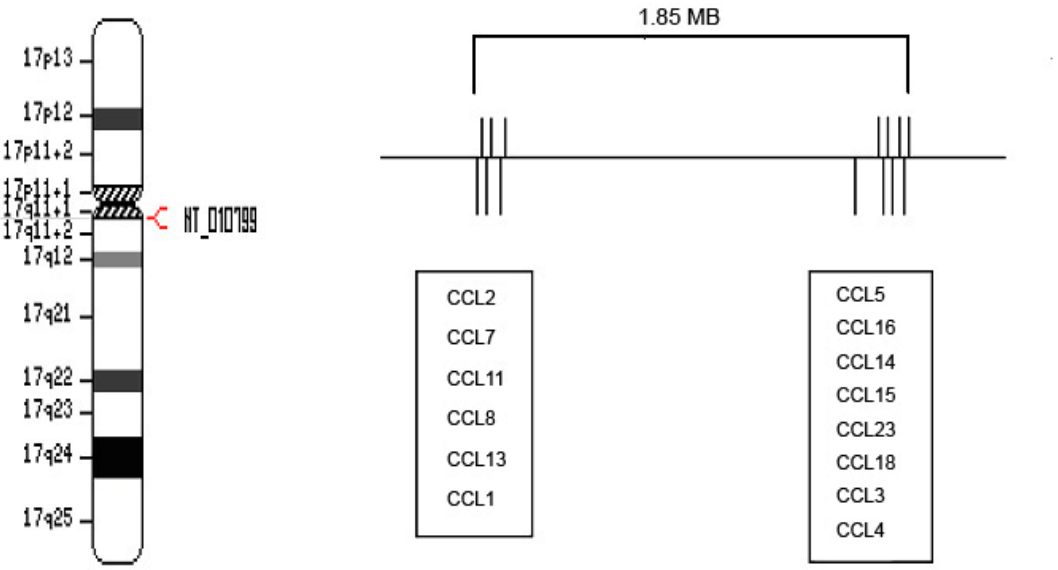

This figure demonstrates the position of the CCL cluster in 17q11 (left side). The enlarged CCL region (right side) shows the distribution of individual genes in two subclusters within a 1.85MB region. The distance between CCL1 and CCL5 is 1.5 MB.

While CC chemokine receptors (CCRs) generally bind multiple chemokine ligands and vice versa, the most efficient interaction may occur between a single receptor and its primary ligand (e.g. CCL2 – CCR2). CCRs are G-protein coupled receptors with seven-transmembrane-domains. A high affinity interaction between CCL-CCR molecules leads to signal transduction initiated by the dissociation of G-protein complex into Gα and Gβγ subunits. Gα induces the activation of the phosphoinositidine 3-kinase pathway, while the Gβγ subunits activate phospholipase C and induce Ca^{2+} influx and protein kinase C activation. Ten CC chemokine receptors (CCRs), 6 CXCRs, one CX_3CR1 and one XCR1 are currently known (85-86).

The transmigration of autoreactive immune cells via the BBB is an early and critical process in EAE and MS, and is regulated by CC chemokines produced at the BBB and in the CNS. Subcellular signals induced by a specific CCL-CCR engagement lead to an increased avidity of integrins (VLA4) on leukocytes to their receptors (VCAM1) on endothelial cells, followed by a facilitated migration of leukocytes towards the chemokine gradient in the CNS (87-88). In addition, chemokines are involved in the regulation of T cell differentiation, apoptosis, cell cycle, angiogenesis and metastatic processes as well as of the generation of soluble inflammatory products (85,89). The differential effects of various

chemokines on TH1, Th17 and TH2 polarization may also be significant in the development of inflammatory demyelination.

A meta-analysis of three MS genome scans detected the highest NPL score= 2.58 at 17q11 (73). While numerous candidate genes are located in this region (e.g. NOS2A, OMG, NF1), a 1.85 MB segment at 17q11.2-q12 encodes a cluster of β-chemokines (Figure 3). Two quantitative trait loci (QTL) in EAE, *eae6* and *eae7*, were mapped to a region of mouse chromosome 11 synthenic to human 17q11. *Eae6* and *eae7* influence severity and duration of, while e*ae7* also confers susceptibility to EAE (90). Fine mapping revealed two adjacent QTLs, *eae18a* and *eae18b,* on the rat chromosome 10 in a chronic relapsing form of EAE (91). *eae18b* is orthologous to the human 17q11 region and encodes β-chemokine genes.

The recognition of the β-chemokine gene region as susceptibility and quantitative trait locus in EAE, the human data revealing 17q11 as a susceptibility locus in MS, and the well defined immune regulatory functions of these gene products strongly suggests the involvement of β-chemokine variants in the development of inflammatory demyelination.

2.2 PATIENTS AND METHODS

2.2.1 Studies on 17q11: phase I - LD mapping

Patients, families and DNA specimens

DNA specimens from families with various structures were obtained from the Multiple Sclerosis DNA Bank (MSDB), University of California San Francisco, San Francisco (UCSF), CA, the collection of the Canadian Multiple Sclerosis Collaborative Group (CMSCG) (Dr. Ebers) and the Multiple Sclerosis Treatment and Research Center (MSTRC), Minneapolis, MN (Dr. Birnbaum) (Table 1). Human subjects were studied in this and all the following sections in compliance with the rules of US Human Subject Protection Programs (IRB and HIPAA). The diagnosis of MS for patients whose DNA specimens were obtained from existing collections (MSDB, CMSCG) was made by the Poser criteria (28). Patients whose specimens were prospectively collected for this study were diagnosed using the McDonald's criteria (29). The diagnosis of PP-MS was established if sustained progression of disability was observed for at least one year in the absence of relapses (30). If one or more relapses occurred superimposed on a progressive course from onset, PR-MS was diagnosed.

To test if the inclusion of patients with PP-MS caused any bias in the outcome, in a subanalysis we removed all PP-MS nuclear families and trios from the total DS101-115 dataset. The majority (over

94%) of patients in DS101-104, DS106-108, DS109-112 and DS113-114 has RR / SP-MS. DS105 and DS115 are exclusively composed of PP-MS trios and PP-MS incomplete families. Patients with PR-MS were assigned to the PP-MS group (27). There were 47 PP-MS trios and incomplete families, and 217 RR/SP-MS families in the stratified analyses (trios, affected sib pair and multiplex families).

Table 1. Families in DS101-115

Dataset	Total families	Individuals	Trio	ASP	Incomplete	Multiplex	Origin
DS101-105	66	365	7	34	10	15	MSDB, UCSF
DS106-108	66	198	66	0	0	0	MSDB, UCSF
DS109-112	50	300	0	39	0	11	CMSCG
DS113-114	58	174	42	0	16	0	MSDB, UCSF
DS115	17	48	2	0	15	0	MSTRC
Total	257	1085	117	73	41	26	

Specimens of North-American Caucasian MS patients and their families were obtained in five shipments (DS101-105, DS106-108, DS109-112, DS113-114 and DS115) from two existing DNA collections of the UCSF based MS DNA Bank (MSDB) and the London, ON based collection of the Canadian MS Collaborative Group (CMSCG), and from a prospective collection of the MS Treatment and Research Center (MSTRC), Minneapolis, MN. DS101, DS102 … DS115 represent subsets of specimens in separate 96 well plates. All specimens were similarly genotyped and the analyses of combined data from 257 families are presented below. Definitions: ASP=affected sib pair family: two or more affected and one or more unaffected children with their unaffected parents; trio: an affected child with unaffected parents; incomplete family: an affected individual with one unaffected parent and / or an unaffected sibling; multiplex family: multiple affected and unaffected family members in two or three generations.

Genotyping

We contracted ACGT, Inc (Northbrook, IL), a biotech company that uses the 5’ Nuclease (or TaqMan) assay for allelic discrimination of SNPs with high sensitivity and specificity on an ABI7900HT Instrument (ABI PE Inc, Foster City, CA). PCR amplification of the template DNA was performed with unlabeled forward and reverse primers in the presence of a specific TaqMan probe with a non-fluorescent quencher plus a minor groove binder attached to the 3’ end, and a reporter fluorescent label (Fam or Vic) attached to the 5’ end. A fully hybridized probe remained bound during strand displacement, and resulted in efficient cleavage of the reporter dye by the 5’ nuclease activity of TaqGold DNA polymerase. Each reaction mixture contained two probes having a single nucleotide difference and

Fam or Vic labels. The release of the reporter dyes correlated with the fraction of the matching alleles. The genotyping error rate with this method was <0.5%.

SNPs

Table 2. SNPs genotyped (Contig NT010799, chromosome 17q11.2-q12.)

Gene with SNP	Alternative names	NCBI SNP #	Contig location (bp)	Interval distances (bp)	Heterozygosity	Minor allele frequency
CCL2B	MCP-1	rs2857657	7316912		0.32	0.21
CCL2X	MCP-1	rs13900	7317691	779	0.38	0.29
CCL7X	MCP-3	rs3091237	7331583	13892	0.26	0.15
CCL7N	MCP-3	rs3091322	7333640	2057	0.22	0.13
*CCL11X	Eotaxin	rs3744508	7346674	13034	0.27	0.21
CCL11B	Eotaxin	rs1860184	7346912	238	0.43	0.35
CCL8X	MCP-2	rs3138036	7381324	34412	0.27	0.16
CCL8Y	MCP-2	rs138037	7381524	200	0.32	0.19
CCL13A	MCP-4	rs159313	7418169	36645	0.45	0.42
CCL13B	MCP-4	rs2072069	7418771	602	0.49	0.46
CCL1N	I-309	rs3136682	7421222	2451	0.09	0.04
CCL1A	I-309	rs2282692	7421963	741	0.41	0.33
CCL1X	I-309	rs3138032	7422822	859	0.20	0.11
CCL5B	RANTES	rs1065341	8932373	1509551	0.09	0.05
CCL5A	RANTES	rs2280789	8940783	8410	0.28	0.15
CCL16X	NCC4	rs2063979	9037346	96563	0.39	0.29
CCL16A	NCC4	rs917015	9039305	1959	0.35	0.25
CCL14Y	HCC1	rs2075746	9059312	20007	0.09	0.05
CCL15O	MIP1δ	rs864104	9059550	238	0.31	0.20
*CCL15M	MIP1δ	rs854625	9062241	2691	0.08	0.05
CCL15N	MIP1δ	rs2075746	9062512	271	0.50	0.45
*CCL23M	MPIF-1	rs1003645	9074064	11552	0.30	0.19
CCL23A	MPIF-1	rs1719208	9078021	3957	0.32	0.19
CCL18B	MIP-4	rs2015052	9125793	47772	0.08	0.04
CCL18X	MIP-4	rs712042	9126660	867	0.24	0.14
CCL18A	MIP-4	rs14304	9132275	5615	0.38	0.28
CCL3B	MIP-1α	rs1719130	9150026	17751	0.33	0.22
CCL3A	MIP-1α	rs1719134	9150726	700	0.33	0.22
CCL4X	MIP-1β	rs3744597	9165650	14924	0.18	0.09
*CCL4P	MIP-1β	rs3744595	9165758	108	0.18	0.09
CCL4B	MIP-1β	rs1719147	9165905	147	0.33	0.23

Table 2 shows the experimental designation of SNPs in β-chemokine genes using the current terminology (CCL2, etc…) and alternative names (MCP-1, etc…), the NCBI Rs numbers, contig positions, inter-marker distances, heterozygosity and minor allele frequency of SNPs. SNPs are indicated with a letter attached to the gene name (e.g. CCL2B). Nonsynonymous SNPs (CCL11X, CCL15M, CCL23M and CCL4P) are labeled with "*". Abbreviations for the alternative β-chemokine names: MCP-1: monocyte chemotactic protein-1; MCP-3: monocyte chemotactic protein-3; Eotaxin: eosinophil chemotactic protein; MCP-2: monocyte chemotactic protein-2; MCP-4: monocyte chemotactic protein-4; I-309: inflammatory protein homologous to mouse TCA-3; RANTES: Regulated upon Activation, Normally T Expressed, and Presumably Secreted; NCC4: homologous to mouse macrophage inflammatory protein-1; HCC1: enhance proliferation of CD34 stem cells and share homology with the mouse MIP-1α and MIP-1β; MPIF-1: myeloid progenitor inhibitory factor -1; MIP-4: macrophage inflammatory protein-4; MIP-1α: macrophage inflammatory protein-1α; MIP-1 β: macrophage inflammatory protein-1β.

Nonsynonymous, untranslated region and intronic SNPs within CCL genes were selected from the NCBI database (http://www.ncbi.nlm.nih.gov/SNP). We intended to have at least 2 SNPs per gene and all nonsynonymous SNPs listed in the database as of November 2002, when the study was initiated. Thirty-one assays were successfully developed, validated and genotyped in DS101-105, DS106-108, DS109-112. In DS113-14 and DS115, data only from 27 assays were obtained as assays of CCL2B, CCL7N, CCL11X and CCL15M SNPs were not included. Table 2 summarizes the list of included SNPs and their characteristics.

Analyses

-Files

Mendelian inconsistencies were screened by Pedcheck and genotyping errors were manually corrected or deleted dependent on the reliability of information obtained from the scatter plot distribution and relative intensity of fluorescent signals. Allele and genotype frequencies were calculated for 356 unrelated parents in DS101-115. Deviation from the Hardy-Weinberg equilibrium (HWE) was tested by using the χ^2-statistics in MERLIN (Multipoint Engine for Rapid Likelihood Inference, http://www.sph.umich.edu/csg/abecasis/Merlin/) (92).

-Power estimate

Different methods have been used to estimate the required sample size (N) in the TDT / PDT, taking into consideration varying estimates of the genotypic risk ratio (λ_s=1.5 - 4), allele frequency (p=0.01 - 0.80), and proportion of heterozygous parents (0.025 - 0.500), and different modes of inheritance (multiplicative, additive, recessive or dominant). Based on four methods of power assessment in the TDT of one candidate SNP, a sample size of 53 to 55 is required for λ_s=2, and a sample size of 192 to 195 is required for λ_s=1.5 to achieve 80% power, when assuming a disease-predisposing allele frequency of 0.1 and a multiplicative model (79,93-94). Therefore N=257 in MS appears to be a reasonable sample size in a TDT or PDT based analysis of SNPs in candidate genes with an expected range of λ_s= 1.5 - 2 (41,95).

-PDT

We chose to use the pedigree disequilibrium test (PDT), developed from the classical transmission disequilibrium test (TDT), to determine if a marker locus and the hypothetical disease locus are linked or are in linkage disequilibrium (95-96). Under Mendelian inheritance, all alleles have a 50% chance of being transmitted to offspring by the parents. An allele may be associated with the disease risk, if it is

transmitted more often than 50% of the time, indicating a transmission distortion. PDT can utilize data from trios, nuclear families and discordant sibships within extended pedigrees.

-TRANSMIT

Haplotype-based analyses were conducted using the TRANSMIT version 2.5 program (http://www-gene.cimr.cam.ac.uk/clayton/software/) (97). This program tests for association between genetic markers and disease by examining the transmission of markers and haplotypes from parents to affected offspring. TRANSMIT can analyze multilocus haplotypes, even if phase is unknown and parental haplotypes are missing. The tests are based on a score vector which is averaged over all possible configurations of parental haplotypes and transmissions consistent with the observed data. Data from unaffected siblings may be used to restrict the number of possible parental genotypes to be considered. When transmission is fully observed, this test is similar to the Pearson χ^2 -test. The program calculates the following χ^2-statistics: 1) For each haplotype or allele, a test for excess transmission of that haplotype; and 2) a global test for association (H-1 df, where H is the number of haplotypes for which transmission data are available). In brief, TRANSMIT v. 2.5 estimates the maximum log-likelihood of haplotype probabilities of paired marker alleles. The haplotype-based score test evaluates the difference in the observed and expected transmission of each possible haplotype from parents to affected children by using the χ^2 statistics. We performed the bootstrap significance test using 10,000 bootstrap samples of haplotypes.

-Ldmax

Ldmax in the GOLD program provides maximum likelihood estimates of pair-wise disequilibrium (http://www.sph.umich.edu/csg/abecasis/GOLD/docs/stats.html) by using the Slatkin and Excoffier implementation of the expectation-maximization algorithm (98-99). SNP alleles were taken from unrelated parents in 356 unrelated parents in DS101-115 to assess haplotype frequencies. Computation of the δ^2, D and D' values can be found at the web site. In brief, pair-wise LD can be estimated as $D = x_{11} - p_1q_1$, where x_{11} is the frequency of haplotype A_1B_1, and p_1 and q_1 are the frequencies of alleles A_1 and B_1 at loci A and B, respectively. A standardized LD coefficient, δ, is defined by $D/(p_1p_2q_1q_2)^{1/2}$, where p_2 and q_2 are the frequencies of the other alleles at loci A and B, respectively. D' is given by $D' = D/D_{max}$, where $D_{max} = \min(p_1q_2,p_2q_1)$ when $D < 0$ or $D_{max} = \min(p_1q_1,p_2q_2)$ when $D > 0$. The χ^2 statistics for a contingency table is also generated to calculate significance from an asymptotic distribution with *(r-1)(c-1)* degrees of freedom, where r and c are the count of alleles for the pair of markers being considered. The statistics and p-values, as well as δ^2 and D' values, where D' ranges between 0 and 1 (greater values indicating stronger LD), are included in the output file (100).

-Computation

PDT, TRANSMIT vs 2.5, MERLIN and the GOLD program were run in Unix and Linux based computational environments at the AMDeC Bioinformatics Core Facility at the Columbia University.

2.2.2 Studies on 17q11: phase II - LD mapping

Patients, families and DNA

Specimens of DS116-132 (Table 3) were obtained from sources (UCSD MSDB and CMSCG) and with criteria (28,29) as described above in 2.2.1 (82,83).

Table 3. Families in DS116-132

Dataset	Total families	Individuals	Trio	ASP	Incomplete	Multiplex	Origin
DS116-117	47	141	47	0	0	0	MSDB
DS118-120	59	221	0	8	5	46	CMSCG
DS121-123	57	238	26	0	7	24	MSDB
DS124-132	198	769	50	120	2	26	CMSCG
Total:	361	1369	123	128	14	96	

DNA specimens of Caucasian patients and their families (DS116-132) were received in four shipments from existing collections of the Multiple Sclerosis DNA Bank (MSDB), UCSF and of the Canadian Multiple Sclerosis Collaborative Group (CMSCG), London, ON. Each DS (dataset) designates a subset of specimens in separate 96 well plates. Definitions: ASP=affected sib pair family: two or more affected and 0 or more unaffected children with their unaffected parents; trio: an affected child with his / her unaffected parents; incomplete family: an affected individual with one unaffected parent and / or an unaffected sibling; multiplex family: multiple affected and unaffected family members in two or three generations.

Genotyping

High through-put SNP genotyping was performed at Genaissance Pharmaceuticals using the Sequenom MassARRAY^{TM} System, which employs MALDI-TOF mass detection of extended primers. The genotyping success rate for each validated marker averaged 96%, while the error rate was 0.5% based on comparisons of data from sequence and MALDI-TOF analyses. The error rate identified by checking for Mendelian inconsistencies was 0.2% in our data sets.

SNPs

Out of 326 SNPs initially selected (http://www.ncbi.nlm.nih.gov/SNP), 261 assays were successfully developed and validated (80% assay conversion rate). A higher rate of assay development failure was noted for non-synonymous and other coding region SNPs as compared to intergenic SNPs. After the exclusion of monomorphic markers (18 SNPs) and of those with deviation from the HWE (11 markers with HWE $p<0.03$ excluded), 232 markers were retained in the study. These 232 markers (numbered here continuously according to the sequential inclusion of SNPs from centromeric to telomeric direction in 17q11) included tagging SNPs which define haplotypes (http://www.hapmap.org) and achieved an average pacing <8 kb. The total number of non-synonymous mutations was 21, 5 of which were located within CCL genes. The total number of SNPs within genes was 103, 50 of which were located within CCL genes.

Analyses

Mendelian inconsistencies were identified by using Pedcheck. Mismatching genotypes were deleted. Allele and genotype frequencies and heterozygosity in DS116-132 were determined in 755 unrelated parents by using MERLIN (http://www.sph.umich.edu/csg/abecasis/Merlin/) (92). Deviations from the HWE were tested by using the χ^2-statistics (92).

The PDT and TRANSMIT version 2.5 were used as described in 2.2.1.4.3 and 2.2.1.4.4. In the TRANSMIT program, first the transmission of two-marker haplotypes (n-1=231 marker pairs, each with 4 possible haplotypes of which 3 are independent, resulting in a total of 693 independent 2-marker-haplotypes) was examined, followed by the extension of haplotypes in both directions in regions with p-values <0.05. Thus, an additional array of 28 three-marker and 2 four-marker combinations were tested by TRANSMIT. In the bootstrap significance test, 10,000 bootstrap samples of haplotypes were applied.

In addition to PDT, we used the family based association test (FBAT). FBAT examines association and linkage or association in the presence of linkage, while excludes spurious associations caused by population admixtures (101-102). FBAT, based on the original TDT (95), integrates tests of different genetic models, different sampling designs and different disease phenotypes. It can also perform tests with missing parents. FBAT compares the distribution of observed and expected (Mendelian segregation) genotypes in affected individuals under the null hypothesis assuming “no linkage and no association” or “no association, in the presence of linkage”. As the built in conditioning on the sufficient statistics eliminates all nuisance parameters, the technique avoids confounding due to model misspecification as well as admixture or population stratification (101). To complement TRANSMIT, we

included here the haplotype based association test (HBAT). HBAT is a family-based test of association between disease and haplotypes constructed from tightly linked markers.

We used here the method of spectral decomposition (SpD) to perform correction for multiple testing for SNPs in LD with each other (http://genepi.qimr.edu.au/general/daleN/SNPSpD/) (103). A collective correlation among variables is measured by the variance of eigenvalues (λs) derived from the correlation matrix. High correlation among variables results in high λs. If all variables are fully correlated, the first λ equals the number of variables in the correlation matrix (M), and the rest of λs are zero. If no correlation exists among variables, all of the λs will be equal to one, and the set of λs will have no variance. The ratio of observed eigenvalue variance, Var (λ_{obs}) to its maximum (M) gives the proportional reduction in the number of variables in a set. The effective number of variables (M_{eff}) is calculated as $M_{eff}=1+(M-1)\ (1-Var(\lambda_{obs})/M)$ (103). Merlin-format pedigree and map files are analyzed by an altered version of ldmax (GOLD) to estimate haplotype frequencies and to calculate the pair wise LD statistics. A Perl script creates a matrix of pair wise Δ measures, from which SNPSpD calculates λs. The SpD output includes the matrix of pair wise Δ measures, M, λs, Var (λ_{obs}), M_{eff} and the Sidak-corrected (104, similar to Bonferroni correction) significance threshold for M_{eff} tests required to keep the type I error rate at 5%.

Ldmax (GOLD) was used as described in 2.2.1.4.5. The distribution of LD is also estimated here by the D' values, where D' ranges between 0 and 1 (greater values indicate stronger LD). The computation environment was similar to that described in 2.2.1.4.6.

2.2.3 Studies on 17q11: Phase III - Sequencing of a MS associated haplotype within CCL3

Patients and families

Altogether, 17 affected and 8 unaffected unrelated individuals were identified with an MS associated three-marker haplotype encompassing CCL3 in 1369 individuals from 361 trio, affected sibpair, incomplete and multiplex Caucasian families in the Phase II CCL genetic study. All positive individuals were heterozygous for this haplotype defined by the A-T-C alleles of SNPs 278-277-273 (84).

Automatic sequencing

A 3500 bp DNA segment, including the MS-associated three-marker haplotype (1,180 bp) and its 5' (1,750 bp) and 3' (570 bp) flanking regions, was amplified by PCR in 7 overlapping fragments. The DNA fragments were directly sequenced on an ABI Prism 3700 DNA Analyzer

(Genaissance Pharmaceuticals, Inc, New Haven, CT). Sequences were aligned with the corresponding segment of the NC_010799 contig on chromosome 17 http://www.ncbi.nlm.nih.gov/entrez/viewer.fcgi?val=37544509&view=gbwithparts.

Genotyping:
SNPs revealed by sequencing in 25 individuals carrying the haplotype of interest were genotyped using the Sequenom MassARRAY System in the original 361 families including 1369 individuals.

Analyses
Associations of these alleles and haplotypes with MS were tested by using the pedigree disequilibrium test (PDT) and TRANSMIT version 2.5 program (82,96,97).

2.2.4 Expression of CCL molecules in MS brains

Patients and specimens
Frozen brain samples were obtained from the Rocky Mountain Multiple Sclerosis Brain Bank (RMMSBB), Denver, CO, and the Human Brain and Spinal Fluid Resource Center (HBSFRC), Los Angeles, CA. Corresponding sets of adjacent NAWM, NAGM and chronic active plaque specimens were obtained from frontal lobes of 10 patients with PP-MS and SP-MS, with a mean age of 51.6±10.2 years and a post mortem time of 13.52±9.6 hours. Histological criteria of specimen selection were defined as described by Lu et al (105). In brief, normal appearing and pathological tissues were selected by gross examination. The presence of small plaques, microglial proliferation, and perivascular or parenchymal infiltration by mononuclear cells in NAWM and NAGM specimens were excluded by microscopic examination of cryosections stained by Haematoxylin&Eosin and Luxol Fast Blue. For indication of macrophage / microglia activation and up-regulation of the MHC Class I molecule, immunohistochemical analysis was performed by using anti-CD68 and anti-β_2-microglobulin staining. A chronic active plaque was defined by the presence of inflammatory activity, hypercellularity around regions showing demyelination, oligodendrocyte loss and some degree of astrogliosis (Figure 4).

Corresponding sets of white matter (WM) and gray matter (GM) specimens were obtained from 3 normal controls with a mean age of 70±3.92 years and a post mortem time of 10.13±4.32 hours. Specimens from normal controls in the age range of MS patients were not available in the Tissue Banks, however, we included the available specimens for the intra-individual normal WM-GM comparisons. WM and GM specimens from 3 patients with Alzheimer's disease, a mean age of

72.0±13.23 years and a post mortem time of 11.37±7.9 hours were also included. We also obtained frozen postmortem WM and GM specimens from two patients with Herpes Simplex and postinfectious encephalitis. The age of these patients was 86 and 58 years. Histological evaluation using Haematoxylin & Eosin, Luxol Fast Blue, anti-CD68 and anti-β_2-microglobulin staining revealed inflammatory activity in both the white and gray matters of these specimens (histological documentation not shown).

Figure 4. Inflammation, immune activation and demyelination in plaque, NAWM and NAGM.

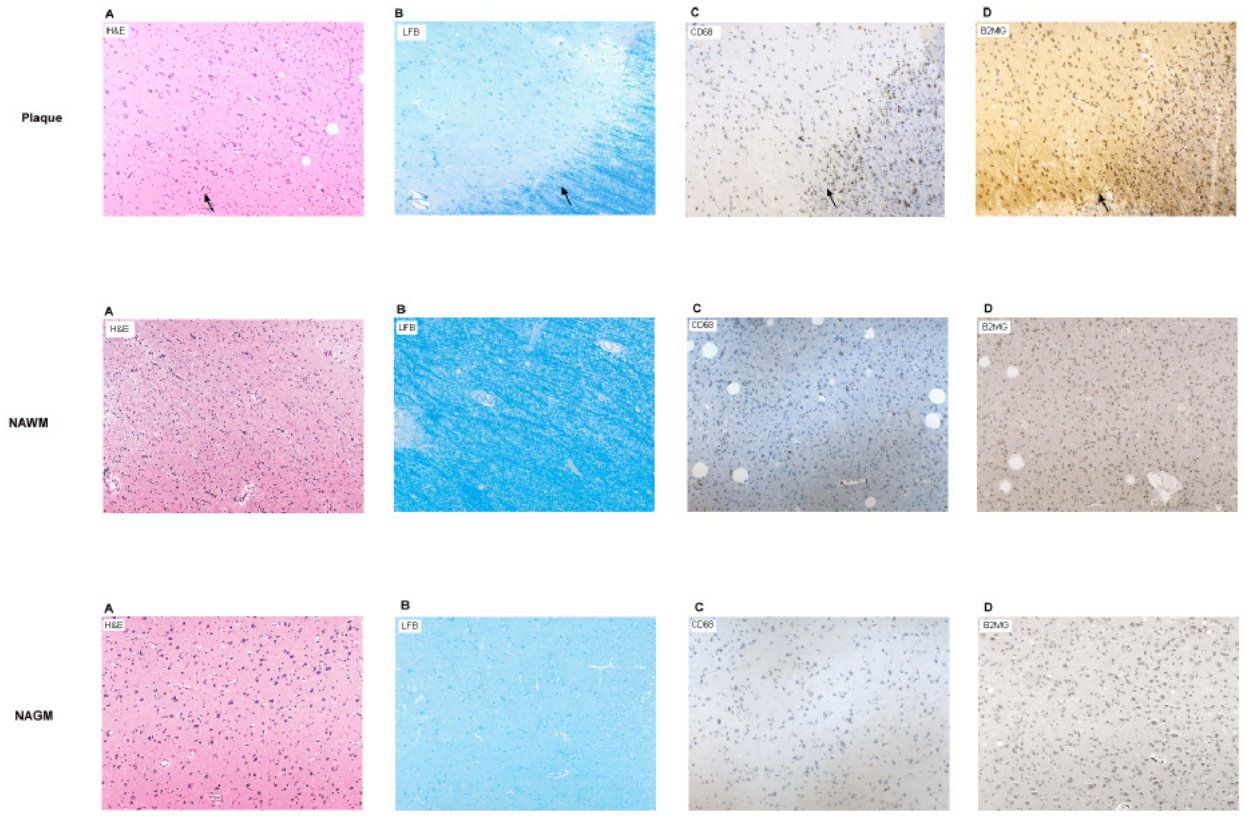

Plaque, NAWM and NAGM containing specimens were selected from adjacent frontal lobe regions of all patients. Columns a-d show Haematoxylin & Eosin, Luxol Fast Blue, anti-CD68 and anti-β_2-microglobulin staining of a plaque (first row), NAWM (second row) and NAGM (third row) of a representative patient. Note the separation of demyelination and the border zone of inflammation in a chronic active plaque (arrow), and the striking differences in the degree of inflammation and CD68 and β_2-microglobulin expression in plaque, NAWM and NAGM.

Isolation of RNA

RNA extraction from frozen brain tissues was carried out by using a Qiagen RNA isolation kit (Qiagen, Valencia). RNA concentration was adjusted to 1 ug/ul and cDNA was synthesized by using the Promega Reverse Transcription Kit with random primers (Promega, Wisconsin, MN).

Real Time PCR

mRNA of CCL2, CCL3, CCL5, CCL7, CCL8, CCL13 and CCL15 was quantified relative to β-actin (ACTB) using the LightCycler – FastStart DNA Master^{PLUS} SYBR Green I kit on a Roche Light Cycler System 2.0 (Roche, Indianapolis).

The primers were designed by the Roche Light Cycler Probe Design Program:

	Forward primers	Reverse primers
CCL2:	5`- TGTGCCTGCTGCTCATAGC – 3`	5` - TGTGGAGTGAGTGTTCAAGTCT – 3`
CCL3:	5` - TTGGGAACATGCCTCTGACC – 3`	5` - ACTGCCTACACAGGCTGAT – 3`
CCL5:	5` - TCGCTGTCATCCTCATTGCTAC – 3`	5` - GCTCATCTCCAAAGAGTTGATGTAC - 3`
CCL7:	5` - AAGGAGATCTGTGCTGACCC – 3`	5` - AAGCTTTATGTTCDAAAACCCAC – 3`
CCL8:	5`- GTGAGGTCACTTTGCTGAGC - 3`	5`- AACCTTCATCTTGGAGGGC- 3`
CCL13:	5` - GCTGGAGTACGTGAAATGACT – 3`	5` - GGAACCGAATACAAACCCACTG – 3`
CCL15:	5` - GCTAACACCTCCTGGTTGGA – 3`	5` - AGAACAAGGCTGAGAGTGC – 3`
ACTB:	5` - AAGACCTGTACGCCAACAC – 3`	5` - GGGTGTAACGCAACTAAGT – 3`

As an external standard, five different concentrations [$5x10^6$ copies/5ul; $5x10^5$ copies/5ul; $5x10^4$ copies/5ul; $5x10^3$ copies/5ul; $5x10^2$ copies/5ul] of a β_2 -microglobulin cDNA sample were amplified along with the experimental samples in each run (Roche, Indianapolis). Each PCR mixture consisted of 2 uL cDNA, 50 pmol of forward and reverse primers, 4 uL of SYBR Green reaction mix with the FastStart^{PLUS} Enzyme and H_2O was added to a final volume of 20 uL. The PCR conditions were as follows: denaturation at 95°C for 600s; amplification at 95°C for 10s, 62°C for 13 sec, 72°C for 13 sec in 45 cycles. The melting curve reading rose 0.21°C/sec continuously until it reached 97°C from 70°C. Cooling proceeded until the machine reached 40°C. The experimental samples were plotted along the slope of the β_2 -microglobulin external standard to automatically extrapolate their concentrations by using the Roche analysis software version 4.0.

Analyses of data

Regional differences in the mRNA expression in NAWM, NAGM and plaque or WM and GM were analyzed by the Wilcoxon Signed Rank Test.

2.3 RESULTS

2.3.1 Studies on 17q11: phase I – LD mapping (82)

Allele and genotype frequencies

Genotyping of DNA was similarly performed in all datasets. SNP allele and genotype frequencies were compared among the datasets, and also calculated for the unrelated parents in the combined DS101-115 dataset. No deviations from the HWE were observed.

Markers showing allelic associations with MS

Analysis of data was initially carried out separately in each dataset, and then in the combined DS101-115 set. Since all datasets contain North-American families with European background and with similar allele frequency distributions, the results from the combined DS101-115 families are presented here (Table 4). The analysis reveals transmission distortion for SNPs CCL2B, CCL11B, CCL5A, CCL18B, CCL18X and CCL3B (Table 4). Considering that 94% of the DS101-115 families include patients with RR/SP-MS, it is reassuring to detect similar trends of findings in the unstratified and the RR/SP-MS data sets. Although the PP-MS group is small, allelic associations are significant at CCL18B and CCL18X. However, the p-values are modest and become non-significant after Bonferroni correction for multiple comparisons.

Haplotypes associated with MS

While no SNP in Table 4 has direct relevance to MS, they may still define disease associated haplotypes. Therefore, twenty-seven 2-marker haplotypes generated in a pair-wise manner from the list in Table 2 (but skipping subregions with a gap >30kb), and five 3-marker haplotypes in subregions of 2-marker haplotype associations were tested by TRANSMIT (Table 5a and 5b). We detected significant p-values for several two-marker haplotypes including CCL2bx, CCL11b-CCL8x, CCL8y-CCL13a, CCL13ab and CCL15om in both DS101-115 and the RR/SP-MS groups and for CCL3ba in the RR/SP-MS group. Only one three-marker haplotype, CCL15omn showed significant distortion in the two groups. However, the variance value of observed and expected transmissions (<2.5) of the CCL15om and CCL15omn haplotypes was too low to make reliable conclusion (97). As indicated in Table 5a and 7b, the removal of the PP-MS families from DS101-115 did not markedly change the outcome of the

analyses, and the PP-MS subgroup alone was too small to reliably define a pattern of phenotype specific associations.

Table 4. Allelic associations as determined by PDT.

	Alleles	DS101-115 χ^2	DS101-115 p-value	RR/SP-MS χ^2	RR/SP-MS p-value
CCL2B	**C** /G	**4.900**	**0.0269**	**6.366**	**0.0116**
CCL2X	C / T	0.643	0.4227	0.021	0.8841
CCL7X	C / G	1.584	0.2082	1.780	0.1821
CCL7N	A / G	0.736	0.3910	0.083	0.7731
CCL11X	A / G	0.540	0.4626	0.128	0.7208
CCL11B	**A** / T	**7.134**	**0.0076**	3.777	0.0520
CCL8X	A / G	0.705	0.4010	0.332	0.5642
CCL8Y	A / C	0.120	0.7293	0.229	0.6320
CCL13A	C / T	1.615	0.2038	2.661	0.1029
CCL13B	A / G	0.019	0.8913	0.024	0.8759
CCL1N	A / G	0.119	0.7299	0.701	0.4025
CCL1A	G / T	0.004	0.9469	0.086	0.7697
CCL1X	C / T	0.326	0.5680	0.835	0.3608
CCL5B	A / G	0.582	0.4455	0.129	0.7193
CCL5A	**C** / T	**3.968**	**0.0464**	3.234	0.0721
CCL16X	A / G	1.421	0.2333	1.245	0.2645
CCL16A	A / G	0.439	0.5077	0.447	0.5039
CCL14Y	C / T	1.506	0.2197	1.582	0.2085
CCL15O	A / G	0.003	0.9551	0.527	0.4679
CCL15M	C / T	3.712	0.0540	1.997	0.1576
CCL15N	A / G	0.804	0.3700	1.839	0.1751
CCL23M	A / G	0.137	0.7108	0.145	0.7037
CCL23A	C / T	0.164	0.6854	0.137	0.7115
CCL18B	**A** / C	**6.132**	**0.0133**	2.133	0.1442
CCL18X	**A** / G	**4.195**	**0.0405**	1.292	0.2556
CCL18A	A / G	0.353	0.5523	1.412	0.2347
CCL3B	**C** / T	3.201	0.0736	**5.614**	**0.0178**
CCL3A	C / T	1.460	0.2269	2.905	0.0883
CCL4X	A / C	0.345	0.5570	0.562	0.4536
CCL4P	A / G	0.000	0.9986	0.010	0.9223
CCL4B	A / G	0.618	0.4317	0.001	0.9712

PDT used 253 individual families, 243 trios and 446 discordant sib pairs in 27 assays (DS101-115), and 178 individual families, 199 trios and 411 discordant sib pairs in 4 assays (CCL2B, CCL7N, CCL11X, CCL15M, see methods) (DS101-112). In the RR/SP-MS group, 213 individual families, 228 trios and 402 discordant sib pairs or 159 individual families, 188 trios and 387 discordant sib pairs were used, respectively. PP-MS families (42 individual families, 16 trios and 32 discordant sib pairs) did not show any association, except for CCL18B (χ^2=6.00 p-value=0.0143) and for CCL18X (χ^2=6.756 p-value=0.0093). Bonferroni correction for multiple comparisons would require a p= or < 0.00165 to bring back the overall α level to 0.05. Thus, after Bonferroni correction, none of the above p-values indicate significant deviation from the expected distribution of marker allele transmission.

Table 5a. Results of two-marker haplotype analysis by TRANSMIT

Gene	DS101-115					RR/SP-MS				
Haplotypes of marker alleles	Observed	Expected	Var(O-E)	Chisq(1df)	p-value	Observed	Expected	Var(O-E)	Chisq(1df)	p-value
CCL2bx Haplotype G C	137	153	45.38	5.68	0.0121	116	133	41.94	6.71	0.0086
CCL11b-CCL8x Haplotype T A	422	448	85.47	8.22	0.0039	370	390	74.00	5.62	0.0181
CCL8y-CCL13a Haplotype A C	237	257	70.40	5.72	0.0158	208	228	61.84	6.96	0.0065
CCL13ab Haplotype T G	39	27	12.29	10.26	0.0001	38	25	11.58	12.70	0
CCL15om Haplotype G T	0.5	2.5	1.02	4.12	0.0062	0.4	2.4	1.02	4.12	0.0005
CCL3ba Haplotype T C	572	558	65.56	2.89	0.0701	499	481	59.32	5.16	0.013

Table 5b. Results of three-marker haplotype analysis by TRANSMIT

Gene	DS101-115					RR/SP-MS				
Haplotype	Observed	Expected	Var(O-E)	Chisq(1df)	p-value	Observed	Expected	Var(O-E)	Chisq(1df)	p-value
CCL15omn Haplotype G T G	0.5	2.5	0.99	4.13	0.0007	0.4	2.4	0.99	4.12	0.0011

Significant distortion of two-marker (a) and tri-marker (b) haplotype transmissions is shown in the DS101-115 and RR/SP-MS dataset, when using a cut off p-value =/> 0.02. The number of nuclear families with transmission to affected offspring was 283 in DS101-115 and 242 in the RR/SP-MS subgroup.

LD distribution

Table 6 shows the distribution of the MS associated haplotypes in correlation with the distribution of inter-marker LD in 17q11.2-q12. Pair wise distributions of D' values indicate that strong LD extends from CCL2B to CCL11B, then it drops markedly and there is no LD between CCL2A and the CCL13A markers. The D' values generally correlate with the inter-marker distances, and the highest D' values (0.7-1.0) can be observed up to 20 kb. As haplotypes of CCL2bx, CCL13ab, CCL15omn and CCL3ba are defined by markers in strong LD with each other, further investigation of these haplotypes may reveal disease relevant mutations. The varying strength and discontinuous nature of LD observed at CCL11b-CCL8x and CCL8y-CCL13a may be related to the relatively low frequency of marker alleles

involved, and suggest that re-investigation of these subregions with alternative markers will be necessary.

Table 6. LD distribution and the MS associated haplotypes within 17q11.

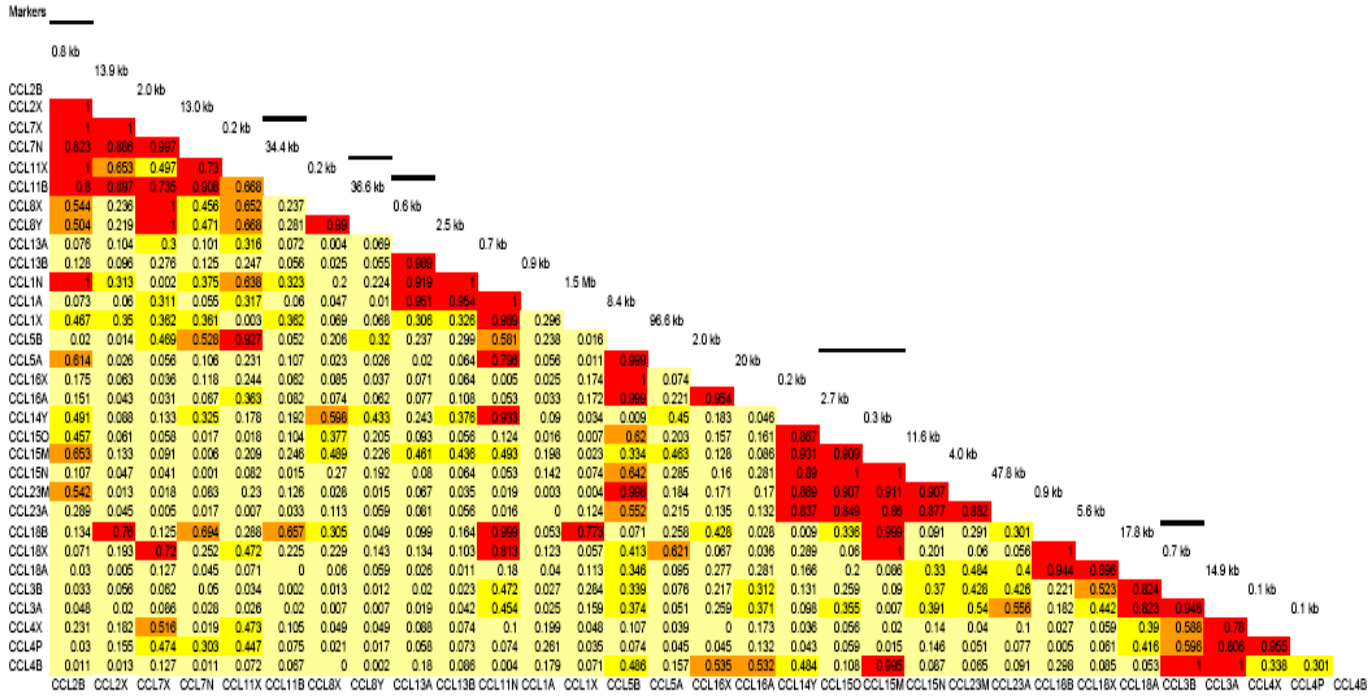

The distribution of inter-marker D' values. Red color designates D'>0.70; orange designates D'<0.70 and D'>0.50; dark yellow designates D'<0.50 and D'>0.30; light yellow designates D'<0.30. Inter-marker distances are indicated above the LD map. Horizontal bars above distance estimates indicate regions where associations with MS were detected by TRANSMIT.

Summary of findings

These analyses suggest that variants of CCL genes are associated with MS. Using methods of association in families, we confined the 10 cM susceptibility locus defined by linkage to haplotypes of 0.7-37 kb sizes in the CCL region. We note that candidate genes showing association with all MS phenotypes overlap with those detected in the RR/SP-subgroup. The inclusion of PP-MS in the combined analyses did not noticeably modify the outcome, and as a subgroup alone, did not have enough power to draw conclusions regarding differential associations. These observations merit follow up investigations.

2.3.2 Studies on 17q11: phase II – LD mapping (83)

Results from PDT and FBAT

The analyses reveal that markers with $p<0.05$ are located within CCL (one marker between CCL2 and CCL7, and others within CCL5, CCL15 and CCL18), and non-CCL genes (LOC440525, CCT6B, AP2B1, TAF15, FLJ32830, LOC57151). Three SNPs, SNP15 (no gene close by), 62 (between genes of CCL2 and CCL7) and 116 (telomeric to CCL1) have $p<0.05$ in both tests (Table 7). The SpD test estimates 219.8 effective independent loci when LD among the 232 markers is taken into consideration. With 219.8 independent loci, a $p<0.00023$ would be required to bring back the overall α level to 0.05, suggesting that none of the marker alleles have direct relevance to MS. SNP 62 has a PDT p-value of 0.0008 and a FBAT p-value of 0.000789, approaching but not reaching the required significance level by SpD.

Results from TRANSMIT and HBAT

Only observations with $p<0.01$ in TRANSMIT and $p<0.05$ in HBAT are listed for markers with a variance of 2.5 or greater in Table 8. The highlighted haplotypes with a simultaneous presence of $p<0.01$ in TRANSMIT and $p<0.05$ in HBAT are located between genes of CCL2 and CCL7, within the CCL15 promoter and coding regions, and the CCL3 coding region. Several of the preferentially transmitted marker haplotypes have low frequency, but still reaching a variance of 2.5 or higher in the TRANSMIT statistics. Possible associations with haplotypes are also detected within non-CCL genes including LOC124842, FLJ10458 and CMYA4. Although most of the haplotypes are defined by alleles of two SNPs, there are also three-marker haplotypes within LOC124842, FLJ10458, CMYA4 and CCL3. In addition, there is a four-marker haplotype within FLJ10458-CMYA4. All MS associated haplotypes include at least one minor allele of two or three SNPs.

Table 7. PDT and FBAT results

SNP#	NCBI rs#	Heterozygosity	PDT p-value	PDT Chi-sq	FBAT p-value	FBAT Var(S)	Chromosome position	Gene
15	**1844737**	**0.26**	**0.0334**	**4.527**	**0.040282**	**61.684**	**29132773**	**No gene close by**
31	929259	0.47	0.0717	3.245	0.044966	116.959	29489922	LOC440425
62	**8079244**	**0.01**	**0.0008**	**11.308**	**0.000789**	**3.750**	**29618681**	**Between CCL2 and CCL7**
113	732807	0.49	0.0307	4.669	0.123815	113.793	29835900	120 kb telomeric to CCL1
116	**961575**	**0.24**	**0.0207**	**5.348**	**0.008292**	**53.633**	**29885018**	**170 kb telomeric to CCL1**
117	758411	0.24	0.0803	3.059	0.047593	63.883	29901059	
132	2062101	0.47	0.0907	2.863	0.041968	103.826	30278969	CCT6B
190	226089	0.27	0.0044	8.112	0.067482	63.468	31041048	AP2B1
202	4251719	0.23	0.0280	4.831	0.056286	55.862	31166475	TAF15
204	3785764	0.20	0.0376	4.322	0.120609	48.112	31184877	TAF15
207	2306630	0.23	0.0423	4.123	0.074584	55.362	31206454	FLJ32830
216	8069014	0.30	0.0354	4.427	0.058246	72.271	31224111	CCL5
217	4796120	0.21	0.0437	4.068	0.106289	48.662	31225004	CCL5
218	9889874	0.23	0.0362	4.390	0.084068	54.612	31226410	CCL5
220	2280789	0.24	0.0213	5.301	0.050818	53.362	31231116	CCL5
227	2280784	0.38	0.0439	4.061	0.053041	87.534	31288659	LOC57151
248a	7208990	0.15	0.1208	2.407	0.025802	37.954	31353588	CCL15 promoter
265	854472	0.38	0.0330	4.547	0.059189	81.978	31421721	CCL18
296	757121	0.42	0.1876	1.736	0.043557	108.380	31479495	

Table 7 includes the study designation, NCBI rs# and heterozygosity of SNPs, PDT p-value and chi-square value, FBAT p-value and variance, the position of markers on 17q11 (http://www.ncbi.nlm.nih.gov/SNP) and the co-localizing genes. Only those markers are listed which have $p<0.05$ at least in one of the two tests. Highlighted markers have $p<0.05$ in both PDT and FBAT.

Table 8. Results of TRANSMIT and HBAT

SNP#	Haplotype	Haplotype frequency	Transmit p-value	Var(O-E)	HBAT p-value	Var(S)	Ldmax D'	Gene
62-63	**C-T**	**0.01**	**0.0013**	**3.7087**	**0.001341**	**3.500**	**1**	**Between CCL2 and CCL7**
109-110	**C-C**	**0.01**	**0.0012**	**4.2442**	**0.000509**	**4.002**	**0.943**	**No known gene**
116-117	G-G	0.85	0.1457	65.594	0.009418	55.442	1	No known gene
116-117	C-A	0.15	0.1329	65.324	0.007593	55.192	1	No known gene
120-121-122	A-C-G	0.01	0	3.4717	-	-	0.154-0.938	FLJ44815-LOC124842
121-122	**C-G**	**0.02**	**0.0025**	**7.6896**	**0.006632**	**7.612**	**0.938**	**LOC124842**
121-122-124	**C-G-G**	**0.01**	**0.0041**	**6.7575**	**0.009041**	**6.689**	**0.938-0.337**	**LOC124842**
152-153	G-A	0.43	0.0026	118.35	0.078006	110.841	1	DKFZp434H2215
157-158-159-160	**C-C-C-G**	**0.02**	**0.006**	**6.6689**	**0.022601**	**6.486**	**1-0.937-0.858**	**FLJ10458-CMYA4**
157-158-159-160	C-C-T-G	0.04	0.0246	17.626	0.019746	16.056	1-0.937-0.858	FLJ10458-CMYA4
158-159-160	**C-C-G**	**0.02**	**0.0067**	**7.9276**	**0.021835**	**7.732**	**0.937-0.858**	**FLJ10458-CMYA4**
159-160	**C-G**	**0.02**	**0.0074**	**7.9383**	**0.020968**	**7.733**	**0.858**	**CMYA4**
159-160-161	**C-G-A**	**0.02**	**0.0069**	**7.937**	**0.030368**	**7.478**	**0.858-1**	**CMYA4**
236-238	C-C	0.78	0	85.873	0.644172	81.383	0.99	CCL15
236-238	T-T	0.21	0	84.36	0.527147	80.300	0.99	CCL15
246-247	T-A	0.06	0	31.697	0.733445	21.165	1	Promoter CCL15 -696, -777
246-247	A-T	0.94	0	32.966	0.733450	21.165	1	Promoter CCL15 -696, -777
248-248a	A-C	0.92	0.0197	44.246	0.009926	35.517	0.932	Promoter CCL15 -880, -944
248-248a	**A-G**	**0.02**	**0**	**12.428**	**0**	**10.992**	**0.932**	**Promoter CCL15 -880, -944**
248a-249	C-A	0.90	0.0958	48.905	0.046699	42.354	0.812	Promoter CCL15 -944, -1004
248a-249	**G-A**	**0.02**	**0**	**10.397**	**0.000003**	**8.974**	**0.812**	**Promoter CCL15 -944, -1004**
248a-249-250	**G-A-T**	**0.02**	**0**	**10.151**	**0.000001**	**8.742**	**0.812-0.986**	**Promoter CCL15 -944,-1004, -1034**
264-265	T-C	0.29	0.0094	106.19	0.108009	76.783	0.996	CCL18
264-265	C-T	0.70	0.0086	108.84	0.140478	78.783	0.996	CCL18
273-277-278	**C-T-A**	**0.02**	**0.0023**	**4.5398**	**0.007638**	**4.248**	**0.982-0.986**	**CCL3**
277-278	**T-A**	**0.02**	**0.0001**	**5.5614**	**0.004554**	**5.250**	**0.986**	**CCL3**

Table 8 indicates SNP marker haplotypes, marker alleles, frequency of haplotypes, TRANSMIT and HBAT p-values and variance values, D' value from ldmax and the co-localizing genes. Where SNPs fall into promoter regions, the positions of markers relative to the genes are indicated in the last column. Applying Bonferroni correction based on 693 independent tests of two-marker haplotypes, a p-value of 0.00007215 would be required to bring back the overall α level to 0.05. The A-G haplotype of SNP 248-248a and the G-A haplotype of SNPs 248a-249 within the CCL15 gene promoter remain significant after this correction.

LD assessment

Table 9a-c demonstrates the distribution of pair wise D' values from ldmax. These analyses reveal extensive LD within the 1.85 MB region studied with high resolution SNP coverage. Where LD drops at one or two markers within continuous regions of extended LD, these interruptions are uniformly associated with low marker heterozygosity. If markers with <0.10 heterozygosity are removed, there appear to be three continuous chromosomal blocks between markers 33-107c (190 kb), 179-221 (366 kb) and 232b-295 (121 kb). The MS-associated haplotypes (indicated by horizontal bars above the columns in Table 9a-c) fall in regions characterized by extensive LD. The haplotype between CCL2 and CCL7 encompasses 95 bp, while the sizes of haplotypes within CCL15 and CCL3 are 154 bp and 1,200 bp, respectively.

Legend to Table 9.

This table indicates pair-wise LD estimates of D' values in ldmax (GOLD). Markers with <0.01 heterozygosity were excluded. The investigated region is broken into three parts (a-c) for the purpose of presentation. The X and Y axis indicate the numerical codes of SNPs. D' estimates between paired markers are indicated in a color-coded manner. D'</=0.30: light yellow, 0.30<D'</=0.50: dark yellow, 0.50<D'</=0.70: brown, 0.70<D'</=0.95: red and 0.95<D'</=1: black. Horizontal bars below the LD distribution indicate the position of genes that have MS associated haplotypes (light blue promoter, dark blue coding segment). In Table 10a: CCL2, CCL7, CCL11, CCL8, CCL13; in Table 10b: CCL1, LOC124842, FLJ10458, CMYA4; in Table 10c: CCL5, CCL16, CCL14, CCL15, CCL23, CCL18, CCL3, CCL4. Horizontal bars above the LD table indicate MS associated haplotypes.

Table 9a-c. Pair-wise LD distribution in the 1.85 MB CCL region of 17q11

Table 9a. Pair-wise LD among markers #1-100.

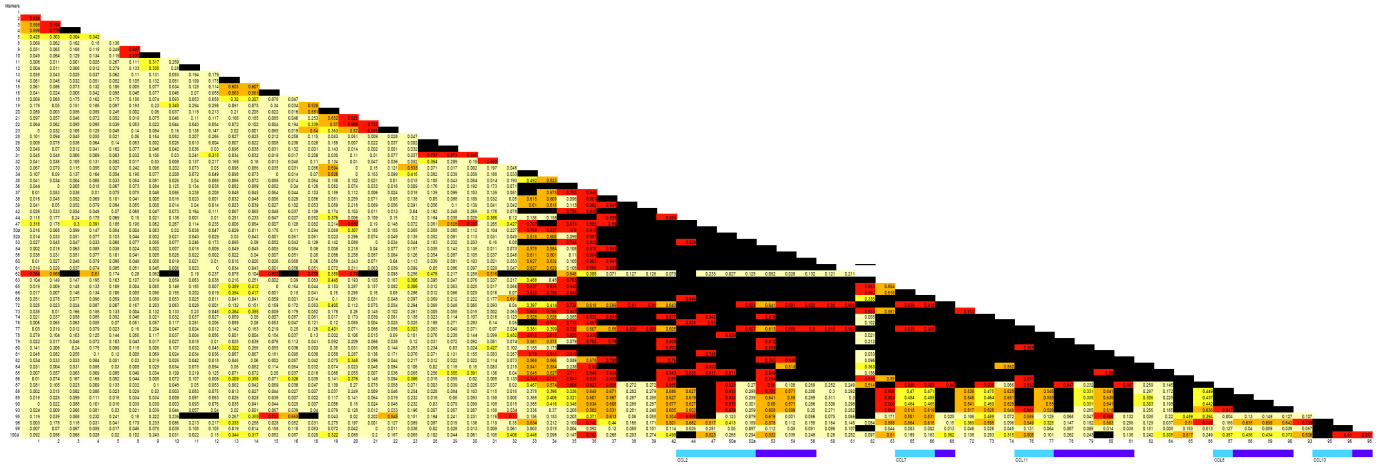

Table 9b. Pair-wise LD among markers #101-200.

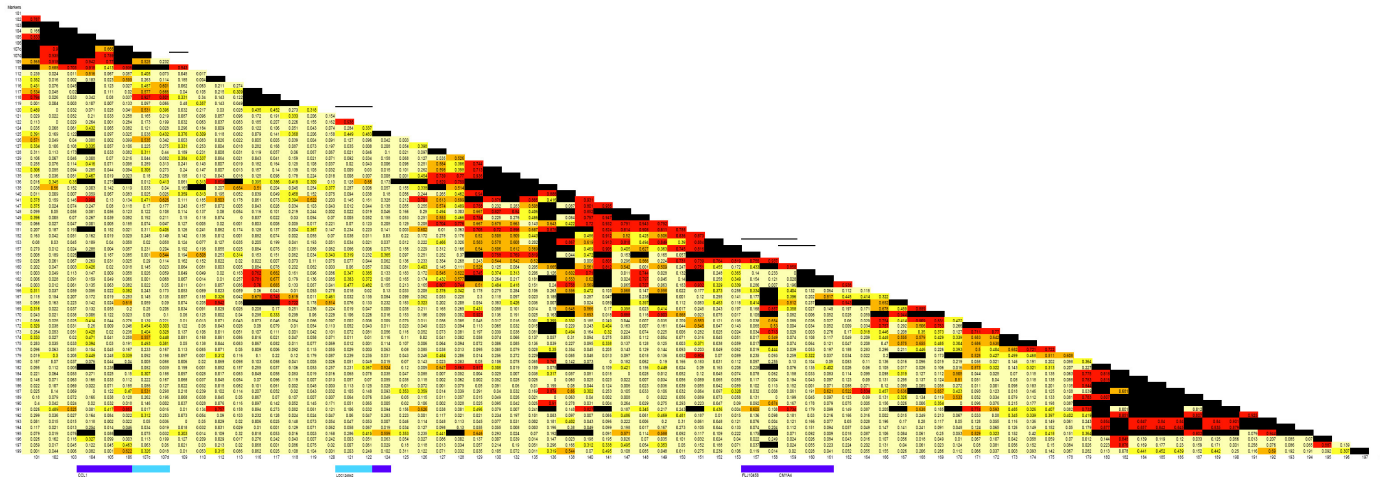

Table 9c. Pair-wise LD among markers #201-300.

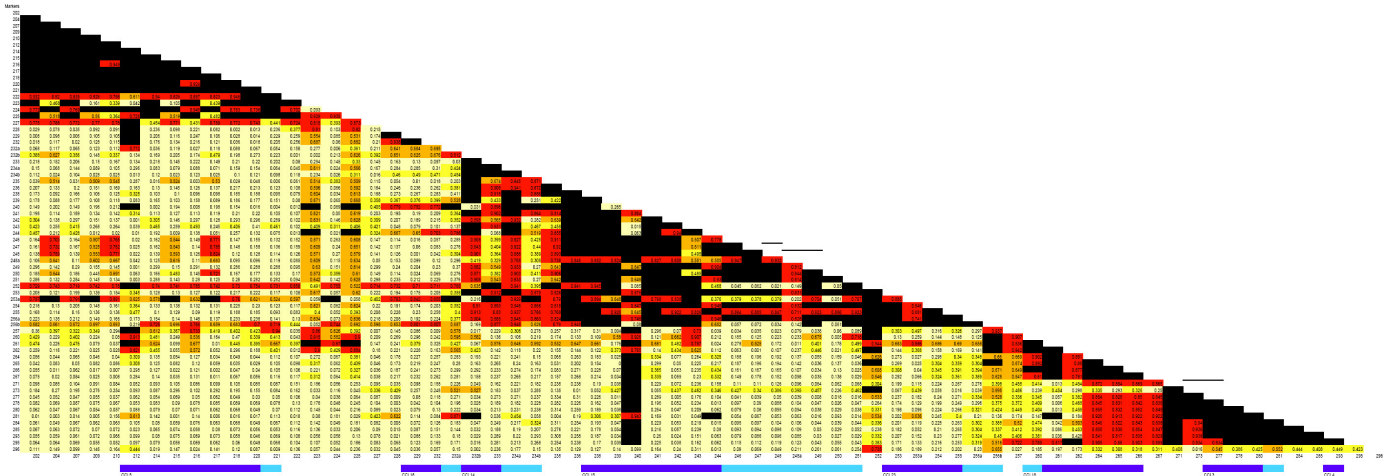

Summary of findings

This second, high resolution SNP scan in 17q11 confirms that MS associated haplotypes are located between CCL2 and CCL7 in the centromeric region, and within the CCL15 and CCL3 genes in the telomeric cluster. The second study corroborated the previously suggested associations of MS with haplotypes in genes of CCL15 and CCL3 (telomeric cluster), identified a new haplotype between CCL2 and CCL7 close to the previously detected ones (centromeric cluster), and revealed relatively large LD blocks in the 17q11 region. Overlapping finding from the phase I and phase II studies are summarized in Figure 5.

Figure 5. Overlapping findings in CCL study I and II

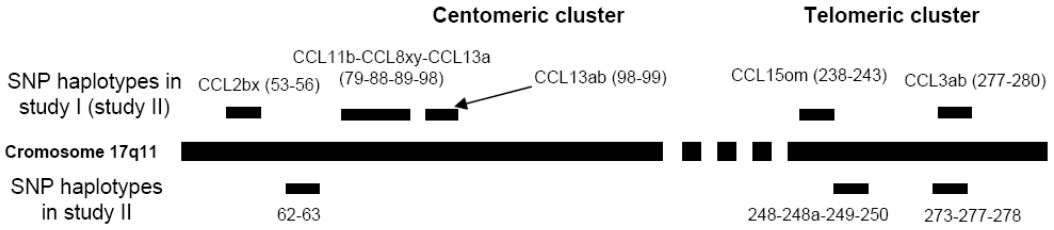

Figure 5 indicates the relative position of MS associated SNP haplotypes in Study I (upper part of figure; numbering of markers differed in the 2 studies, therefore corresponding numbering of markers in study II is indicated in parenthesis) and Study II (lower part). Markers in the overlapping haplotypes of CCL15 and CCL3 (Telomeric cluster) were identical in the two studies.

2.3.3 Studies on 17q11: Phase III – Sequence analyses (84)

Sequence analyses and genotyping

The findings in Phase I and II CCL study raised the question if disease relevant variants are located within or in the proximity of the MS-associated haplotypes. For sequencing, we selected the best defined MS-associated haplotype encompassing CCL3 (SNPs 273-277-278) which segregated in 25 of the 361 families in the CCL study II (83) and was also found in association with MS in study I (82). In search for new mutations within or in the proximity of this haplotype, we sequenced 3,500 bps of the extended haplotype in all 25 positive individuals from Study II.

Sequencing revealed no new mutations, but 16 SNPs and 1 insertion / deletion variant within this haplotype (Figure 6). Genotyping these “new” variants in DS116-132 (families in study II) identified haplotypes in association with MS which overlap with the haplotype of SNP278-277-273 found in Study I and II. The strongest and most consistent association was the T-A allelic

combination of haplotype 277-278, suggesting that an interaction between these alleles may play a role in MS (83).

Figure 6. The sequenced haplotype of SNPs 273-277-278 within CCL3

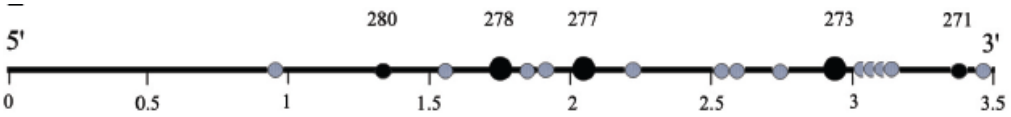

Large black dots: SNPs defining the MS-associated haplotype in Study I-II. Small grey dots: new SNPs revealed by sequencing.

Summary of findings

Sequence analyses of the CCL3 encompassing haplotype SNPs 277-278-280 (that was found in association with MS in two independent LD mapping studies) along with its flanking regions reveal no pathogenic mutation. Testing of all variants revealed in this region confirms that it is the T-A allelic combination of haplotype 277-278 that has the strongest association and likely contributes to MS.

2.3.4 Expression of CCL molecules in MS brains (62)

Regional mRNA expression of β-chemokines in MS brains

We present here intra-individual comparisons of mRNA levels in MS brain regions to avoid confounding effects of variations in age, post-mortem time and tissue handling in a potential inter-group comparison. Testing the β-actin-normalized mRNA copy numbers of CCL2, CCL3, CCL5, CCL7, CCL8, CCL13 and CCL15 molecules in NAWM, NAGM and plaque regions reveals a significant increase in the messages of CCL2 in plaques as compared to NAWM (p=0.022), and of CCL7 both in NAWM and plaque as compared to NAGM (p=0.047) (Table 10). In contrast, mRNA for CCL8 appears to be decreased in chronic active plaques as compared to corresponding NAWM and NAGM regions (p=0.047).

No differences are observed when we compare the normalized CCL values in WM and GM specimens of normal controls, and of the AC or EC groups alone. However, normalized values of CCL7, CCL8 and CCL13 are slightly higher in the WM as compared to the GM in the combined AC+EC (OND) group (p=0.043, 0.047, 0.043, respectively).

Summary of findings

This corollary study reveals a differential regional mRNA expression for CCL2, CCL7 and CCL8 in the brains of MS patients. Although the distribution of β-chemokines is likely to vary from the early to late stages of a plaque evolution, the above observation indicates that the expression of these three CCL

molecules correlates with the distribution of pathology, at least in chronic stages of inflammation, demyelination and neurodegeneration.

Table 10. Distribution of normalized values of β-chemokine ligands in MS brains.

	CCL2		CCL3		CCL5		CCL7		CCL8		CCL13		CCL15	
MS	Mean	SD	Mean	SD	Mean	SD	Mean **	SD	Mean	SD	Mean	SD	Mean	SD
NAWM	0.0103	0.0127	0.2069	0.1792	0.0186	0.0282	**0.0602**	0.0690	0.0732	0.0414	0.0664	0.0605	0.0551	0.0495
NAGM	0.0372 *	0.0758	0.1640	0.2732	0.0456	0.0894	0.0290 ***	0.0408	0.0667 *****	0.0746	0.0339	0.0558	0.0243	0.0403
Plaque	**0.0555**	0.1151	0.1734	0.1700	0.0180	0.0271	**0.0643**	0.0838	**0.0392**	0.0340	0.0668	0.0689	0.0507	0.0536
AC														
WM	0.0149	0.0119	0.3168	0.1690	0.1370	0.0916	0.0606	0.0363	0.0164	0.0098	0.0680	0.0375	0.0535	0.0320
GM	0.0211	0.0207	0.2665	0.3198	0.4214	0.4266	0.0092	0.0067	0.0014	0.0010	0.0146	0.0168	0.0068	0.0055
EC														
WM	0.0260	0.0355	0.2533	0.0948	0.0710	0.0598	0.1328	0.1067	0.0568	0.0585	0.1511	0.1339	0.1033	0.0826
GM	0.0275	0.0387	1.4274	1.5858	0.3643	0.0646	0.0898	0.0657	0.0139	0.0115	0.0971	0.0678	0.0713	0.0368
OND							****		****		****			
WM	0.0193	0.0205	0.2914	0.1332	0.1106	0.0800	**0.0896**	0.0712	**0.0326**	0.0373	**0.101**	0.0851	0.0734	0.0544
GM	0.0236	0.0245	0.7308	1.0412	0.3986	0.3050	0.0414	0.0553	0.0064	0.0090	0.0476	0.0578	0.0326	0.0400
NC														
WM	0.0152	0.0144	0.1444	0.0558	0.0186	0.0077	0.0230	0.0166	0.7649	1.3035	0.0231	0.0142	0.0225	0.0126
GM	0.0170	0.0211	0.0910	0.0437	0.0261	0.0085	0.0051	0.0018	0.3028	0.4517	0.0101	0.0040	0.0082	0.0049

* p= 0.022 Plaque vs. NAWM
** p=0.047 NAWM vs. NAGM
***p=0.047 Plaque vs. NAGM
**** p= 0.043 WM vs. GM
*****p=0.047 Plaque vs. NAGM and NAWM

This table summarizes the copy numbers of CCL mRNA molecules normalized with those of corresponding β-actin values as determined by real-time PCR in NAWM, NAGM and plaque regions of 10 MS patients. Similar measurements in WM and GM regions of 3 controls with Alzheimer's disease (AC), of 2 controls with encephalitis (EC), of 5 combined AC+EC controls (OND) and of 3 normal controls (NC) are shown. The Wilcoxon Signed Rank Test was used to compare the normalized mRNA values in corresponding brain regions.

2.4 DISCUSSION: THE ROLE OF CCL MOLECULES IN MS

The involvement of CCL molecules in inflammatory demyelination is well established by comprehensive experimental data in the EAE model. The available MS data are less comprehensive or congruent, and are mostly derived from descriptive studies of selected CC chemokine ligands (62). Our genetic studies identify haplotypes in specific CCL coding regions in MS and reveal the architectural complexity of 17q11. The mRNA expression studies provide further support to the involvement of these gene products in lesion development. Here we integrate our observations into existing CCL data of inflammatory demyelination, and further develop the concept concerning the role of CCL molecules in the pathogenesis of MS.

2.4.1 Association studies identify haplotypes in the CCL genes within 17q11

Linkage studies successfully defined several susceptibility loci in MS. However, these loci still encompass 2-20 cM chromosomal segments. To further refine the genetic data, we chose using methods of association that assisted identifying a significant number of candidate genes within linkage defined susceptibility loci of complex disorders (106). We genotyped and analyzed SNPs within candidate genes located in chromosome 17q11, a previously defined susceptibility locus of MS (73). In the phase I study, the selected 31 markers encompassed the coding regions of CCL genes in a 1.85 MB chromosomal segment (Figure 3), leaving two gaps between CCL1 and CCL5 (1.5 MB) and CCL5 and CCL16 (97 kb). Within CCL genes, the inter-marker distances extended from a few hundred to a few thousand base pairs. Although none of the marker alleles showed direct association with MS after adjusting for multiple comparisons, transmission distortion indicated association with several SNP haplotypes in genes of CCL2, CCL3 and CCL11 – CCL8 – CCL13 (Table 4-6). Because of the low number of transmissions, the indicated association for a haplotype within the CCL15 region remained tentative. Overall, the first phase of studies confined the regions of interest to 0.7 – 37 kb chromosomal segments and identified specific CCL gene regions involved in defining susceptibility to MS. The D' values (Table 6) indicated that LD extends at least up to 20 kb between paired markers in this region. This distribution of LD assisted the design of a next SNP scan to confirm and refine the MS relevant chromosomal segments.

The second phase of studies increased the number of markers from 31 to 232, encompassing now not only the CCL but also other genes with less than 8 kb average pacing in the 1.85 MB segment of 17q11. Out of the successfully validated 261 SNP markers, we used 232 SNPs in the analyses after excluding 18 monomorphic SNPs and 11 markers with HWE violation. In the data analyses, we decided to complement PDT with FBAT and TRANSMIT with HBAT in order to increase the stringency of

observations. FBAT and HBAT can also assist eliminating spurious outcomes related to population stratifications. Finally, we implemented the method of SpD for correction for multiple comparisons.

PDT and FBAT did not identify any markers with significant p-values after correction for multiple comparisons. SNP 62, between genes of CCL2 and CCL7, approached most but did not reach the significance level required by SpD. However, combined data from TRANSMIT and HBAT revealed consistent observations within several CCL genes.

In the phase I scan, markers 53-56 (as designated in the present study and corresponding to CCL2bx in the phase I study), 79-88-89-98 (CCL11b-CCL8xy-CCL13a), 98-99 (CCL13ab), 238-243 (CCL15om) and 277-280 (CCL3ba) showed association with MS. These haplotypes are within the CCL2, CCL11-CCL8-CCL13 and CCL13 genes. In the phase II scan, we detected a 95 bp MS-associated haplotype of SNPs 62 and 63 located between CCL2 and CCL7. SNP 62 lies 10 kb telomeric to the CCL2 gene, and SNP 63 is 2.6 kb centromeric to the CCL7 gene. Flanking regions of haplotype 62-63 in both directions are characterized by extensive and strong LD encompassing 190 kb (Table 9a). Although LD appears to be moderate between some SNPs in the continuous stretch of high D' values (Table 9a), this virtual drop results from the low heterozygosity of those markers. The finding of haplotype 62-63 between CCL2 and CCL7 does not challenge the previous data, rather refines the primary location of a MS associated haplotype in the centromeric cluster where several functionally relevant genes are encoded (CCL2, CCL7, CCL11, CCL8, and CCL13, see Figure 3) (62,82-83).

The more telomeric CCL cluster includes CCL5, CCL16, CCL14, CCL15, CCL23, CCL18, CCL3 and CCL4 (Figure 3). One of the MS associated haplotypes within the CCL3 gene is defined by identical markers in both study I and II (Tables 5 and 8, Figure 5). The markers defining the MS associated haplotypes within the CCL15 gene also greatly overlap in Study I and II (Figure 5). Study II confirms the data for CCL15 in Study I, in which we had some uncertainties due to the low variance in the TRANSMIT analysis. This problem did not occur in Study II and two SNP haplotypes in CCL15 showed association with MS even after correction for multiple testings (Table 8). Although the MS associated haplotypes are within a region with extensive LD (121 kb) (Table 9c), the haplotypes encompassing CCL3 and CCL15 were consistently found in two independent studies and their sizes are small (1,200 bp and 154 bp in CCL3 and CCL15, respectively). While sequence analyses of the haplotype encompassing CCL3 did not reveal new mutations, additional genotyping confirmed that the strongest and most consistent

association was the T-A allelic combination of haplotype 277-278, suggesting that an interaction between these alleles may play a role in MS (84).

Our analyses also reveal that both the centromeric and the telomeric clusters of CCL genes are located within chromosomal blocks with strong and extensive LD (Table 9a and c) in consensus with data by others (107-109). A whole-genome SNP scan in three human populations shows that the largest “bin” with the most SNPs in European-Americans is located within chromosome 17. This chromosomal block has an unusual pattern of variation with two haplotypes extending across 518 SNPs in an 800 kb distance (107-109). These regions with extensive LD are characterized by low recombination, a structure likely reflecting functional significance. Because of the architectural complexity including segmental duplications, long-range rearrangements (109-110) and extensive LD, further refinements of candidate genes and variants may require next generation sequencing within chromosome 17.

Years after the completion of our 17q11 studies, platforms for genome-wide association studies (GWAS) and copy number variation (CNP) studies became available. GWAS confirm the established association of MS with the HLA DR locus ($p=8.94x10^{-81}$) (111) and identify non-HLA determinants with very small effects. The list of non-HLA susceptibility candidates is still incomplete and thus far includes variants in genes of IL2Rα, IL7Rα, CD58, IRF8, TNFRSF1A and KIF1B (111-116). GWAS only revealed a moderate score in the 17q11 region (111). This finding is, however, not incompatible with ours, considering the small effects of non-HLA genes, the different populations studied and heterogeneity of MS. CNV studies are still in progress and the data are preliminary(reviewed in 117).

In summary, our multi-stage CCL genetic studies demonstrate the associations of MS with haplotypes within genes of CCL15 and CCL3, and possibly between CCL2 and CCL7. These analyses also show large LD blocks with possible functional relevance in the 17q11 region. Due to this LD distribution and the architectural complexity of chromosome 17, further identification of the MS associated variants may require next generation sequencing of this chromosome or its subregions.

2.4.2 Expression and function of the identified gene products in MS

The above genetic data suggesting MS susceptibility variants within or close to genes of CCL2, CCL7 and CCL3 are in consensus with expression and functional studies. CCL3 (MIP-1α) is involved in the recruitment of MNCs into the CNS and in the pathogenesis of both MS and EAE. Blockade of CCL3 prevents the development of acute and relapsing forms of EAE, and the immigration of MNCs into the

CNS (118). The increase of CCL3 and CCL5 in the CSF during a relapse correlates with the increased expression of their main receptors, CCR1 and CCR5 on TH1 lymphocytes in blood and CSF (119-121). Monocytes entering to the CNS are derived from a minor pool of CCR1+ / CCR5+ MNCs in the peripheral circulation. Both CCR1+/CCR5+ monocytes and CCR1-/ CCR5- microglial cells evolve into a CCR1-/CCR5+ phenotype from early to late stages of the histological type II but not of type III lesions (19,118). Based on our genetic data, CCL3 variants may differentially regulate the development of various histological lesion types.

A review of data in blood, CSF and CNS of MS patients and the results of descriptive, transgenic, knockout and neutralizing antibody studies in EAE establish that CCL2 (MCP-1) and CCR2 also play key roles in the development of inflammatory lesions in the CNS (62,89,122-130). CCL2 is a chemoattractant for CCR2+ monocytes and microglia as well as memory T, dendritic and natural killer cells. The expression of CCL2 can be induced in various cell types, and has been predominantly detected in residential immune cells of the CNS (89). CCR2+ immune cells of hematogenous origin follow the crescendo CCL2 gradient from the peripheral circulation to the CNS. A CCL2 - TH2 co-regulation is well established. CCL2 induces polarization of regulatory TH2 cells and vice versa, CCL2 expression is controlled by TH2 cytokines such as IL4. CCR2+ T cells express predominantly TH2 phenotype and are present with higher frequency in the blood of patients with SP-MS (130). The consistently observed low CSF levels of CCL2 during relapses (119,121,128-130) correlate with a decreased TH2 lymphocyte activity. Clinical improvement and normalization of the TH1 - TH2 balance after corticosteroid treatment also correlate with the normalization of CCL2 in the CSF.

In the MS brain, CCL2 (MCP-1), CCL8 (MCP-2) and CCL7 (MCP-3) are expressed in high amounts in the lesion centers, but sharply decrease at the edges of acute and chronic active plaques (131). There is an inverse correlation between the age of plaques and the expression of these proteins, with only a scanty appearance of immunoreactive astrocytes in silent lesions. CCL3 and CCL4 are predominantly detected in macrophages/microglia, CCL3 is also present in astrocytes (132-134) and CCL5 in perivascular MNCs and astrocytes (133-135).

We assessed the mRNA expression levels for CCL2, CCL3, CCL5, CCL7, CCL8, CCL13 and CCL15 relative to β-actin in corresponding NAWM, NAGM and chronic active plaque containing specimens characterized by haematoxylin & eosin, Luxol Fast Blue and immune staining for CD68 and β_2-microglobulin (62,136). The selection of these CC chemokines was based on two considerations. First, we detected MS associated SNP haplotypes in the genes of CCL2, CCL2-CCL7, CCL11-CCL8-CCL13,

CCL15 and CCL3 (82-83, sections 2.3.1, 2.3.2). Second, immunohistochemical studies suggested the involvement of CCL2, CCL7, CCL8, CCL5 and CCL3 in plaque development (131,137). While neither our genetic nor our mRNA studies revealed positive findings for CCL5, the three MCP chemokines CCL2 (MCP-1), CCL7 (MCP-3) and CCL8 (MCP-2) showed altered regional expressions in chronic active plaques. We detected an increased expression of CCL2 in plaques as compared to NAWMs, and an increased expression of CCL7 in both plaques and NAWMs as compared to NAGMs. This analysis of CCL mRNA molecules in various regions of MS brains complements the data from previous immunohistochemical studies, and further confirms the involvement of CCL2 and CCL7 (and possibly of CCL8) in the development of pathology. In consensus with others, however, we also note an increased CCL7, CCL8 and CCL13 expression in the white matter as compared to the gray matter in 5 other neurological disease controls (1 viral and 1 post-infectious encephalitis, 3 Alzheimer disease) (137). No differences were observed for any of these molecules in the white and gray matters of normal controls. We postulate that the expression of CCL molecules may be detected in various inflammatory conditions of the CNS, however, the temporal and cell specific upregulation of certain CCL and CCR molecules is pathology dependent. Therefore, further exploration of the expression kinetics of these molecules may facilitate a better understanding of MS pathogenesis.

In summary, experimental evidence from several studies using different methods now in consensus suggests that mRNA and protein products of CCL2, CCL3, CCL4, CCL5, CCL7 and CCL8 can be detected in higher amounts in lesions of MS and EAE, but in a lesion age - dependent manner (acute, chronic active or chronic silent) (131,134,137,138). Our genetic and mRNA expression studies further support the role of CCL2, CCL7, CCL8 and CCL3 in MS, and refines previous observations regarding the distribution of CCL expression in chronic active plaques, NAWM and NAGM.

2.4.3 Overall importance of CCLs as inflammatory mediators in MS

Data from our genetic studies underscore the importance of variants within or close to genes of CCL2-CCL7, CCL15 and CCL3 in conferring susceptibility to MS. The corollary gene expression studies in consensus with existing observations from EAE and MS establish that CC chemokine ligands (most prominently CCL2, CCL7, CCL8 – in our and other studies, but also CCL1, CCL3, CCL4, CCL5, CCL19 and CCL21) expressed by residential immune cells in the CNS or by endothelial cells at the BBB are major chemoattractants for hematogenic immune cells (primarily monocytes / macrophages [CCL2, CCL7, CCL8, CCL22] dendritic cells [CCL19, CCL20, CCL21, CCL22] and T lymphocytes [CCL1, CCL2, CCL3, CCL4, CCL5, CCL19, CCL21, CCL22]) via interactions with their G-protein-coupled receptors (CCR1-CCR10). These CCL - CCR interactions play a key role in the recruitment, activation

and retention of immune competent cells in the CNS, with the CCL1 – CCR8, CCL2 – CCR2, CCL3 – CCR1 / CCR5, CCL5 – CCR1 / CCR5, CCL7 – CCR1 / CCR2 / CCR3, CCL8 – CCR3, CCL20 – CCR6, CCL19 / CCL21 - CCR7, CCL22 – CCR4 interactions being the best characterized among them (Figure 7). The EAE model suggests that CCL19 and CCL21 produced by endothelial cells induce G-protein-mediated signaling via their receptor CCR7. This signaling leads to an enhanced adhesion of the leukocyte α4-integrin (VLA-4) to the endothelial VCAM-1 and results in a facilitated transmigration of leukocytes via the BBB. CCL-CCR interactions also define the differentiation and chemotaxis of T cell subpopulations, and thus may control the dynamic changes in the local balance of TH1 (CCL3 - CCR1 / CCR5, CCL5 – CCR1 / CCR5) and TH2 (CCL1 – CCR8, CCL2 – CCR2, CCL22 – CCR4) cell populations in lesion. Different CCL – CCR expression kinetics may characterize the different (initial, height, self-limiting) phases and histological subtypes (type II or type III) of inflammatory demyelination. This differential involvement of chemokines and their receptors in various stages and forms of MS, and the arising information concerning relevance of CCL variants in the disease suggest that small CCR antagonists represent a useful strategy in controlling inflammatory activity and may be considered in the personalized treatment of MS patients (62).

Figure 7. Interaction between CCL and CCR molecules at the blood-brain barrier

Legend to Figure 7: This figure depicts CCL-CCR interactions at the BBB (endothelial cells and astrocytic processes) interfacing a venule and the CNS. CCL molecules (most prominently CCL2, CCL3, CCL7 and CCL8, but also CCL1, CCL4, CCL19 and CCL21) are produced by residential microglia, astrocytes and endothelial cells throughout the course of lesion development, and by infiltrating MNCs (CCL5) during late phases of plaque formation, and attract functionally different subsets of monocytes / macrophages, dendritic cells and T lymphocytes from the circulation via the BBB into the CNS. The temporal and spatial regulation of molecular events, the association of distinct CCR molecules with different histological subtypes of demyelination and the involvement of different CCL-CCR interactions in T cell polarization are detailed in the text. Here we illustrate in a simplified and cross-sectional manner the main groups of interacting receptors on various hematogenous cells and ligands released by residential immune cells of the CNS or by components of the BBB.

Group A of receptors expressed by and ligands acting on monocytes / macrophages, respectively: CCR1 / CCR2 / CCR3-CCL7, CCR2-CCL2, CCR3-CCL8, CCR4-CCL22;

Group B of receptors expressed by and ligands acting on dendritic cells, respectively:
CCR4-CCL22, CCR6-CCL20, CCR7-CCL19 / CCL21;

Group C of receptors expressed by and ligands acting on T lymphocyes, respectively:
CCR1-CCL3 / CCL5, CCR2-CCL2, CCR4-CCL22, CCR5-CCL3 / CCL4 / CCL5, CCR7-CCL19 / CCL21, CCR8-CCL1.

Figure 7.

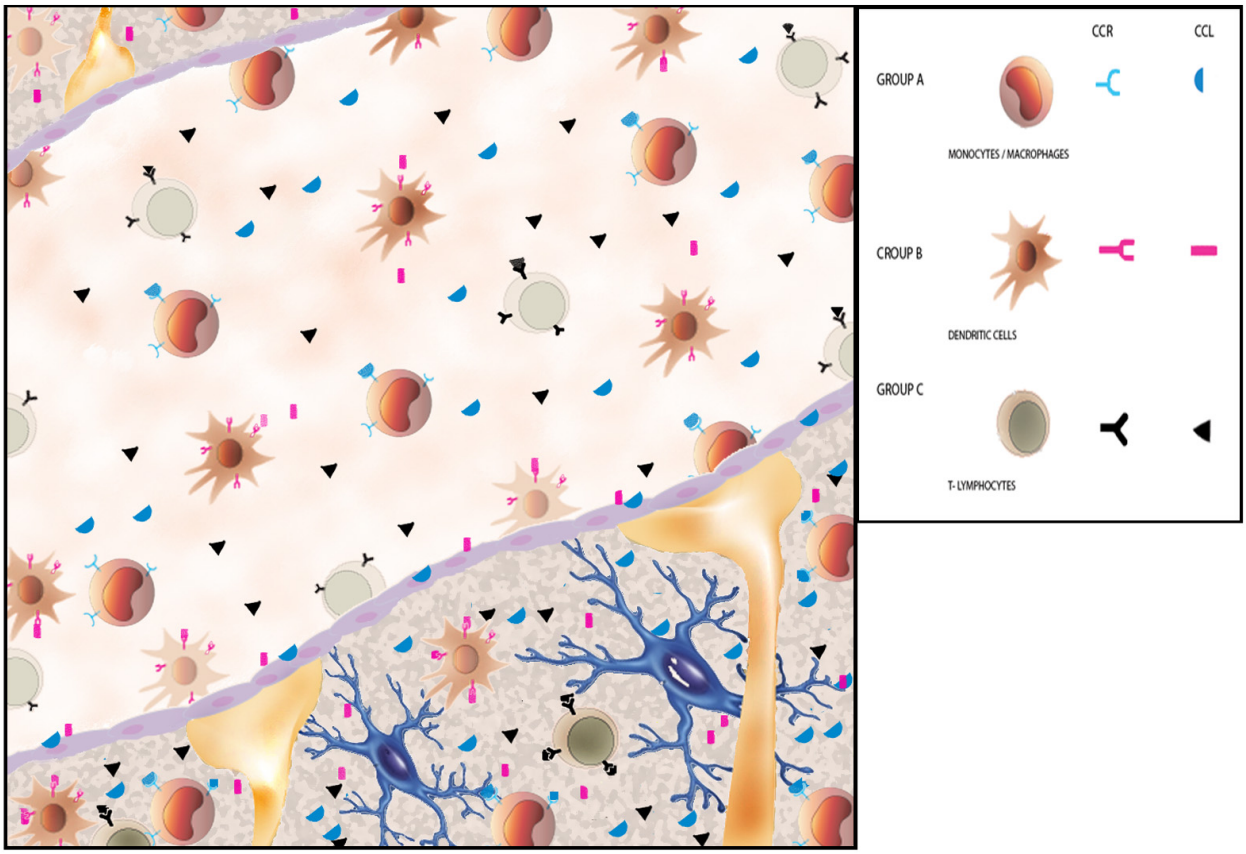
CCR
CCL
GROUP A
MONOCYTES / MACROPHAGES
CROUP B
DENDRITIC CELLS
GROUP C
T- LYMPHOCYTES

3. MITOCHONDRIAL GENETICS AND MECHANISMS OF NEURODEGENERATION IN MS

(16,17,20,21,81,105,136,139-149,228,261).

3.1 BACKGROUND

The involvement of mitochondrial molecules and mechanisms in the pathogenesis of MS are discussed here in three parts. The first section investigates if mitochondrial (mt)DNA mutations, polymorphisms and haplotypes confer susceptibility to MS, prominent optic neuritis (PON) or neuromyelitis optica (NMO). The second section extends the investigation of mtDNA encoded genes to nuclear (n)DNA encoded genes of Complex I. The third section addresses if inflammation affects mitochondrial macromolecules and alters the activity of Complex I, a potential mechanism contributing to neurodegeneration in MS.

3.1.1 Involvement of mtDNA in MS, PON and NMO

3.1.1.1 Mitochondrial genetics and inflammatory demyelination

An extranuclear part of the genome is mtDNA, which is maternally inherited. This 16.5 kb double-stranded circular molecule has been sequenced in its entirety (150) and encodes 22 transfer (t)RNA molecules, 13 protein subunits and 2 ribosomal (r)RNA molecules (Figure 8).

The higher mother to child as compared to father to child transmission of MS in families with parent-child concordance suggests the involvement of a maternally inherited genetic factor (10). The observed association of inflammatory demyelination with Leber's Hereditary Optic Neuropathy (LHON), a disease caused by mtDNA point mutations, also supports the mitochondrial hypothesis of MS (151-154). mtDNA point mutations with pathogenic significance for blindness were detected in a number of MS patients (138-142), while inflammatory demyelination was also noted in LHON patients (151-161).

Deleterious mtDNA point mutations cause early onset neurodegenerative diseases, many of them associated with myelin impairment (143). Mildly deleterious mtDNA point mutations are detected in patients with late onset neurodegenerative disorders including Alzheimer's and Parkinson's diseases (162). In addition to the involvement of mtDNA in neurodegeneration, its potential contribution to immune response was proposed when a maternally transmitted minor histocompatibility antigen was identified in mice (163). This molecule is presented on the cell surface and recognized by cytotoxic T lymphocytes. Antibodies specific for mitochondrial proteins were detected in a subgroup of patients with encephalomyopathies related to a point mutation in the $tRNA^{Leu}$ mtDNA gene (164-165).

Figure 8. Mitochondrial DNA and OXPHOS

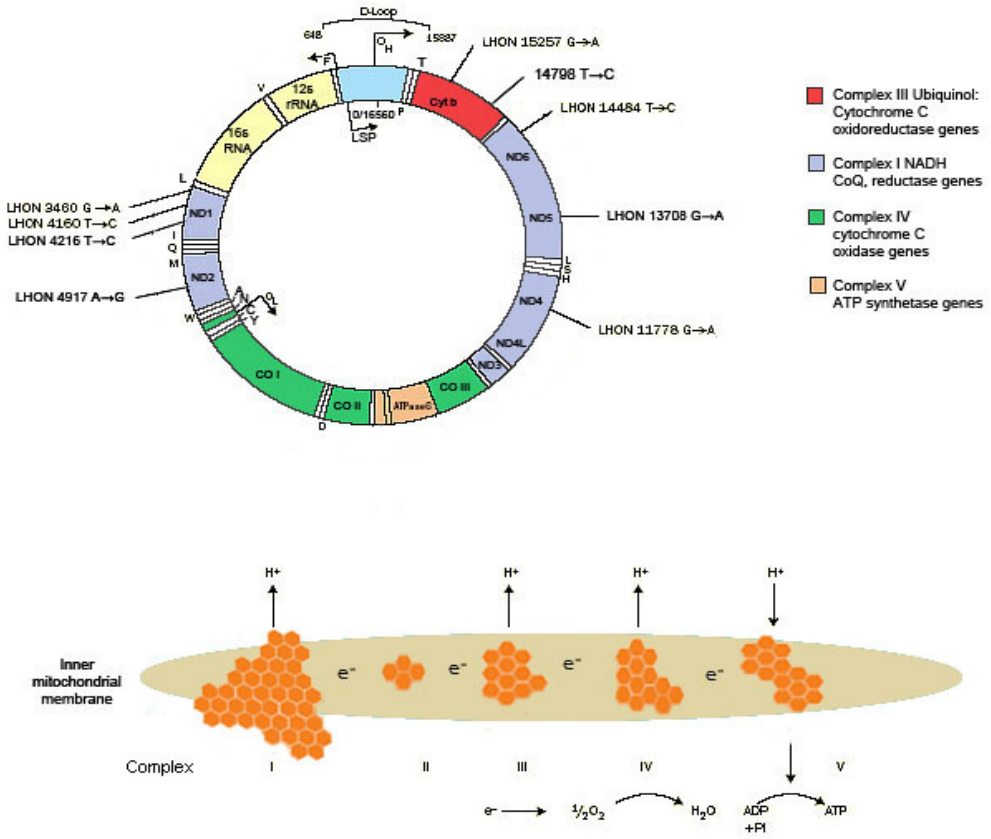

The upper part of Figure 8 depicts mtDNA as a double stranded circular molecule encoding 13 protein subunits in Complexes I, III, IV and V, and 22 tRNA and 2 rRNA molecules. Protein coding regions are separated from each other by tRNA genes. The only non-coding part, the D- (displacement) loop region plays a role in replication and gene expression regulation. O_H: origin of heavy strand replication. O_L: origin of light strand replication. Primary and secondary LHON mutations, and a variant at 14,798 (see study) are indicated outside of the mtDNA symbol. The lower part of Figure 8 depicts Complex I through V embedded in the inner mitochondrial membrane, the site of oxidative phosphorylation. With the exception of Complex II, subunits of all other complexes are encoded by both nDNA and mtDNA. Electrons (e^-) derived from substrate oxidation enter into the electron transfer chain at the level of Complex I. Protons are pumped out by Complexes I, III and IV, and re-enter mitochondria at Complex V. Complex V is also called ATP synthetase that catalyzes ATP synthesis from ADP and Pi (164-165).

3.1.1.2 Phenotypes of ON, PON, NMO and LHON

Optic neuritis (ON) may be a disease of the optic nerve(s) alone or part of MS. Typically, acute painful visual loss affects one eye, less frequently both eyes, resulting in color vision impairment, central

scotoma, visual field defect, or complete loss of light perception. Inflammatory disc swelling can be seen in about 20-40% of cases, but the fundus also may appear normal during an acute attack. Spontaneous visual improvement occurs over weeks or months, and recovery attains an acuity level of 20/30 or better in 75% to 90% of uncomplicated cases (166-169). Intravenous methylprednisolone followed by oral prednisone accelerates the recovery of vision but does not change the five-year cumulative probability of clinically definite MS (167-169). In an unusual form of ON, here referred to as prominent ON (PON), the acute visual loss is followed by no recovery, or a progressive visual deterioration leads to blindness within a few years. This subgroup comprises less than 10% of patients with ON, and has little or no benefit from intravenous methylprednisolone even in short terms (167-166-169). The cause of distinct clinical behavior of patients with PON is unknown, but the influence of genomic and mitochondrial genetic factors is possible.

Devic's neuromyelitis optica (NMO) is characterized by inflammation, demyelination and necrosis restricted to the optic nerves and spinal cord (40,170-173). NMO may occur in any ethnic groups, but it is most commonly seen in those with low risk for typical or Western type of MS. Pathogenic significance of immunoglobulins and complement, the abundance of distinct cell types (e.g. eosinophils, neutrophils) and hyalinized blood vessels in NMO lesions have long been recognized (172,174). Both clinical and pathological observations had generated debates on as to NMO is a variant of MS or a distinct entity, until anti-Aquaporine-4 antibodies as disease markers were identified and their pathogenic significance was defined (170-174). The distribution, necrotic nature and vascular involvement in pathology suggest some similarities between NMO and mitochondrial diseases such as LHON (distribution), MELAS or mitochondrial encephalopathy-lactic acidosis-stroke-like episodes (vascular involvement) and Leigh's syndrome (subacute brain tissue necrosis). These features raise the question if there is a role of mitochondria in NMO.

In contrast to ON, the visual loss in LHON is subacute and painless. Affected individuals are usually young men (175). The pathology typically is restricted to the anterior optic pathway without signs of inflammation. However, additional neurological abnormalities including inflammatory demyelination were historically noted in several LHON pedigrees (176-179). Went (179) reviewed eight families with LHON and MS (151-154). In the most often cited pedigree (153), an affected woman had five children, three of whom presented with LHON and two of these three children developed symptoms of MS. In a Dutch family, combinations of optic nerve atrophy, spastic paraparesis, dystonia and MS were noted (154). These studies suggest associations between LHON and CNS diseases, particularly MS.

3.1.1.3 LHON mutations in MS, PON and NMO

MtDNA abnormalities associated with LHON were identified between 1988 and 1992, and were classified either as primary or secondary mutations based on their biochemical and clinical effects (180-183). Primary LHON mutations are pathogenic, and are located at nucleotides (nt) 11,778, 3,460 and 14,484 within the NADH dehydrogenase (ND)-4, ND-1 and ND-6 subunits of Complex I, respectively (180-182). Pathogenic mtDNA mutations are usually heteroplasmic (both the mutated and wild-type molecules are present in a cell). Secondary LHON mutations are sequence polymorphisms found in a small percentage of the normal population and in a higher percentage of LHON patients. These mutations are biologically neutral, reach a homoplasmic state over time (only the mutated molecules are present in a cell) and show linear accumulation in haplotypes. The most frequent secondary mutations (variants) are located at nt 4,216 (ND-1), nt 4,917 (ND-2) and nt 13,708 (ND-5) in the respiratory Complex I genes (183).

Numerous case reports described LHON mutations in MS patients (138-142). First Harding et al (155) reported eight women with an MS-like illness and the 11,778 mutation. Flanigan and Johns (156) also found this mutation in four patients with demyelinating disease and LHON in their families. Kellar-Wood et al (157) screened twenty MS patients with PON without family history for LHON. Three patients carried either the 11,778 or the 3,460 mutation. However, neither of these mutations was found in 307 random MS patients (157). Subsequently, further cases of MS with primary LHON mutations were documented (158-159). A survey of LHON patients revealed that five of eleven (45%) females with the 11,778 mutations had an MS-like illness on MRI with or without clinical manifestation (161). In the above mentioned Dutch family with LHON-dystonia and MS (154), point mutations at 11,696 (ND-4 gene), and at 14,596 (ND-6 gene) were identified (160). Horvath et al (184) described a patient with a MS-like disease associated with the 14,484 mutation. Autopsy report of this patient revealed the presence of both typical and atypical forms of plaques, inflammation with macrophages and CD8+ T cells, axonal damage and cystic necrosis in the white matter, and an upregulation of inducible nitric oxide synthase and mitochondrial manganese superoxide dismutase (185). In contrast to MS, primary LHON mutations were not detected in NMO (186,187). Secondary LHON mutations (at nts 4,216, 4,907 and 13,708) also were only reported in some MS cohorts, but not in NMO (188-189).

As mtDNA is maternally transmitted, highly polymorphic and free of recombinations, mtDNA polymorphisms that sequentially align in haplotypes provide phylogenetic information (162,190,191). Each human race has a characteristic mtDNA haplotype and haplogroup distribution depicted in the phylogenetic tree. Sequence variations in the most variable part of mtDNA, the D-(displacement)-loop

region, have also been used in phylogenetic analyses. Our preliminary study of D-loop sequences in Caucasian MS patients and controls suggested an association between certain mtDNA polymorphisms / haplotypes and MS (141). These above observations and considerations prompted us performing a comprehensive study to evaluate the role of mtDNA mutations, polymorphisms and haplotypes in MS, PON and NMO.

3.1.2 Mitochondrial and nuclear DNA encoded genes of Complex I

3.1.2.1 Complex I (NADH-ubiquinone oxidoreductase):

Complex I is the first and largest enzyme complex in the mitochondrial electron transport chain, and is composed of 38 nDNA and 7 mtDNA encoded subunits (ND-1 to ND-6 and ND-4L) (192-193). Primary and secondary LHON mutations are located in the ND-1, ND-2, ND-4, ND-5 and ND-6 mtDNA encoded subunits of Complex I. The fully assembled enzyme has a L-shape configuration with the hydrophilic part emanating into the mitochondrial matrix and the hydrophobic part embedded in the inner mitochondrial membrane (IMM) (Figure 9). Both the flavoprotein (NDUFV1-NDUFV3) and the iron-sulphur protein subunits (NDUFS1-NDUFS6, NDUFA5) are hydrophilic and are involved in electron transfer. All mtDNA encoded subunits and the remaining nDNA encoded subunits are hydrophobic and mediate proton translocation (192). Electrons generated by substrate oxidation enter in the electron transfer chain at the level of Complex I to contribute to oxidative phosphorylation (OXPHOS).

3.1.2.2 Pathogenic mutations and functional impairment of Complex I:

Pathogenic mutations in nDNA encoded genes of NDUFS2, NDUFS4, NDUFS7, NDUFS8 and NDUFV1 have been identified in pedigrees presenting with Complex I deficiency, leukodystrophy, CNS tissue necrosis (Leigh’s syndrome) or degeneration (encephalopathy) (193,194). In an experimental system, the expression of the NDUFA1 mRNA was suppressed by hammerhead ribozyme (195). Mice treated with the ribozyme developed loss of retinal ganglion cells, axonal degeneration and demyelination in the retrobulbar portion of optic nerves, proving directly the involvement of Complex I in the maintenance of myelin and neuronal integrity (143,192,193).

Figure 9. Schematic depiction of Complex I

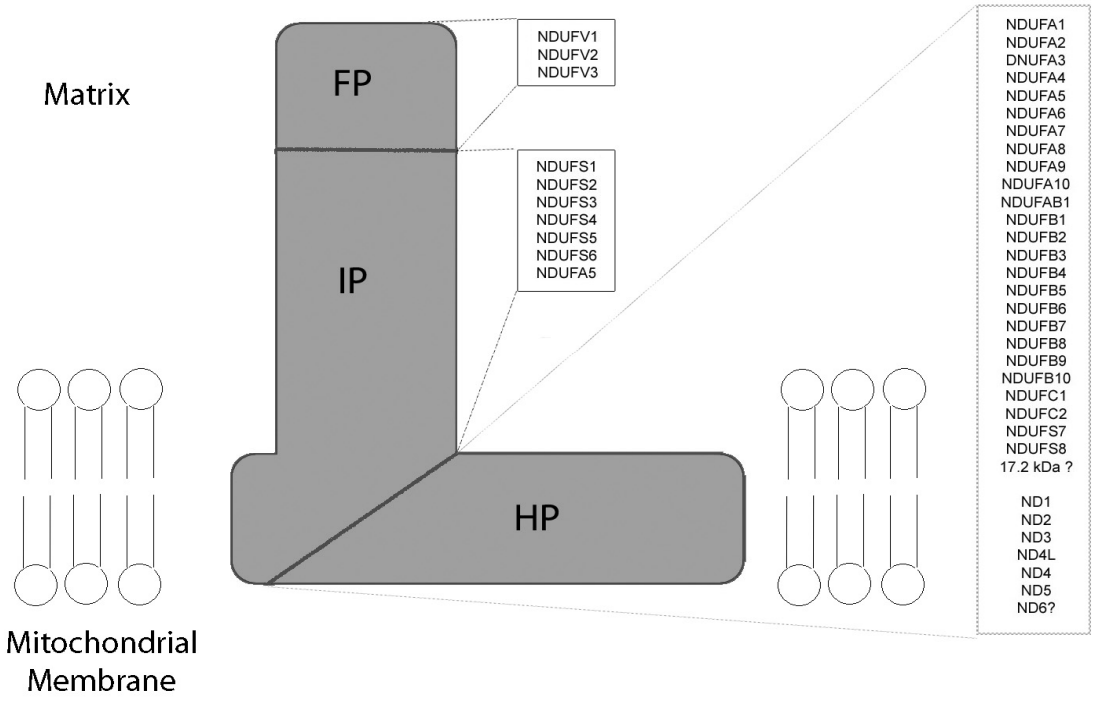

Complex I is composed of a hydrophobic fraction (HP) embedded in the inner mitochondrial membrane, and a flavoprotein (FP) and iron-sulphur protein (IP) fraction protruding into the mitochondrial matrix. The HP fraction is the largest part, that includes all mtDNA encoded and at least 25 nDNA encoded subunits (193).

3.1.2.3 Possible involvement of Complex I variants in MS

Several nuclear genes of Complex I are located within or close to chromosomal regions where lod scores suggesting linkage were detected in MS families. Of the flavoprotein subunits, NDUFV1 in chromosome 11q13 is located 30 cM away from a MS susceptibility locus (68), but the 11q13 region is orthologous to the mouse chromosome 7 D7Mit37 locus conferring susceptibility to EAE (197). Among the iron-sulphur subunits, NDUFS6 is encoded in chromosome 5ptel - p15.33 (Canadian MS locus) and NDUFS4 is encoded in chromosome 5q11.1 (British MS locus). NDUFA5 (7q32) is less than 10 cM away from and NDUFS5 (1p34.2-p33) is within a published linking-defined susceptibility locus of MS (68-69). The remaining subunits are hydrophobic, and 16 of them are within or close to previously identified regions of interest in MS linkage studies (41,68-69). The NDUFA2 hydrophobic subunit is encoded in 5q31.2, 40 cM away from a US susceptibility locus for MS. An autosomal dominant leukodystrophy mimicking PP-MS was also linked to 5q31 (198). These studies raise the possibility that

genetic variations in nDNA encoded genes of Complex I have a role in MS pathogenesis, and support analyses of Complex I genes in MS families.

3.1.3 Possible involvement of Complex I in neurodegeneration secondary to inflammation

Myelin specific immunoglobulins, tumor necrosis factor (TNF) -α, glutamate, NO and ROS (O_2^-, H_2O_2, OH^-) are known to damage myelin and oligodendrocytes directly (22,199-204) (Figure 1). A contribution of proteolytic enzymes and the above molecules to damaging demyelinated axons and neurons also has been proposed (20-22,56). Axonal loss develops in association with infiltrating macrophages within acute plaques and at the edges of chronic active plaques, while neuronal degeneration and apoptosis appear in association with activated microglia in cortical and deep gray matter regions (56,67,207). MRS and histological observations suggest the development of biochemical abnormalities (drop of NAA, rise of choline) (208-210) and altered energy (ATP) metabolites (206). Since NAA is synthesized in mitochondria of neurons, a decreased NAA measure may reflect mitochondrial dysfunction and neuro-axonal loss (52-53,209-210).

As an extension of our mitochondrial genetic studies, we aimed to explore a mechanism that can contribute to degenerative changes in plaques. We previously demonstrated that activated MNCs of MS patients produce increased amounts of ROS as compared to those of normal or OND controls (148-149), and that oxidative damage to DNA develops in association with inflammation in chronic active plaques (148). Oxidative damage to DNA is likely to be a consequence of higher ROS / NO production by activated macrophages and microglia (47,206,211). MtDNA is about ten times more susceptible to oxidative damage than nDNA because of the lack of protective histones and less efficient repair (212). Therefore, the damage we previously detected in total DNA (148) might predominantly reflect damage accumulated in mtDNA. This oxidative damage not only is capable of causing somatic mtDNA mutations and deletions, but may also be an indicator of an overall damage affecting macromolecules in mitochondrial membranes and enzymes. If this is the case, oxidative damage may interfere with the energy metabolism of cells and contribute to degenerative changes in MS. To explore this potential pathway, we investigate below effects of inflammation-associated oxidative stress, damage to mtDNA and activity of mitochondrial respiratory chain complexes in paired plaques and NAWMs.

3.2. PATIENTS AND METHODS

3.2.1 MtDNA mutations, variants and haplotypes in MS, PON and Devic's disease

3.2.1.1 MtDNA mutations and variants in MS

Patients and specimens

Fifty-three unrelated Caucasian MS patients and 74 controls matched by age, gender and ethnic distribution were studied. PBL was obtained from 50 patients with clinically definite or laboratory supported definite MS (28) in the MS Clinic at Thomas Jefferson University. In addition to the 50 clinical cases, 3 NAWM specimens from autopsy MS brains were included. Three age and sex matched autopsy NAWM controls were added to the 71 healthy Caucasian PBL controls. Brain specimens were provided by the RMMSBB, Englewood, CO and by HBSFRC, Los Angeles, CA.

Table 11. PCR primers and products

Gene	Mutations	5' primer	3' primer	size	enzyme/ sequencing
ND-4	(11,778)	11,642-11,661	11,961-11,980	338	sequencing
ND-1a	(3,460)	3,400-3,419	3,866-3,885	485	sequencing
ND-1b	(4,136, 4,160, 4,216) 4,216	3,817-3,836	4,243-4,262	445	sequencing *Nla*III
ND-2	4,917	4,704-4,721	5,103-5,120	416	*Bfa*I
ND-5	13,708	13,570-13,587	13,990-14,007	437	*Bst*N1
ND-6	(14,484)	14,240-14,257	14,638-14,855	415	sequencing
cyt b	15,257	15,044-15,061	15,437-15,454	410	*Acc*I

Mutations within the ND-4, ND-1 and ND-6 genes in 20 MS patients were identified by direct sequencing of the amplified segments of mtDNA in both directions. In the remaining 33 MS patients and 74 controls, the 4,216, 4,917, 13,708 and 15,257 mutations were detected by restriction endonucleases, *Nla*III, *Bfa*I, *Bst*N1 and *Acc*I, respectively. The mutation at position 4,216 (T to C) creates a restriction site for *Nla*III (**C**ATG) resulting in a 399 and a 46 bp fragment of the wild type uncut PCR product. The mutation at position 4,917 (A to G) creates a new restriction site (CTA**G**) for *Bfa*I restriction endoduclease, resulting in a 203 bp fragment in addition to the cleaved wild type fragments. The mutation at position 13,708 (G to A) eliminates a restriction site for *Bst*N1 restriction endonuclease (CCTG**G**), resulting in an uncut fragment of the amplified mitochondrial DNA (437 bp) instead of the wild type (299 and 138 bp) fragments. A mutation at position 15,257 (G to A) eliminates the restriction site for *Acc*I, in which case the 410 bp PCR fragment can be seen instead of the wild type 213 and 197 bp cleaved fragments. LHON mutations are placed in parenthesis when sequencing was applied, since by this technique other mutations could also be revealed in the region studied.

DNA extraction, amplification, sequencing and restriction endonuclease analyses

DNA from PB MNCs or from NAWM tissues was extracted using a QIAamp Tissue Kit (Qiagen, Chatsworth, CA). Six portions of mtDNA, including almost the entire ND-1 and parts of the ND-2, ND-4, ND-5, ND-6 and cytochrome b (cyt b) genes, were amplified by PCR (Table 11). The PCR products were purified with a Qiaquick-spin PCR Purification Kit (Qiagen). DNA segments of the ND-1 (a and b), ND-4 and ND-6 regions were sequenced directly in 20 patients using the dyedeoxy terminator reaction chemistry on the Applied Biosystem Model 373A DNA Sequencing System, and homology with the published human mitochondrial DNA was searched (150,213). In the remaining 33 patients and in the 74 controls the mutation at 4,216 (ND-1) was screened by *Nla*III restriction endonuclease (New England Biolabs, Beverly, MA). In every individual studied, the mutations at nt 4,917 (ND-2), nt 13,708 (ND-4) and nt 15,257 (cyt b) were screened by digesting the purified PCR products with *Bfa*I, *Bst*N1 and *Acc*I, respectively (New England Biolabs) (Table 12). The digested fragments were separated on a 1.5% agarose gel.

3.2.1.2 Screening for LHON mutations in patients with PON

Patients and specimens

Twenty-two patients with PON were selected by reviewing the charts of the Multiple Sclerosis Clinic, Thomas Jefferson University Hospital. None of these patients were addicted to tobacco, alcohol or drugs, were exposed to neurotoxins, deficient in vitamin intake or malnourished. PON was established if no or minimal recovery followed the acute, usually severe visual loss from ON, or if a progressively disabling visual deterioration developed either with or without clinical exacerbations of ON over the years. Patient selection was based on a residual visual acuity of 20/70 or worse if ON affected both eyes, and 20/200 or worse if ON predominantly affected only one eye. Patients received intravenous corticosteroid with no improvement. Patient characteristics are detaled in Tables 13 and 14.

Table 12. Characteristics of MS in patients with PON

Patient No.	Ethnic	Age	Gender	DG of MS or ON (years before study)	Course	MRI	EDSS (in 1995)	FAMILY
1.	B	45	F	13	RR	MWL	5.5	MS:Mother
2.	W	48	M	20	RR, SP	MWL	8.5	-
3.	W	41	F	21	RR	MWL	3.5	-
4.	W	30	F	8	RR,SP	MWL	6.0	MS: maternal aunt
5.	W	39	M	14	RR	MWL	1.5	-
6.	B	51	F	28	RR,SP	MWL	7.0	-
7.	W	54	F	17	RR,SP	MWL	7.5	-
8.	W	40	M	9	RR,SP	MWL	4.5	-
9.	W	42	F	7.5	RR	NOL	2.0	-
10.	W	39	F	23	RR	MWL	6.0	MS: paternal cousin
11.	W	52	M	6	PP	NOL	3.5	-
12.	B	37	F	7	RR	MWL	5.5	-
13.	W	40	F	19	RR	MWL	2.0	-
14.	B	21	F	3	PP	MWL	8.5	MS: Father
15.	W	53	F	1	RR	MWL	1.5	-
16.	W	54	M	7	RR	MWL	3.5	-
17.	W	27	F	1.5	RR	MWL	7.0	-
18.	W	42	F	8	RR,SP	MWL	7.0	-
19.	W	50	F	3	RR,SP	MWL	6.0	-
20.	W	44	F	19	RR,SP	MWL	6.0	-
21.	B	63	M	1	PP	MWL	7.0	-
22.	W	62	F	30	RR,SP	MWL	5.5	-
		44.3+/-10.2		12.0+/-8.7			5.0+/-2.2	

This table indicates the patients numerical code, ethnicity, age at the time of the study, gender, how many years before the study was the diagnosis of MS or ON made, course of the disease, MRI and EDSS at the time of the study, and the family history. Abbreviations: W: White, B: Black, F: female, M: male, RR: relapsing-remitting, SP: secondary progressive, PP: primary chronic progressive, MWL: multiple white matter lesions (at the time of study), NOL: no lesion

Table 13. Characteristics of ON in the PON patients

Patient	Dg of ON (years before study)	VA onset	VA current	VL at onset	Rec.	Prog.	SR	11,778	3,460	14,484
1.	8	FC 20/20	FC 20/20	+	-	-	-	-	-	-
2.	11	20/60 FC	20/50 FC	+	-	-	-	-	-	-
3.	21	BLIND BLIND	BLIND BLIND	+	-	-	-	-	-	-
4.	8	20/200 20/400	20/200 20/200	+	-	-	-	-	-	-
5.	7	20/400 20/400	20/400 20/400	+	-	-	-	-	-	-
6.	28	20/400 20/50	20/100 20/25	-	7	-	+	-	-	-
7.	17	20/800 20/20	20/800 20/70	-	-	+	-	-	-	-
8.	9	20/100 20/70	20/400 20/70	-	3	-	-	-	-	-
9.	7.5	20/80 20/20	20/200 20/30	-	4	-	-	-	-	-
10.	23	20/20 20/200	20/30 20/100	+	-	-	-	-	-	-
11.	6	20/25 20/30	20/80 FC	-	-	+	-	-	-	-
12.	6	NA BLIND	20/200 20/100	+	-	-	+	-	-	-
13.	19	NA NA	20/30 20/70	-	3	-	+	-	-	-
14.	3	20/400 20/20	BLIND BLIND	-	-	+	-	-	-	-
15.	1	20/50 20/100	20/50 20/100	+	-	-	-	-	-	-
16.	3	20/200 20/400	20/100 20/100	+	-	-	+	-	-	-
17.	1.5	20/800 20/800	20/400 20/600	-	2	-	+	-	-	-
18.	6	20/30 20/800	20/200 20/400	-	-	+	-	-	-	-
19.	3	20/200 20/25	FC 20/200	-	-	+	-	-	-	-
20.	19	20/30 20/25	20/70 20/200	-	-	+	-	-	-	-
21.	1	20/200 20/200	20/400 20/800	-	-	+	-	-	-	-
22.	30	20/200 20/50	20/800 20/400	-	3	-	-	-	-	-

10.4+/-9.2

Abbreviations: VA: visual acuity, FC: finger counting, NA: not available, VL: visual loss, Rec: recidive VL, Prog: progressive VL, SR: steroid responsiveness, Visual acuities are in the order of OD, OS.

There were 5 black and 17 white patients, 16 of whom were females (Table 12). The age range was 21 to 63 (mean: 44.3+/-10.2) years. Twenty patients suffered from MS (28). Two patients had isolated ON without clinical or MRI signs of disseminated inflammatory demyelination. Fourteen of the 20 MS patients had ON as a first presentation, and 6 patients developed ON 1 to 9 years after the diagnosis of MS. Only 3 patients (No. 15, 17 and 21) had a recent onset of ON (1 and 1.5 years ago). The remaining patients developed clinical ON three or more years before the study (range 3 to 30) (Table 13). At the time of this study all but one patient (No.1) had bilateral decrease in visual acuity. Acute exacerbations (two to seven episodes) of ON were documented in six patients (No. 6, 8, 9, 13, 17, 22), with each exacerbation resulting in further visual impairment. Six patients (No. 7, 11, 14, 18, 19, 20) developed progressive visual impairment without apparent clinical relapse, while nine patients (No. 1-5, 10, 12, 15, 16) had one severe episode of ON followed by only moderate improvement or no recovery.

Methods

DNA from PB MNCs was extracted as in 3.2.1.1. Three segments of mtDNA encompassing regions of the ND-1, ND-4 and ND-6 genes were amplified by PCR (Table 11, section 3.2.1.1). The presence of primary LHON mutations was determined by using restriction endonuclease analyses and sequencing. The mutation at nt 3,460 results in a recognition site loss for *Bsa*HI (New England Biolabs) (157). The mutation at nt 11,778 introduces a site gain for *Mae*III (Boehringer Mannheim, Germany) (155-159). The presence of the mutation at nt 14,484 was tested by sequencing (Table 11, Section 3.2.1.1). Restriction fragments were separated on a 1.5% agarose gel by electrophoresis and visualized by ethidium bromide.

3.2.1.3 Sequence analyses of the entire mtDNA in patients with MS and NMO

Patients

-*MS patients*: The entire mtDNA of two patients with clinically definite, laboratory supported (MS-R4, MS-R51) and one pathologically confirmed MS (MS-1NP) was sequenced (28).

1. Patient MS-R4 is a 42 y.o. Caucasian female with a 10 year history of RR-MS associated with blurred vision and weakness, spasticity, paresthesia, decreased position and vibratory sensation in her lower extremities. Increased deep tendon reflexes, extensor plantar reflexes, gait ataxia and dyssynergia of the bladder sphincters of varying severities were also noted. Somatosensory and visual evoked potentials showed abnormalities compatible with a demyelinating process. T2 weighted cranial MRI revealed multiple periventricular and parietal white matter signal abnormalities. IgG and IgG index were within normal limits, but oligoclonal bands were present in the CSF. The history of this Ashkenazi

Jewish family was positive for idiopathic dystonia with autosomal dominant inheritance on the mother's side (214). A first cousin on the father's side had MS.
2. Patient MS-1NP (autopsy case) was a 43 y.o. Caucasian female with PP-MS characterized by the decline of cognitive functions, seizures, blurred vision and weakness in her lower extremities in the 1980-ies. Visual evoked potentials were delayed. IgG was increased in the CSF. CT scan of the brain showed atrophy without focal lesions. The patient died 3 years after the clinical onset. Histology showed active plaques with gliosis and moderate lymphocyte collection, and striking demyelination in the periventricular white matter.
3. MS-R51 is a 39 y.o. Caucasian female who presented with ON first on the left, then on the right 20 years before the study. After initial improvement, both eyes rapidly worsened despite ACTH and she was blind bilaterally within a year. Concurrent with the ON, she had episodes of seizures which were treated with Dilantin. Ten years later she developed waxing and waning tingling, fatigue, clumsiness, urinary urgency and recurrent vertigo. On exam, she exhibited no light perception in either eye, marked optic pallor and no pupillary response to light. Nystagmus was observed on lateral and up gaze, but no other cranial nerve abnormality was noted. She exhibited full strength in all extremities with increased deep tendon reflexes and flexor plantar responses. Mild decrease of vibration and pin prick sensation in the lower extremities was detected. Her tibial sensory evoked potentials were abnormal. Repeated MRI of the brain and the cervical cord showed disseminated white matter abnormalities consistent with MS. Her family history was negative for MS or mitochondrial diseases.

-*NMO patients:* Three spinal cord specimens with NMO pathology were studied (NMO-A, B, C) (170). Two frozen specimens were obtained from the RMMSBB, Englewood, CO. One paraffin-embedded tissue was provided by Dr. Raul Mandler. All three patients were Caucasians. After the identification of a new mtDNA variant in NMO-B, a screening for this mutation was performed in mtDNA of 65 Caucasian MS patients and 80 controls.

Methods:
Genomic DNA was extracted from the PB MNCs or the NAWM of MS patients and controls, and from the spinal lesion of NMO patients as in 3.2.1.1. The entire mtDNA of the three MS and three NMO patients was amplified in about 600 bp overlapping fragments. The PCR products were purified with a Qiaquick-spin PCR Purification Kit (Qiagen). DNA portions were sequenced directly using the dyedeoxy terminator reaction chemistry on the Applied Biosystem Model 373A DNA Sequencing System. In each patient a number of mtDNA alterations were detected relative to the Cambridge sequence (150). Eight unusual mtDNA variants identified in the 3 MS patients and one new variant detected in a NMO patient

were chosen for further analyses. The presence of these nine new mtDNA variants was confirmed in the probands and tested in a cohort of MS patients and controls by amplifying the appropriate region of the mtDNA and by restriction endonuclease digestion of the PCR product.

The section below in italics describes design of assays and the technical details of how each of the nine mutations detected by sequencing in the MS and NMO probands was confirmed by a restriction endonuclease analysis.

To confirm the mutation at 980 (T to C) PCR was performed using a sense (590-609) and a mismatching antisense (981-1,004) primer which replaces the two Cs by Gs at positions 983 and 984 to create a restriction site for Bst NI (New England Biolabs, Beverly, MA) (CCAGG) in the presence of the mutation. While the presence of the mutation in MS-R4 was confirmed by this test, its homoplasmic nature was verified by using less complex primers. In the mismatching sense primer (955-979) an A was replaced by G at nt 977, to create a recognition site for Hinf I (New England Biolabs) (GANTC) in the presence of the wild type T nucleotide at 980 (Fig.10a). The antisense primer encompassed nt 1,193-1,212.

To confirm the mutation at 1,888 (G to A) PCR was performed by a sense (1,590-1,609) primer and a mismatching (1,889-1,912) antisense primer. In the antisense primer a C was replaced by G at position 1,889, and the A nucleotides at 1,891 and at 1,892 were replaced by Ts to create a restriction site for Hind III (New England Biolabs) (AAGCTT) in the presence of the mutation. To verify the homoplasmic nature of the mutation in the mtDNA of MS-1NP, PCR was performed by using a mismatching sense primer (1,865-1,887), in which an A was replaced by C at nt 1,887 to create restriction site for Hha I (New England Biolabs) (GCGC) in the presence of the wild type G at nt 1,888 (Fig.10a). The antisense primer encompassed nt 2,198-2,217.

The mutation at 8,684 (C to T) was evaluated by using a mismatching sense primer (8,656-8,683) and an antisense primer (8,899-8,918) for amplification. The sense primer had T instead of C at nt 8,680 to create a restriction site (ATTAAT) for Ase I (New England Biolabs) in the presence of the mutation at 8,684 (Fig.10b).

The mutation at 9,300 (G to A) was tested by using a mismatching sense primer (9,278-9,299) in which C is replaced by T at 9,297 to create a recognition site (TTAA) for Mse I (New England Biolabs) in the presence of the mutation at 9,300 (Fig.10b). The antisense primer encompassed nt 9,852-9,871. The presence of the mutation in MS-R4 was also confirmed by Bfa I (New England Biolabs) digestion of the PCR products (generated by a set of sense [8,762-8,781] and antisense [9,341-9,360] primers, or another set of sense [9,236-9,255] and antisense [9,852-9,871] primers). The G to A mutation at 9,300 results in a site loss (CTAG to CTAA) for Bfa I (data not shown).

The mutation at 10,463 (T to C) was detected by using a mismatching sense (10,436-10,462) and an antisense (10,830-10,849) primer for PCR. The sense primer had G instead of A at 10,460 to create a restriction site (AGATCT) for Bgl II (New England Biolabs) in the presence of the mutation at 10,463 (Fig.10b).

To detect the mutation at 13,966 (A to G) PCR was performed using a sense primer (13,570-13,589) and a mismatching antisense primer (13,967-13,993). In the antisense primer A was replaced by C at 13,969 to create a restriction site (GCGC) for Hha I (New England Biolabs) in the presence of the mutation at 13,966, and G was replaced by A at 13,970, to eliminate a restriction site for Hha I in the vicinity of the site of interest (Fig.10b).

The mutation at 14,798 (T to C) was confirmed by using a sense (14,559-14,578) and a mismatching antisense (14,799-14,825) primer for amplification. In the antisense primer T at 14,802 was replaced by G to create a recognition site (CTNAG) for Dde I (New England Biolabs) in the presence of the mutation at 14,798 (Fig.10b).

The mutation at 15,928 (G to A) creates a recognition site (GAAGAN$_8$) for Mbo II enzyme (New England Biolabs). PCR was performed using the nt 15,761-15,780 sense and the 16,401-16,420 antisense primers (Fig.10b).

The only new mtDNA mutation at nt 4,695 (T to C) in NMO patient B was confirmed by a restriction endonuclease analysis with Ear I specific for the wild type CTC TTC (N)1 sequence.

Statistical analyses: To test differences in the occurrence of mtDNA variants between patient and control cohorts, χ^2 test was applied.

3.2.1.4 A comprehensive screening of mtDNA in Caucasian MS patients and controls

Patients and controls:

Seventy-seven Caucasian patients with RR and SP-MS were included. Heparinized PB was obtained from 75 patients who were recruited based on standard criteria (28) from the MS Clinics at the Thomas Jefferson University Hospital and at the Allegheny University of the Health Sciences, Philadelphia. Brain tissue specimens from two additional patients were obtained from the RMMSBB, Englewood, CO and from the HBSFRC, Los Angeles. Charts of patients were reviewed to analyze the phenotypic characteristics of the disease. The age range of patients was 23 to 71 (mean: 45.2+/-8.7) years, and fifty-five patients were females. The range of Kurtzke's EDSS score was 1 to 8 (mean: 3.7+/-1.8). The history of MS was 3 to 33 (mean: 12.5+/-7.4) years long. The age of onset was in the range of 15 to 64 (mean: 32.7+/-10.0) years. Altogether 19 patients with PON were involved, 18 of whom participated in the previous study (3.2.1.2). PON was defined as in 3.2.1.2. ON as a presenting symptom was recorded in 31 of the 77 patients (42%). There were two patients with relatives with MS (a maternal aunt and a daughter) likely sharing identical mtDNA. Four patients had cousins with MS. Two of the

cousins were on the fathers' side. The parental side of the other two cousins could not be identified. In addition, a father-son concordance was noted.

PB was drawn from 81 Caucasian healthy controls recruited from personnel in the Department of Neurology, Thomas Jefferson University, or from healthy blood donors in the Blood Donor Center, at Allegheny University of the Health Sciences. Brain tissue specimens were obtained from 3 additional normal Caucasian controls from the HBSFRC, Los Angeles. Except for the brain tissue specimens, controls and patients were collected from the same geographic area and special care was taken to ensure a similar ethnic distribution among Caucasians. mtDNA of an African-American control was designated as outgroup in the phylogenetic analysis.

Methods:

PB MNCs were separated by Ficoll-Paque gradient centrifugation. Genomic DNA from PB MNCs or brain specimens was extracted as above. To perform a high resolution restriction site polymorphism and haplotype analysis (162,190,215), we amplified by PCR the entire mtDNA of each individual in nine overlapping fragments. Primers were designed and the nucleotides were numbered based on the human mtDNA light (L) chain sequences (150). Primers: I sense 0-19, antisense 1193-1212; II sense 1126-1145, antisense 3433-3452; III sense 3402-3421, antisense 5598-5617; IV sense 5469-5488, antisense 7651-7670; V sense 7598-7617, antisense 9852-9871; VI sense 9741-9760, antisense 11,961-11,980; VII sense 11,932-11,951, antisense 13,988-14,007; VIII sense 13,942-13,961, antisense 16,031-16,050; IX sense 15,976-15,995, antisense 658-677. For all reactions, 35 cycles of 95^{o}C-55^{o}C-72^{o}C, each for one minute, were performed. Each of the 9 PCR fragments was digested by 14 restriction endonucleases: *Alu*I, *Ava*II, *Bam*HI, *Dde*I, *Hae*II, *Hae*III, *Hha*I, *Hinc*II, *Hinf*I, *Hpa*I, *Msp*I, *Mbo*I, *Rsa*I, *Taq*I (New England Biolabs, Beverly, MA) (162,190,215). In addition, mtDNA was screened by *Bst*NI and by *Nla*III enzymes (New England Biolabs) to determine the presence of 13,708 and 4216 mutations, respectively. To test the relevance of the 13,966 (A to G, Thr to Phe) and 14,798 (T to C, Phe to Leu) mutations to MS, mtDNA of each individual in the study was amplified by sense and mismatching antisense primers and digested by *Hha*I and *Dde*I, respectively, as in section 3.2.1.3.2. Restriction fragments were separated by electrophoresis in 1-4% SeaKem plus NuSieve agarose gel of various ratios, depending on the expected fragment sizes. When the identity of a new nucleotide change causing restriction site loss or gain could not be determined based on the enzymatic analysis, direct sequencing of the PCR fragment was performed. We investigated the potential association of each new mtDNA variant with MS by using the Fisher's exact - test.

For haplotype analysis, the presence or absence of restriction sites were converted in a binal format (1 indicating the presence, and 0 indicating the absence of a site). Applying a modified version of the MEGA program (NJBOOTW, by K. Tamura) we performed alignment and bootstrap analyses of data (216). The Kimura two-parameter method was used for distance estimation, and the neighbor joining (NJ) method was used to create the phylogenetic trees.

3.2.2 Genetic analysis of Complex I in MS

Patients, families and DNA specimens

DNA specimens from families were obtained from the UCSF MSDB, San Francisco, CA and from the collection of the CMSCG, London, ON (Table 14). The diagnosis of MS (28,29) and the definition of phenotypic subtypes (30) was similar to that described in section 2.2.1.1. Although the proportion of families with PP-MS was low in DS101-112, we addressed as to how the inclusion of clinical sub-groupings could influenced the outcome. There were 26 PP-MS trios and incomplete families, and 163 RR/SP-MS families (trio, ASP, multiplex, incomplete).

Table 14. Families studied

Dataset	Total families	Individuals	Trio	ASP	Incomplete	Multiplex	Origin
DS101-105	66	365	7	34	10	15	MSDB, UCSF
DS106-108	66	198	66	0	0	0	MSDB, UCSF
DS109-112	50	300	0	39	0	11	CMSCG
Total	182	863	73	73	10	26	

Definitions: ASP=affected sib pair family: two or more affected (and usually one or more unaffected) children with their unaffected parents; trio: an affected child with his / her unaffected parents; incomplete family: an affected individual with one unaffected parent and / or an unaffected sibling; multiplex family: multiple affected family members in two or three generations. These families also were included in a simultaneously conducted, larger phase I study on chromosome 17q11 (section 2.2.1).

Table 15a. Complex I nuclear genes and SNPs studied

Chromosome	Subunit gene	SNP designation (nucleotides) [amino acid]	NCBI rs#	Heterozygosity %
1p34.2-p33	NDUFS5	A (t/c)	2889683	0.38
		X (t/g)	3768325	0.29
		D (g/a)	6981	0.09
2q33-34	NDUFS1	X (g/t)	2045858	0.51
3q13.33	NDUFB4	A (a/g)	804986	0.46
		B (g/a)	804970	0.47
		X (c/t)	12762	0.23
4q28.2-31.1	NDUFC1	X (c/t)	3816413	0.35
		A (a/a)	1802239	0.00
		M (a/g)	4863646	0.36
5pter-p15.33	NDUFS6	E (c/a)	2242412	0.14
		M (c/t)	3776149	0.18
		G (t/c)	1018120	0.46
		X (t/c)	3756344	0.18
5q11.1	NDUFS4	X (c/g)	2279516	0.48
		C (t/c)	923610	0.32
		Z (t/c)	370594	0.36
		A (a/a)	1044692	0.00
5q31.2	NDUFA2	O (a/g)	702398	0.52
		A (a/t)	778592	0.39
		N (t/c)	778594	0.49
7p21.3	NDUFA4	X (c/t)	1681289	0.19
		M (g/a)	218979	0.26
		Y (c/t)	1616965	0.52
7q32	NDUFA5	B (t/t)	11004	0.00
		X (t/a)	3779262	0.43
7q34	NDUFB2	M (c/t)	1046515	0.17
11q13	NDUFV1	E* (t/a) [Phe/Ile]	1800670	0.04
		X (t/c)	3741165	0.03
11q13	NDUFS8	B (t/c)	2075626	0.36
11q13.3	NDUFC2	M (a/g)	731639	0.35
		E (c/t)	1470710	0.53
		Y (a/t)	522683	0.25
		X* (c/g) [Val/Leu]	8875	0.49
12p13.3	NDUFA9	E (t/c)	2159352	0.50
		C (t/g)	2074984	0.49
		A (a/g)	2240760	0.46
16pter-p13.3	NDUFB10	X (c/t)	2302175	0.04
		C (c/a)	338790	0.28
		Y (g/a)	758335	0.32
19p13.3	NDUFS7	X* (t/c) [Pro/Leu]	3180032	0.49
		N (a/g)	2074897	0.53
		B (a/g)	809359	0.16
19p13.2	NDUFA7	X (g/c)	2288414	0.09
		Y (c/t)	561	0.29
		N (g/a)	2241590	0.50
19p13.12-13.11	NDUFB7	Y* (a/g) [Lys/Glu]	1042349	0.07
		X* (c/g) [Gly/Arg]	3752220	0.05
		M (g/t)	3752221	0.30
19q13.42	NDUFA3	X (c/t)	254259	0.47
		F (g/a)	254257	0.46
22q13.2-q13.31	NDUFA6	D (t/c)	7245	0.43
		B* (c/t) [Val/Ala]	1801311	0.40

Columns include the chromosomal and gene location, experimental designation (nucleotide change) [amino acid change], NCBI Rs number and heterozygosity of selected Complex I SNPs, respectively. The SNP designation with letters of the alphabet was introduced to make the marker discrimination and handling simpler than using the Rs numbers. *indicates non-synonymous SNPs; with a few exceptions, intragenic inter-marker distances vary between 200 and 5000 base pairs. NDUFB7Y and NDUFB7X markers are only 45 base pairs apart.

Table 15b. Mitochondrial DNA variants studied

Nucleotides : nt1719; nt4216; nt4529; nt4917; nt7028; nt9055; nt10398; nt13708; nt14798; nt16069; nt16391

Haplotypes : K* 9,055 / 14,798 / 10,398

J* 13,708 / 16,069 / 10,398 / 14,798

K* and J* haplotypes are defined by variants at the indicated nucleotide positions in the Caucasian haplogroups K and J, respectively (sections 3.2.1, 3.3.1, 3.4.1 and ref 145).

SNPs

Sixty-four assays were developed and validated. The assays included 11 mtDNA variants (Table 15b) found previously, either as a single allele or as determinants of haplotypes, associated with MS (144, 145). The remaining assays included 53 SNP variants in 20 nDNA encoded Complex I genes (http://www.ncbi.nlm.nih.gov/SNP). Table 15a shows the list of included nuclear genes and SNPs and the heterozygosity of markers. From the distribution of marker alleles, the genotype frequencies were calculated in the unrelated parents. By using MERLIN (http://www.sph.umich.edu/csg/abecasis/Merlin/) (92), deviations from the HWE and heterozygosity of markers were assessed. Table 15b lists the tested mtDNA variants and haplotypes.

Genotyping Genotyping was performed as in section 2.2.1.

Methods of analyses for nDNA variants

For the description of preparation and cleaning files, power estimation, PDT, TRANSMIT and computation, see previous sections 2.2.1. In ldmax analyses, SNP alleles were taken from unrelated parents in DS101-112 to assess haplotype frequencies.

Analysis of mtDNA variants

To test if mtDNA variants of interest are enriched among affected children in DS101-112, we compared maternal (transmitted) vs. paternal (non-transmitted) mtDNA variants using the Fisher exact test. Haplotypes in maternal vs. paternal lineages were similarly tested.

3.2.3 Oxidative damage to mtDNA, activity of mitochondrial enzymes, somatic mtDNA deletions and expression of apoptosis-related molecules in lesions of MS

3.2.3.1 Oxidative damage and activity of OXPHOS

Autopsy brain tissues

Frozen brain tissues were obtained from the RMMSBB, Englewood, CO and from the HBSFRC, Los Angeles, CA. For the DNA studies, five pairs of cerebellar chronic active plaques and corresponding NAWM tissues, and eight pairs of hemispheral chronic active plaques and corresponding NAWM tissues were collected from patients who had SP-MS or PP-MS based on clinical and pathological evaluation. For biochemistry, an additional 10 pairs of hemispheral plaque and NAWM tissues were obtained. Normal appearing and pathological tissues were first selected by gross examination and then evaluated by microscopic examination as described in 2.2.4 (Figure 4). NAWM tissues were free of microscopic pathology. Patients ranged between 18 to 54 years of age, and brain tissues were frozen less than five hours after clinical death. Although we obtained and assayed in the DNA studies specimens from the cerebellar white matter of non-neurological disease controls matched for age- and sex with patients, these control tissues had a significantly longer post mortem time (13.5 to 15 hours) than the MS tissues (2 to 5 hours), and were only available from the HBSFRC, Los Angeles, (while most of the MS tissues were obtained from the RMMSBB, Englewood). Our previous studies showed that oxidative damage in NAWM / NW of age, sex and post mortem time matched MS patients and controls does not differ (148). However, we found that postmortem time and handling of tissues are strong *ex vivo* modifiers of the detected oxidative damage to DNA. Therefore, to minimize the effect of undesired modifiers on the outcome, we omitted the groupwise comparison between these partially matched controls and patients available at the time of the present study. All comparisons were made in a pairwise manner between corresponding plaque and NAWM tissues derived from the same patient. For immunohistochemistry, five pairs of paraffin embedded NAWM and plaque tissues were obtained from the RMMSBB.

Southern blot detection of oxidative damage to mtDNA

The method of Southern blot analysis was adapted from Pfeifer et al (217,218) and Driggers et al (219). Briefly, DNA from NAWM and plaque containing specimens was extracted with a QiaAmp Tissue Kit (Qiagen, Valencia, CA). *Bam*HI digested DNA samples (*Bam*HI linearizes mtDNA) were purified by ethanol precipitation and dissolved in Tris buffer. Following quantitation, samples were divided into two equal aliquotes. One of each pair was incubated with either endonuclease III (Endo III) or formamidopyrimidine DNA glycosylase (FPG) (Trevigen, Inc., Gaithersburg, MD) which introduce single strand breaks at oxidized pyrimidines and purines, respectively. To produce single strand breaks at all abasic or sugar-modified sites in DNA, both aliquotes of each sample pair (non-treated and Endo III or FPG treated) were incubated with sodium-hydroxide. DNA samples were then separated by alkaline gel electrophoresis and vacuum transferred to a nylon membrane. Membranes were hybridized

either with a double stranded biotinylated mtDNA probe (Gibco BRL, Grand Island, NY) or with ^{32}P-labeled single stranded (light or heavy strand) probes encompassing the nts 14,559-15,112 mtDNA region. Single stranded probes were generated as described (219). Membranes were washed under high stringency condition and developed by using the PhotoGene Nucleic Acid Detection System (Gibco BRL) when the biotinylated probe was used, or exposed directly to a film when ^{32}P-labeled probes were used. The linearized 16.5 kb mtDNA bands were measured by densitometry on the autoradiograms. The break frequency was determined by using the Poisson expression $s=-\ln P_0$, where *s* is the number of breaks per fragment and P_0 is the fraction of fragments free of breaks, calculated as densitometric volume of FPG+alkali / alkali treated DNA (217). DNA from Jurkat cells and Alloxan (10 mM) treated Jurkat cells were used to optimize the experimental conditions. Alloxan induces oxidative damage to mtDNA. In the non-treated Jurkat cells, the proportion of mtDNA molecules free of breaks (P_0) was 0.96 (96%) when the FPG + alkali treated sample was compared to the alkali treated counterpart, resulting in a break frequency of s=0.038 per 16.5 kb linearized mtDNA. In the Alloxan treated Jurkat cells, the fraction of linearized mtDNA molecules free of break was P_0= 0.75 (75%) giving a break frequency of s=0.286.

Immunohistochemical detection of oxidative damage to DNA

Four um sections of paraffin embedded NAWM and chronic active plaque specimens were exposed to a mouse IgG1 to 8-OH-dG (Trevigen, Gaithersburg, MD) to observe the *in situ* distribution of oxidative damage to DNA following the protocol Yarborough et al (218). A horse anti-mouse biotinylated IgG was used as secondary antibody, and reactions were visualized by the Elite Vectastain ABC kit (Burlingame, CA). Slides were weakly counterstained with Haematoxylin to differentiate nuclei. Sections were analyzed on a Nikon Diaphot 300 microscope (Optical Apparatus Co., Inc, Ardmore, PA). Punctate distribution of 8-OH-dG was seen when paraffin embedded frontal brain tissue of a patient with Alzheimer's disease was investigated as a positive control. DNase pre-treatment of the positive control eliminated both the cytoplasmic and nuclear staining, confirming the specificity of the anti-8-OH-dG antibody.

Assays for citrate synthase and respiratory chain complexes

Frozen specimens were homogenized in 9 volumes of ice cold lysis buffer (320 nM sucrose, 1 mM EDTA, 10 mM Tris, pH 7.4) in a fritted glass - fritted glass homogenizer (165,219). After three cycles of freeze / thawing, mitochondrial fragments in homogenates were assayed for citrate synthase and the partial reactions of electron transport using standard enzyme assay methods. Absorbance changes

were continuously monitored at 37°C using a single-beam Perkin-Elmer Lambda 1 UV/VIS spectrophotometer. Sensitivity to enzyme inhibitors was used to confirm assay specificity. NADH dehydrogenase (DH) of complex I was measured at 420 nm as NADH-ferricyanide reductase in the presence of rotenone and azide (222-223). Complex I+III activity was measured at 550 nm as a rotenone-sensitive NADH-cytochrome c reductase (223-224). Complex II was measured at 600 nm as thenoyltrifluoroacetone-sensitive succinate-(2,6-dichlorophenol indophenol) reductase (224-225). Complex II+III was measured at 550 nm as antimycin A-sensitive succinate-cytochrome c reductase (225-226). Complex IV was measured at 550 nm as azide-sensitive ferrocytochrome c oxidase (225). Citrate synthase was measured at 412 nm using 5,5'-dithio-bis(2-nitrobenzoic acid) to detect free sulfhydryl groups in coenzyme A (227). All the measurements were performed in 10% w/v homogenates of NAWM and plaque tissues, and values were given as umol/min/g wet weight tissue. Blind assays were performed in quadruplicates, triplicates or duplicates. The assay conditions for white matter tissues were optimized in preliminary experiments. Protein concentration of each 10% homogenate was determined by a BioRad Protein Assay (BioRad, Hercules, CA) using bovine serum albumin as a standard.

Statistics

The Wilcoxon signed rank test was used to evaluate differences in values of oxidative damage and enzyme activity measured in plaques and NAWMs.

3.2.3.2 Detection of somatic mtDNA deletions

Autopsy brain tissues:

We obtained frozen, postmortem specimens including two trio sets of chronic active plaques, nearby NAGM, and adjacent NAWM from frontal, parietal and occipital lobes of 5 MS patients using similar criteria and sources as in 2.2.4.1 (table 16a). Adjacent hemispheral normal GM and WM specimens were also obtained from 9 non-neurological controls who died either from systemic disorders (cancer, cardiovascular disease) or car accident. Four of the non-neurological controls were matched by age to MS patients, and there were five older controls in order to encompass an age range of 34 to 80 years for the age – mtDNA deletion correlation study. In addition, we obtained frozen brain tissue specimens from 3 other neurological disease controls (OND) that included cortex from 2 patients with advanced Alzheimer's disease (AD) (90 and 94 years of age) and substantia nigra (SN) from 1 patient with advanced Parkinson's disease (PD) (81 years of age) (Table 16b). These specimens served as positive controls.

Preparation of tissues:
Frozen brain tissue specimens were placed in OCT and 16-20 micron sections were prepared by using a Leica CM1900 Cryostate (Leica Microsystems, Bannockburn, IL). The sections were then mounted on slides with steel frames and PET-membrane (Leica Microsystems, Bannockburn, IL) for staining and laser microdissection.

Cytochrome c Oxidase (Cox) / Succinate Dehydrogenase (SDH) histochemistry:
For Cox staining, sections were incubated in cytocrome c oxidase medium composed of 100 uM cytochrome c, 4 mM diaminobenzidine tetrahydrochloride, 20 ug/ml catalase in 0.2 M phosphate buffer pH 7.0 at 37^{o}C for 50 minutes. Subsequently, sections were washed in PBS (pH 7.4) 3 times for 10 minutes each. For SDH staining, sections were incubated in succinate dehydrogenase (SDH) medium composed of 130 mM sodium succinate, 200 uM phenazine methosulphate, 1 mM sodium azide, 1.5 mM nitroblue tetrazolium in 0.2 M phosphate buffer, pH 7.0 at 37^{o}C for 40 minutes. Then, sections were washed again in PBS (pH 7.4) 3 times for 10 minutes each and let dried at room temperature for 30 minutes (228-230).

Cox + / - single neurons (NAGM, GM, SN) and glial cells (NAWM, WM, plaque) were collected according to the manufacturers' protocol in 200 ul PCR tube caps by using a Leica Laser Microdissection Microscope (Leica Microsystems, Bannockburn, IL). Cresyl violet (Merck, Darmstadt, Germany) counter staining was applied for morphometric analyses of cells. In MS patients, we collected and analyzed at least 10 Cox positive and 10 Cox negative neurons and glial cells from each of the two sets of NAGM, NAWM and plaque containing specimens (altogether 2 sets of 3x[10+10]=120 single cells per individual) in the real time PCR experiments. In normal controls, we twice collected and analyzed 10 Cox positive and 10 Cox negative neurons and glial cells from each set of GM and adjacent WM specimens (2 sets of 2x[10+10]=80 single cells per individual) in the real time PCR experiments.

Table 16a. Specimens from MS patients

Code	Diagnosis	Age	Gender	Structure	Autolysis
3413a	MS	38	F	Occipital Plaque, Adjacent NAWM, Nearest NAGM	9.5 hours
3413b	MS	38	F	Occipital Plaque, Adjacent NAWM, Nearest NAGM	9.5 hours
3816a	MS	47	F	Frontal Plaque, Adjacent NAWM, Nearest NAGM	20.7 hours
3816b	MS	47	F	Parietal Plaque, Adjacent NAWM, Nearest NAGM	20.7 hours
4107a	MS	52	F	Frontal Plaque, Adjacent NAWM, Nearest NAGM	20.6
4107b	MS	52	F	Parietal Plaque, Adjacent NAWM, Nearest NAGM	20.6
3891a	MS	53	M	Parietal Plaque, Adjacent NAWM, Nearest NAGM	25.3 hours
3891b	MS	53	M	Occipital Plaque, Adjacent NAWM, Nearest NAGM	25.3 hours
3928a	MS	53	F	Frontal Plaque, Adjacent NAWM, Nearest NAGM	10.3 hours
3928b	MS	53	F	Parietal Plaque, Adjacent NAWM, Nearest NAGM	10.3 hours

Table 16b. Specimens from normal and OND controls

Code	Diagnosis	Age	Gender	Structure	Autolysis
37	NC	34	M	Lobe undefined; WM and adjacent GM	<10 hours
274	NC	46	F	Frontal WM and adjacent GM	<10 hours
214	NC	56	M	Lobe undefined; WM and adjacent GM	<10 hours
202	NC	57	M	Lobe undefined; WM and adjacent GM	<10 hours
3611	NC	64	M	Frontal WM and GM	17.5 hours
3602	NC	66	M	Frontal WM and GM	13.2 hours
3606	NC	71	M	Frontal WM and GM	11.5 hours
3603	NC	74	F	Frontal WM and GM	12 hours
3632	NC	80	M	Frontal WM and GM	25.5 hours
4078	PD	81	F	Substantia Nigra	12 hours
2985	AD	90	F	Lobe undefined Cortical GM	8 hours
2943	AD	94	F	Lobe undefined; Cortical GM	6 hours

Table 16 summarizes the diagnosis, age, gender, origin of brain tissue and postmortem time for MS patients (a) and normal and OND controls (b).

Isolation of DNA from single cells:

Each cell in the 200 ul PCR tube cap was covered with 1 ul of lysis buffer containing 1 ul of 10 mM EDTA pH8.0, 0.5% SDS and 2 mg / ml proteinase K. After 30 minutes of incubation at 37^{o}C, 10 ul of RNase/DNase free water was added to the lysate and gently mixed by pipetting (230). To inactivate proteinase K, the lysate was incubated at 95^{o}C for 2 minutes.

Real-time PCR:

To quantify the proportion of deleted versus full length mtDNA molecules per cell we used the ND4 / ND1 assay (229). This assay is based on the comparative amplification of two mtDNA regions: ND1 that is usually undeleted, and ND4 that is commonly deleted in patients with large mtDNA rearrangements related to mitochondrial diseases, aging and neurodegenerative diseases (229,230). Deletion rates were calculated as 1-ND4 / ND1 copy number values.

Primers:

ND1 forward nt3485-3504 primer: 5' CCCTAAAACCCGCCACATCT 3'

ND1 reverse nt3553-3532 primer: 5' GAGCGATGGTGAGAGCTAAGGT 3'

ND4 forward nt12087-12109 primer: 5' CCATTCTCCTCCTATCCCTCAAC 3'

ND4 reverse nt12170-12140 primer: 5' CACAATCTGATGTTTTGGTTAAACTATAATT3 3'

PCR reactions were carried out as described in 2.2.4 using the QuantiFast Sybr Green PCR kit (Qiagen, Hilden, Germany) for each reaction having 2x QuantiFast Sybr Green PCR Master Mix, 20 -20 pmol of the forward and reverse primers, 5-5 ul of DNA from the 11 ul total DNA lysate of each Cox + and Cox- cell. An internal standard including the human beta-globin gene was amplified yielding a 110 bp PCR product (Roche, Indianapolis, IN).

DNA amplification was carried out in an Applied Biosystems 7000 Real Time PCR machine using the following cycling conditions: 95^{o}C for 5 min followed by 42 cycles of 95^{o}C for 10 sec, 60^{o}C for 30 sec, and then 1 cycle at 60^{o}C for 2 min, and finally hold at 4^{o}C. In each reaction, a negative (no DNA template) and a non-deleted mtDNA control (mtDNA obtained from peripheral blood of a healthy control aged <40 years) was included.

Validation of the ND4 / ND1 test was performed by using a mtDNA template with a 7.44 kb deletion between nt [8,637-8,648] and [16,073-16,084] flanked by a 12 bp direct repeat at both ends. Southern blot analyses determined 35%, while our ND4 / ND1 test defined 37% deletion rate in this heteroplasmic mtDNA specimen that was generously provided by Dr. Shulin Zhang and Sandra Peacock at the Medical Genetics Laboratories of the Baylor College of Medicine.

A quality control experiment was performed to establish the inherent technical variations in the ND4 / ND1 test. We measured mtDNA deletions in 20 Cox positive single neurons from the cortex of a young normal control that was not expected to have deletions. This study revealed a mean ratio of ND4 / ND1 =1.0±0.06 (mean±SE), translating into 0±0.06 deletion.

Statistics:

For statistical analyses the non-parametric Wilcoxon signed rank test was used for intra-individual comparisons of mtDNA deletion values defined by real time PCR. For the inter-group comparisons of mtDNA deletion values, t-test and ANOVA analyses were performed using the SPSS v 14 package.

3.2.3.3 mRNA expression for apoptosis related molecules

Patients and specimens

The same specimens from patients and controls were included in this study as described in 2.2.4. Pre-evaluation of tissues using Haematoxylin & Eosin, Luxol Fast Blue and immunohistochemistry with anti-CD68 and anti-β_2-microglobulin was similar to that in Figure 4.

Isolation of RNA as described in 2.2.4.

Real Time PCR as described in 2.2.4.

mRNA expressions of six molecules (GSHS, SOD-1, Bak, Bcl-2, Bcl-x_L, β_2-microglobulin) involved in apoptosis, immune activation and anti-oxidative processes were studied.

The following primers were designed:

Forward primers	Reverse primers
GSHS: 5' – GCCGGTTTGTGCTAAAG - 3'	5' – CTTGTTCATCACGAGTGTC - 3'
Bcl-2: 5' – ATGGACCTAGTACCCACT - 3'	5' – CGGACTTCGGTCTCCTAA - 3'
Bcl2-x_L: 5' – GTAAACTGGGGTCGCAT - 3'	5' – AGTGTCTGGTCATTTCCG - 3'
Bak: 5' – TCAACCGACGCTATGACT - 3'	5' – TCTTCGTACCACAAACTGG - 3'
SOD-1: 5' – GCATCATCAATTTCGAGCAG - 3'	5' – TCAATAGACACATCGGCC - 3'
β_2-Mg: 5' – CTTGACACCAAGTTAGCCC - 3'	5' – ACATGGTTCACACGGCA - 3'

As an external standard, five different concentrations [$5x10^6$ copies/5ul; $5x10^5$ copies/5ul; $5x10^4$ copies/5ul; $5x10^3$ copies/5ul; $5x10^2$ copies/5ul] of a β_2 -microglobulin cDNA sample were amplified along with the experimental samples in each run (Roche, Indianapolis).

Analyses of data

The Wilcoxon Signed Rank Test, Students t-test and Pearson's correlation in the SPSS program were used.

3.3 RESULTS

3.3.1 Mitochondrial DNA mutations in MS, PON and NMO

3.3.1.1 Mitochondrial DNA mutations in MS (139)

The presence of 8 LHON mutations was tested by sequencing and restriction endonuclease digestion. The mutations included the established primary (at nt 11,778, 3,460, 14,484), a tentative primary (at 4,160) and three secondary mutations (at nt 4,216, 4,917, 13,708, 15,257). Altogether 1,700 basepairs of mtDNA, comprising major portions of the ND-1, ND-4 and ND-6 genes, were sequenced in twenty

MS patients. Although a number of synonymous mutations were detected, no primary LHON mutations or other than secondary LHON type of non-synonymous mutations were found in the regions studied. Because of the detection of secondary LHON mutations in this subgroup of patients, we expanded the study using restriction endonucleases in additional 33 MS patients and 74 controls (Table 17).

Of the 53 MS patients studied, 11 (20.8%) individuals carried two or three simultaneous secondary LHON mutations. Five patients (9.4%) had a mutation at nt 4,917 (ND-2) and 6 patients (11.3%) carried a mutation at nt 13,708 (ND-5), both in association with the mutation at nt 4,216 (20.8%). In one patient with simultaneous mutations at nts 4,216 and 13,708, an additional mutation was also detected at nt 15,257 (cyt b) (1.9%).

Among the 74 controls, 10 (13.5%) persons had secondary LHON mutations. Seven (9.5%) individuals had mutations at nt 4,216 in association with the mutations either at nt 4,917 or nt 13,708. Six (8.2%) persons were positive for the mutation at nt 4,917, and four (5.4%) for the mutation at nt 13,708. Mutation at nt 4,917 alone in two individuals, and mutation at nt 13,708 alone in one individual was detected. One individual with mutations at nts 4,216 and 13,708, also carried a mutation at nt 15,257 (1.4%).

Table 17. Secondary LHON mutations in MS patients and controls

Mutation	MS patients	Controls	*Controls*	*LHON*
4,216	20.8% (11/53)*	9.5% (7/74)	*7-13%*	*38%*
4,917	9.4% (5/53)	8.2% (6/74)	*3-4%*	*17%*
13,708	11.3% (6/53)	5.4% (4/74)	*5-6%*	*31%*
15,257	1.9% (1/53)	1.4% (1/74)	*0.3%*	*7-9%*
individuals with mutations	20.8% (11/53)	13.5% (10/74)		
all simultaneous mutations	20.8% (11/53)*	9.5% (7/74)		
4,216+4,917	9.4% (5/53)	5.4% (4/74)		
4,216+13,708	11.3% (6/53)	4.1% (3/74)		

The left part of the table summarizes the frequency of secondary LHON mutations (number of individuals with mutations/all individuals investigated) in MS patients and controls. * p value=0.036, when comparing the incidence of the mutation at nt 4,216 in the two groups as well as when comparing the incidence of the simultaneous mutations associated with the one at 4,216. The remaining comparisons do not reveal significant differences. The right part of the table with italicized letters and numbers is a citation from previous studies for comparison (231).

Statistical analysis using a one-tailed χ^2 test revealed that the frequency of the mutation at nt 4,216 as well as the simultaneous occurrence of the mutations associated with the one at nt 4,216 (20.8% vs 9.5%) was significantly higher in MS patients than in controls (p-value=0.036). When the frequency of the individual secondary mutations was compared in the two groups, no statistical significance was obtained. Similarly, when all individuals positive for mutations (20.8% vs 13.5%) were considered, the difference between the two groups was not significant.

Both male and female patients with secondary LHON mutations displayed heterogeneity of the clinical phenotypes (Table 18). Two patients had no visual problems (No.2 and 7) confirmed by ophthalmological and visual evoked potential studies. The remaining patients had ON of varying severity. Most patients suffered from RR-MS with mild to moderate disability. The clinical characteristics of the autopsy case (No.5) suggested PP-MS with a fulminant course. LHON was suspected but excluded in one family (of patient No.1). Only one (No.3) of the patients with secondary LHON mutations had relatives with MS, however, on the father's side.

Table 18. Summary of the clinical data of MS patients with secondary LHON mtDNA mutations

Patient	Mutation	Specimen	Gender	MS	course	Right	Left ON
1.	4,216+4,917	PBL	F	RR/SP	severe	+	+
2.	4,216+4,917	PBL	F	RR	mild	-	-
3.	4,216+4,917	PBL	F	RR/SP	severe	+	+
4.	4,216+4,917	PBL	F	RR	severe	+	+
5.	4,216+4,917	NAWM	F	PP	fulminant	+	+
6.	4,216+13,708 +15,257	PBL	F	RR/SP	moderate	+	+
7.	4,216+13,708	PBL	M	RR	mild	-	-
8.	4,216+13,708	PBL	M	RR/SP	severe	+	+
9.	4,216+13,708	PBL	F	RR	mild	+	-
10.	4,216+13,708	PBL	F	RR	mild	-	+
11.	4,216+13,708	PBL	F	RR/SP	moderate	+	+

Table 18 shows the detected mtDNA mutations / haplotypes, specimens studied, gender, course of MS and involvement of optic nerve in patients with secondary LHON mutations. Course mild: EDSS <3 at 10 years from onset; moderate: EDSS 3.5-5.5 at 10 years from onset; severe: EDSS 6 or worse at 10 years from onset; fulminant: EDSS: 10 at 3 years of onset.

In summary, this investigation failed to detect primary LHON mutations, but was the first study to suggest an increased frequency of secondary LHON mutations in patients with MS. The secondary LHON variants aligned in haplotypes. The MS associated polymorphisms and haplotypes were not related to distinct phenotypes (139).

3.3.1.2 LHON type mtDNA mutations in patients with PON (142)

Since we could not detect primary LHON mutations in typical forms of MS, the question arose if these mutations are more prevalent in patients with PON. The study revealed that none of the selected 22 patients with PON carried the 11,778, 3,460 or 14,484 primary LHON mutations (Tables 12, 13). Only two patients (No. 9 and 11) had ON without clinical MS or MRI signs of cerebral white matter lesions. One of these two patients had a progressive visual deterioration, while the other had relapsing-remitting

disease. Among the twenty MS patients with PON, two had a PP-MS course, and the others suffered from RR- or SP-MS. None of these patients had positive family history for LHON, and four of them had another family member with MS (either of the mother's or of the father's side) (Table 12).

MS (PON) patients No. 2, 4, 6, 7, 10, 14, 17, 18, 19, 20 and 21 had severe disability as measured by the EDSS Score (EDSS > 6) in addition to having severe visual impairment. One of these patients (No. 14) with blindness had become bedridden during the first year of the disease. Five patients (No. 4, 17, 18, 19, 21) reached EDSS 6 to 7 in less than ten years from diagnosis. The remaining five patients developed severe disability (EDSS > 6) within 10 to 23 years from diagnosis (Table 12).

Besides patients No. 9 and 11 who had isolated ON, patients No. 3, 5, 13, 15, 16 and 22 had mild or no neurologic findings despite multiple white matter lesions in the brain. The duration of the disease was relatively long in all but one of these patients (21, 14, 19, 1, 7 and 30 years, respectively) (Table 12).

In summary, the data suggest that pathogenic LHON mtDNA mutations do not occur frequently in PON (142). The severity of visual loss may not always correlate with the severity of MS.

3.3.1.3 Sequence analyses of the entire mtDNA in patients with MS and NMO (140,147)

Sequencing of mtDNA in 3 MS and 3 NMO patients

Three MS patients were chosen for the studies: 1) MS-R4 with unusual mtDNA polymorphisms detected in a previous study (139); 2) MS-1NP with a fulminant course of MS; and 3) MS-R51 with PON. The mtDNA was amplified in 35 overlapping 600 bp fragments and directly sequenced. Ambiguities were solved by antisense sequencing, use of additional sequencing primers or restriction endonuclease analysis. All mtDNA sequence changes are reported as L-strand substitutions and according to information available in 1995 (150, http://www.mitomap.org/). Italicized sections discuss details of the analyses not essential for understanding the final results.

Patient MS-R4 had 45 nucleotide alterations in mtDNA relative to the Cambridge sequence (150)(http://www.mitomap.org/). After excluding common polymorphisms, non-coding and synonymous mutations, 4 new mtDNA variants were found in MS-R4. Text in italics describes the details.

Details: Mutations (or nt insertion/deletion) at nts 73, 151, 152, 261, 264, 310, 514, 569, 16,291, 16,304, 16,318, 16,400, 16,519 are located within non-coding (D-loop) regions, and are likely to be non-pathogenic. The mutations detected at nt 750, 1,438 within the 12S rRNA, and at nt 1,811, 2,706 within the 16S rRNA are known

polymorphisms (232235). A T to C transition at nt 980 located in the 12S rRNA gene had not been described, and was thus selected for further studies. The remaining mutations are located within protein or tRNA coding regions. Synonymous nucleotide transitions or transversions (which do not change amino acid sequences) occurred at nt 3,741, 4,769, 4,985, 5,360, 7,028, 7,184, 7,894, 7,903, 11,467, 11,719, 12,372, 14,245, 14,365, 14,569, 14,860, 14,869. Missense mutations (which cause amino acid alteration) at nt 8,860, 9,559, 13,702, 14,199, 14,272, 14,368 and 15,326 are either errors of the Cambridge sequence or common polymorphisms (181-183,232-236). The mutation at nt 12,308 in the $tRNA^{Leu}$ was also described as a polymorphism (181-183,232-236). In addition to the mutation at 980 in the 12S rRNA gene, this patient harbored three missense mutations which were not found in the large reference data base (181-183,232-238). The C to T transition at nt 8,684 in the ATPase 6 gene modifies Thr to Ile. The G to A mutation at nt 9,300 in the CO III gene causes an Ala to Thr exchange. The A to G mutation at nt 13,966 in the ND-5 gene alters Thr to Ala.

Thus, the sequence analyses identified four novel mutations at nt 980, 8,684, 9,300 and 13,966 in MS-R4, which were chosen for frequency comparisons in cohorts of MS patients and controls.

Patient MS-1NP had 40 mtDNA mutations relative to the Cambridge sequence. After excluding common polymorphisms, non-coding and sysnonymous mutations, 3 new mtDNA variants were found in MS-1NP.

Details; Mutations (or nt insertion) at nts 310, 317, 709, 16,126, 16,294 and 16,519 are located within the non-coding region, and thus are likely non-pathogenic. Mutations at nt 750 and at nt 2,706 within the 12S rRNA encoding region had been described in control individuals (232-236). The G to A transition at nt 1,888 within the 16S rRNA was detected in two individuals with LHON and a bipolar disorder (M.D. Brown personal communication). However, its occurrence in the general population or in diseases was not reported. The mutations at nts 3,423, 4,769, 4,985, 7,028, 7,184, 7,193, 7,199, 11,251, 11,335, 11,719, 11,812, 12,441, 13,326, 13,368, 14,233, 14,365, 14,905, 15,607 are synonymous. The detected missense mutations at nts 4,216, 4,917, 8,860, 9,559, 13,702, 14,199, 14,272, 14,368, 15,326, 15,452 are either errors of the Cambridge sequence or known polymorphisms (181-183,213,232-236). The T to C transition at 10,463 in the $tRNA^{Arg}$ gene, and the G to A transition at 15,928 in the $tRNA^{Thr}$ gene of this MS patient were reported in patients with mitochondrial encephalomyopathy and in controls (238).

Therefore, mutations at nt 1,888, 10,463 and 15,928 were identified in MS-1NP and chosen for further analyses.

Patient MS-R51 had 38 mtDNA nucleotide alterations. After excluding common polymorphisms, non-coding and sysnonymous mutations, one candidate mtDNA variant was found in MS-R51.

Details: Mutations (or nt insertion/deletion) occurred within the regulatory region at nts 73, 263, 311, 426, 497, 514, 16,048, 16,224, 16,291, 16,311, 16,519. Polymorphisms were identified at nts 750, 1,189, 1,438 within the 12S rRNA gene, and at nts 1,811, 2,706, 3,106 within the 16S rRNA (181-183,213,232-236). Nucleotide alterations within the coding region at nt 3,423, 3,480, 4,769, 4,985, 7,028, 9,698, 11,719, 12,372, 14,019, 14,046, 14,167, 14,365 are synonymous base substitutions. The detected missense mutations at nts 8,860, 9,055, 9,559, 10,398, 13,702, 14,199, 14,368 and 15,326 are either errors of the Cambridge sequence or known polymorphisms (181-183,213,232-236). The T to C transition at 14,798 causing Phe to Leu modification in the cytochrome b of this patient was described in controls. However, its potential involvement in LHON was also suggested (181,235).

Therefore, the 14,798 T to C variant detected in MS-R51 was selected for further testing in MS patients and controls.

NMO patients A, B and C: Compared to the Cambridge sequence, we identified 44, 43 and 32 homoplasmic variants in the spinal cords of patients A, B and C, respectively (150). Analyses of these variants were similar in NMO as in MS patients (italicized sections). After the exclusion of synonymous mutations and common polymorphisms, only one new homoplasmic variant was identified at T4695C, Phe->Leu in the ND2 gene of patient B (http://www.gen.emory.edu/mitomap.html 2000).

Table 19. Unusual mtDNA variants detected by sequencing in patients with MS and NMO

	nucleotide/amino acid	gene	heteroplasmy	MS patients	controls
MSR4					
980	T/C	12S rRNA	-	1/52	0/63
8,684	C/T Thr/Ile	ATPase6	-	1/52	0/63
9,300	G/A Ala/Thr	CO III	-	1/52	0/63
13,966	A/G Thr/Ala	ND-5	-	2/52	0/63
MS1NP					
1,888	G/A	16S rRNA	-	1/52	0/63
10,463	T/C	$tRNA^{Arg}$	-	5/52	6/65
15,928	G/A	$tRNA^{Thr}$	-	5/52	6/65
MSR51					
14,798	T/C Phe/Leu	cyt b	-	10/52	6/65
NMO B					
4,695	T/C Phe/Leu	ND-2	-	1/65	2/80

In summary, after analyzing the nucleotide alterations in 3 MS and 3 NMO patients, 8 novel or ambiguous mtDNA variants at nt 980, 8,684, 9,300, 13,966 (MS-R4), at 1,888, 10,463, 15,928 (MS-1NP) and at 14,798 (MS-R51) were detected and selected for further studies from the MS group, and 1 mutation at nt 4,695 (NMO-B) was selected for further studies from the NMO group (Table 19).

Characterization of the selected mtDNA variants (Table 19)

The unusual mtDNA variants detected in MS-R4:

The mutation at 980 is a T to C transition in a non-conserved site of the 12S rRNA gene, that creates a recognition site for *Bst* NI restriction endonuclease when the appropriate mismatching primers are used for amplification (150,239-241). This mutation in MS-R4 appeared homoplasmic by sequencing as well as by the first restriction endonuclease analysis. The homoplasmic appearance was further confirmed by a second restriction endonuclease analysis using less complex PCR primers which created a restriction site for *Hinf* I in the presence of the wild type, but not of the mutated mtDNA sequence (Fig.10a). This mutation was only detected in MS-R4, and in none of the additional 51 patients or 63 controls (Table 19).

The mutation at 8,684 is a C to T transition resulting in a threonine to isoleucine exchange in a non-conserved region of the ATPase 6 (Table 20a) (150,239-241). By using mismatching primers for amplification and *Ase* I restriction endonuclease, the presence of this homoplasmic mutation was confirmed in MS-R4 (Fig.10b). The additional screening detected this mutation in 1/52 MS patients (MS-R4) and 0/63 controls.

The mutation at 9,300 is a G to A transition causing a non-conserved alanine to threonine exchange in an otherwise conserved region CO III (Table 20b) (150,239-241). By using mismatching primers and *Mse* I restriction endonuclease, the presence of this homoplasmic mutation was confirmed in MS-R4 (Fig.10b). Screening of the patient and control cohorts detected this mutation in 1/52 MS patients (MS-R4) and in 0/63 controls.

The mutation at 13,966 is an A to G transition resulting in a threonine to alanine exchange in a non-conserved region of ND-5 (Table 20c) (150,239-241). Presence of this mutation in MS-R4 was confirmed by PCR using sense and mismatching antisense primers, and digesting the PCR product with *Hha* I (Fig.10b). This homoplasmic mutation was present in 2/52 MS patients (MS-R4 + 1 additional patient) and in 0/63 controls (χ^2 =2.446, p-value NS). The mutation at 13,966 had not been detected in the large control population of the reference database. The rare mtDNA haplotype of MS-

R4 is indicated by other mtDNA variants including the ones at nts 980, 8,684, 9,300. The second patient with the 13,966 variant belongs to a different mtDNA lineage as he was negative for mutations at nts 980, 8,684 or 9,300. Therefore, this mtDNA mutation may be either a polymorphism associated with infrequent haplotypes or a variant associated with MS in a subgroup of patients.

The unusual mtDNA variants detected in patient MS-1NP:
The mutation at 1,888 is a G to A transition in the 16S rRNA gene. This site is conserved in humans, bovines, mice, Xenopus and sea urchins (150,239-241). Using the appropriate mismatching primers this mutation creates a restriction site for *Hind* III. The homoplasmic nature of the mutation (in addition to sequencing) was confirmed in the mtDNA of MS-1NP in a second restriction endonuclease analysis, in which the primers were designed in a way that the wild type PCR fragment is cleaved, while the mutated fragment remains uncut (Fig.10a). This mutation was not detected in the 63 controls or in the additional 51 MS patients.

The mutation at 10,463 is a T to C transition in the $tRNA^{Arg}$ gene. To confirm the presence of this homoplasmic mutation in MS-1NP, PCR was performed using the appropriate mismatching sense and antisense primers, and the product was digested by *Bgl* II (Fig.10b). Although the T nucleotide at 10,463 is conserved in human, bovine, mouse and Xenopus (150,239-241), the T to C transition had been described in controls (238). We found it in 5/52 (9.6%) patients and 6/65 (9.2%) controls, suggesting no pathogenic significance for MS.

The mutation at 15,928 is a G to A transition in the $tRNA^{Thr}$ gene, which is a variable site in human, bovine, mouse and Xenopus (150,239-241). The presence of this homoplasmic mutation was confirmed in MS-1NP by digesting the appropriate PCR product with *Mbo* II (Fig.10b). The mutation at 15,928 always occurred with the one at 10,463, and was detected in 5/52 (9.5%) patients and 6/65 (9.2%) controls, indicating a lack of association with MS.

The unusual mtDNA variant detected in patient MS-R51:
The mutation at 14,798 is a T to C transition resulting in a phenylalanine to leucine exchange in a relatively conserved domain of cytochrome b (Table 20d) (150,239-241). The presence of this homoplasmic mutation at 14,798 was confirmed in MS-R51 by using the appropriate sense and mismatching antisense primers and digesting the PCR product with *Dde* I (Fig.10b). Screening the two cohorts revealed the presence of this mutation in 10/52 (19.2%) MS patients and 6/65 (9.2%) controls, indicating a trend but not a significant difference in the two groups (χ^2=2.447, p-value NS).

Table 20. Amino acid sequence conservation in new mtDNA variants detected in MS

a. Mutation at 8,684:

Human	I K L ***T*** S K Q
Bovine	L Q L V S K Q
Mouse	V K L I I K Q
Sea urchin	R S N I - L E
Xenopus	L H N - F T T
Drosophila	L L T L H K E

b. Mutation at 9,300:

Human	G L ***A*** M W F H
Bovine	G L T M W F N
Mouse	G L V M W F H
Sea urchin	G M V L W F H
Xenopus	G L A M W F H
Drosophila	G M V K W F H

c. Mutation at 13,966:

Human	G L L ***T*** S Q N L
Bovine	N L S M S Q K S
Mouse	S L K T S L T L
Sea urchin	S L A L S F F S
Xenopus	N L N L A Q N I
Drosophila	F Y P L N Y G Q

d. Mutation at 14,798:

Human	H S ***F*** I D L P
Bovine	N A F I D L P
Mouse	H S F I D L P
Sea urchin	S T F V D L P
Xenopus	N S F I D L P
Drosophila	N A L V D L P

Interspecies comparison of the amino acid sequences within the ATPase 6 (a), CO III (b), ND-5 (c) and cytochrome b (d). Genes of these proteins carried missense mutations (variants) in the three MS patients (150,239-241).

Figure 10. Detection of the mtDNA mutations by restriction endonucleases

(a)

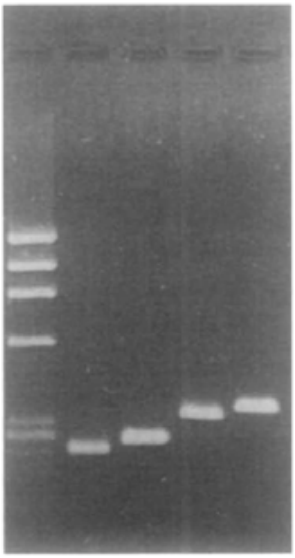

Legend to Figure 10a.

Lane 1: ΦX 174 molecular weight marker; Lane 2: The wild type sequence of the 955-1,212 PCR product (258 bp) from MS-1NP is cleaved into a 235 and a 23 bp fragment by *Hinf* I; Lane 3: *Hinf* I digestion of the 955-1,212 PCR product from MS-R4 results in an uncleaved 258 bp fragment, as the homoplasmic mutation at nt 980 eliminates the restriction site for *Hinf* I; Lane 4: The 1,865-2,217 PCR product (353 bp) from MS-R4 is cleaved by *Hha* I into a 329bp and a 24 bp fragment in the absence of the mutation at 1,888; Lane 5: *Hha* I digestion of the 1,865-2,217 PCR product from MS-1NP results in an uncleaved 353 bp DNA fragment, since the homoplasmic mutation at 1,888 eliminates the restriction site for *Hha* I.

(b)

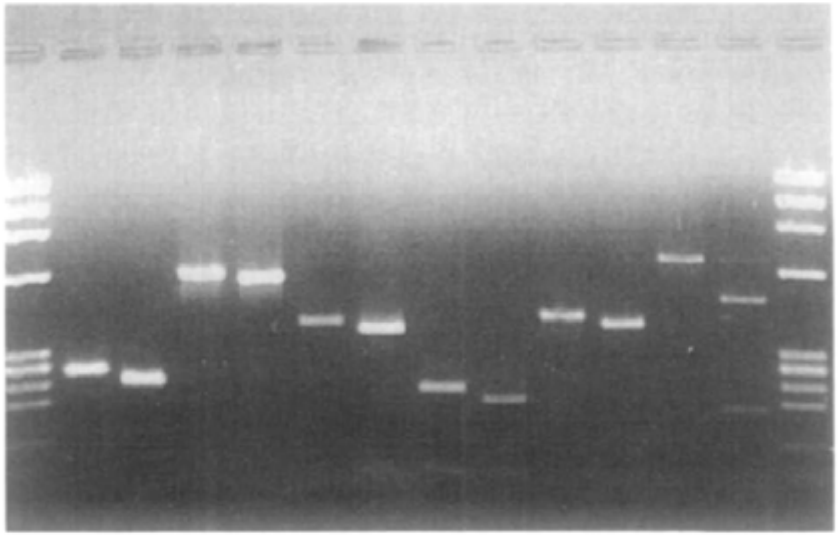

Legend to Figure 10b.

Lane 1: ΦX 174 molecular weight marker; Lane 2: The 8,656-8,918 (262bp) PCR product from MS-1NP is not cleaved by *Ase* I in the absence of the mutation at 8,684; Lane 3: *Ase* I digestion of the 8,656-8,918 PCR product from patient MS-R4 in the presence of the mutation at 8,684 results in a 24bp and a 238bp band; Lane 4: PCR product 9,278-9,871 (593bp) from MS-1NP is uncleaved by *Mse* I in the absence of mutation at 9,300; Lane 5: *Mse* I digestion of the 9,278-9,871 PCR product from MS-R4 in the presence of the mutation at 9,300 results in a 20bp and a 573 bp fragment; Lane 6: *Hha* I digestion of PCR product 13,570-13,993 (423bp) from MS-1NP results in a 398 bp and a 25 bp fragment in the absence of the mutation at 13,966; Lane 7: *Hha* I digestion of the PCR product 13,570-13,993 from MS-R4 results in a 371bp, 27bp and 25 bp fragment in the presence of the mutation at 13,966; Lane 8: *Dde* I digestion of the PCR product 14,559-14,825 (266bp) from MS-1NP results in a 217 bp and a 49 bp band in the absence of mutation at 14,798; Lane 9: *Dde* I digestion of the PCR product 14,559-14,825 from MS-R51 results in a 188bp, 49bp and a 29bp fragment in the presence of the mutation at 14,798; Lane 10: *Bgl* II digestion of PCR product 10,436-10,849 (413bp) from MS-R4 results in an uncleaved 413 bp fragment in the absence of mutation at 10,463; Lane 11: *Bgl* II digestion of PCR product 10,436-10,849 from MS-1NP results in a 23bp and a 390bp band in the presence of the mutation at 10,463; Lane 12: PCR product 15,761-16,420 (659 bp) from MS-R4 is uncleaved by *Mbo* II in the absence of the mutation at 15,928; Lane 13: *Mbo* II digestion of PCR product 15,761-16,420 from MS-1NP results in a 177 bp and a 482 bp fragment in the presence of mutation at 15,928.

The unusual mtDNA variant detected in NMO-B:

After the exclusion of synonymous mutations and common polymorphisms (http://www.gen.emory.edu/mitomap.html 2000), only one new variant, a T->C transition was identified at nt 4,695, resulting in a phenylalanine to leucine exchange in the ND2 subunit of patient B. As no new

variants were detected in patients A and C, we can establish that Devic's disease can occur without mtDNA mutations. The only unique mtDNA mutation at nt T4,695C in patient B was homoplasmic, characteristic of phylogenetically old and biologically neutral mutations. Restriction endonuclease analysis (with *Ear* I specific for the wild type CTC TTC (N)1 sequence) detected the T4,695C variant in 2 of 80 Caucasian controls, and in 1 of 65 Caucasian MS patients, confirming that this polymorphic mutation has no relevance to NMO.

In summary, these analyses establish that both MS and NMO can occur without mtDNA mutations of pathogenic significance. However, certain mtDNA polymorphisms seem to be enriched and remain to be investigated in these patient populations (140, 147).

3.3.1.4 Large scale screening of mtDNA in Caucasian controls and patients with MS (144,145)

The MS associated mtDNA polymorphisms

One hundred and ninety-one restriction sites defined 115 haplotypes in 77 Caucasian MS patients and 84 Caucasian controls. In addition to the published 136 restriction site polymorphisms (190), 55 site gains or losses were identified in these patients and controls. There were 37 new site gains and 18 new site losses. Forty-eight of these 55 new polymorphisms were present in one or two MS patients or controls, without statistical differences between groups, and therefore, we excluded these variants from further analyses. The remaining six site gains and one loss were present in various numbers of patients and controls (Table 21). Five of these 7 sites are known restriction site polymorphisms (at nts 7,828, 14,509 and 16,373), or synonymous mutations without amino acid sequence modification (at nts 14,139 and 14,587). No significant difference in frequencies of these mutations was found (Table21). The 13,966*Hha*I mutation was identified in 3 patients and 2 controls (p=0.674) (Table 21). The frequency of the 14,798*Dde*I mutation was higher in MS patients than in controls (26% vs 13.1%, respectively) (p=0.046) (Table 21).

Among the known Caucasian restriction site polymorphisms, the only observed difference was an increase of the 10,394*Dde*I site in MS patients (26/77) as compared to controls (13/84) (p=0.01).

Table 21. New mtDNA restriction sites detected in more than two patients and controls

Site	Enzyme	Gain/loss	Mutation	Control	MS	p-value
nt 7828	*Hha*I	loss	Rs Pol	8/84	11/77	0.464
nt 13,966*	*Hha*I	gain	ND5 mis	2/84	3/77	0.671
nt 14,140	*Mbo*I	gain	ND5 syn	3/84	1/77	0.622
nt 14,509	*Alu*I	gain	Rs Pol	4/84	1/77	0.370
nt 14,587	*Dde*I	gain	ND6 syn	0/84	3/77	0.107
nt 14,798*	*Dde*I	gain	Cytb mis	11/84	20/77	0.046
nt 16,373	*Mbo*I	gain	Rs Pol	3/84	0/77	0.248

nt: nucleotide; Rs Pol: restriction site polymorphism; mis: missense; syn: synonymous; *Section 3.3.1.3 (Ref 123) suggested a potential relevance of these mutations to MS. p-value: calculated by Fisher's exact test (two-tail).

Among previously described polymorphisms with potential relevance to MS, the T to C transition at 4,216 in the ND1 gene was present in 20 patients (25.9%) and 20 controls (23.8%) (p=0.855). The 13,708 G to A transition in ND5 was found in somewhat more MS patients than in controls (12/77, 15.8% vs. 7/84, 8.6%, respectively), but the difference was not significant (p=0.221). The *Msp*I (an isoschizomer of *Hpa*II) site loss at nt 15,925 of mtDNA was present in 12.9% (10/77) of these of MS patients and 19% (16/84) of controls (p=0.392).

In summary, screening of mtDNA in Caucasian MS patients and controls revealed no pathogenic mutations associated with MS. However, an increase in the frequency of two *Dde*I polymorphisms (at 14,798 and 10,394) was observed in MS.

The MS associated mtDNA haplotypes

We converted the restriction site polymorphisms of each individual into a binal format for computer analysis (0 meaning absence, 1 meaning presence of a site). Following the alignment of individual haplotypes, 1000 bootstrappings were performed, and a consensus tree was created from the resultant 1000 trees by using the NJ method (Figure 11).

Parsimony or NJ method-based analyses of mtDNA restriction site polymorphisms established four (H, I, J and K) major haplogroups in Caucasians (190). Each haplogroup was determined by a single mutation or by a set of mutations (Table 22). Using the NJ program, we also identified four major haplogroups (Table 23, Figure 11). The distribution of the published and our controls among

haplogroups H, I, J and K is similar (Table 23) (190). The distribution of MS patients and controls is also comparable within the four haplogroups (Table 23). Only a trend for increase of MS patients in haplogroup J (defined by -13,704*Bst*I / -16,065*Hinf*I) is observed (p=0.070). Analyses of the subdivisions of the phylogenetic tree (Figure 11) suggest that the distribution of patients relative to controls is similar within haplogroups H and I. However in both haplogroups K and J, an increase of patients with either the +10,394*Dde*I / +14,798*Dde*I / -9052*Hae*II (K*) (p=0.033) or the +10,394*Dde*I / +14,798*Dde*I / -13,704*Bst*NI / -16,065*Hinf*I (J*) (p=0.049) haplotype can be observed (Figure 11, Table 24). Combined comparison of patients (26%) and controls (7%) carrying +10,394*Dde*I/+14,798*Dde*I haplotypes (either in haplogroup K or J) reveals a difference with even a higher degree of significance (p=0.001). The relative risk of individuals with the K*, J* and K*+J* mtDNA haplotypes for developing MS is 1.67, 1.75 and 1.82, respectively (Table 24).

Table 22. Caucasian mtDNA haplogroups are determined by a set of restriction sites (190)

H haplogroup: -10,394/*Dde*I; -7025/*Alu*I

I haplogroup: -1715/*Dde*I; -4529/*Hae*II; +10,028/*Alu*I; +8249/*Ava*II and -8250/*Hae*III; +16,389/*Bam*HI/*Mbo*I; -16,390/*Ava*II

J haplogroup: -13,704/*Bst*NI; -16,065/*Hinf*I

K haplogroup: -9052/*Hae*II; -9053/*Hha*I

Table 23. Distribution of Caucasian haplotypes in the four haplogroups

	Controls* (%)	Controls** (%)	MS*** (%)	p-value*/**	p-value**/***
H	40.0	46.4 (39/84)	39.0 (30/77)	0.349	0.426
I	7.4	3.7 (3/84)	6.6 (5/77)	0.281	0.481
J	9.1	6.0 (5/84)	15.6 (12/77)	0.471	0.070
K	7.4	10.7 (9/84)	15.6 (12/77)	0.476	0.483

*: Caucasian controls in the study by Torroni et al (190). **: Caucasian controls in this study. ***: Caucasian MS patients in this study. p-value: calculated by Fisher's exact test (two-tail)

Table 24. Association between mtDNA haplotypes and MS

Haplotype	Defining sites	Controls	Patients	p-value	RR
K*	-9052*Hae*II/ +14,798*Dde*I/ +10,394*Dde*I	4/84 (4.8%)	12/77 (15.6%)	0.033	1.67
J*	-13,704*Bst*NI/ -16,065*Hinf*I/ +10,394*Dde*I/ +14,798*Dde*I	2/84 (2.3%)	8/77 (10.4%)	0.049	1.75
K*+J*	as above	6/84 (7.1%)	20/77 (26%)	0.001	1.82

P-values were calculated by Fisher's exact test (two-tail). RR: the relative risk for developing MS.

The gain of 10,394*Dde*I site results from an A to G transition at 10,398 changing Thr to Ala in the ND3 gene product. Lack of this mutation is characteristic for the majority of Caucasians and, along with -7,025*Alu*I, determines haplogroup H. The 14,798 mutation is a T to C transition changing Phe to Leu in cytochrome b. This polymorphism was noted more frequently in MS patients than in controls (Section 3.3.1.3, ref 140). The loss of the *Hae*II site at 9,052 results from a G to A transition at 9,055, which changes Ala to Thr in the ATPase 6 gene. This polymorphism determines the Caucasian haplogroup K. The loss of the 13,704*Bst*NI site results from a G to A transition at 13,708, converting Ala to Thr in the ND5 gene. The G13,708A is a known secondary LHON mutation. The 16,065 *Hinf*I site loss is caused by a C to T polymorphic mutation within the D-loop region. Individuals with these polymorphisms in haplogroup J also carry the 4,216*Nla*III site related to a T to C transition within the ND1 gene. The T4,216C polymorphism is another secondary LHON mutation. Analyses of all the tested restriction site polymorphisms reveal association only between the 10,394*Dde*I and 14,798*Dde*I polymorphisms and MS. The phylogenetic tree (Figure 11) demonstrates that these polymorphisms (+10,394*Dde*I / +14,798*Dde*I) accumulated in haplotypes K* and J* that are associated with the disease (Table 24).

In summary, we identified two mtDNA haplotypes K* and J* in association with MS. Secondary LHON mutations which previously showed association with MS, also accumulate in haplotype J*. Individuals with the +10,394*Dde*I / +14,798*Dde*I restriction sites-defined K* and J* haplotypes in haplogroups K or J are at a moderately higher risk for developing MS.

MS phenotypes do not correlate with mtDNA genotypes

Patients with the K* haplotype had an age of onset of MS between 20 and 40 (mean: 30.2+/-6.3) years. Six patients (50%) had ON at onset with or without other neurological focal signs, and one patient developed PON (8.3%). The symptoms at the onset or at the last visit did not suggest preferential distribution of lesions in the CNS in association with this haplotype. Patients had both benign and disabling disease. Although all patients were female, this likely occurred by chance because of the small size of this haplogroup, and because of the relative overrepresentation of females in the study. None of these patients had positive family history for MS. The parameters investigated did not differ statistically in patients with K* compared to those in patients with non-K* haplotypes.

Patients with haplotype J* had an age of onset between 18 to 52 years (mean: 33.1+/-11.2), and half of the patients were female. Five patients (63%) had ON with or without other neurological symptoms at onset, and 3 (37.5%) developed PON. The distribution of the symptoms at onset, or at the last visit, did not suggest preferential involvement of any CNS region in association with this haplotype. Both benign and disabling courses of the disease were observed. Only one familial occurrence, a father to son transmission of MS was noted. The clinical parameters investigated in patients with the J* haplotype did not differ from those with non-J* haplotypes. No statistical difference was revealed when the clinical parameters in patients with the K*+J* haplotypes were compared to those with non-K*+J* haplotypes.

In summary, no distinct phenotypic characteristics of MS seems to correlate with the +10,394*Dde*I/+14,798*Dde*I mtDNA haplotypes (144,145).

Figure 11. Phylogenetic tree of Caucasian MS patients and controls.

Legend to Figure 11. A modified version of the MEGA program (216) (NJBOOTW written by K. Tamura) was used to perform the alignment and the bootstrapping. A consensus tree from 1000 bootstrappings was created by the NJ method. The tree in Figure 11 is a representative of several similar consensus trees investigated. The four major Caucasian haplogroups (H, I, J and K) are indicated (190). MS clusters within haplotype J* in haplogroup J and haplotype K* in haplogroup K are labeled with “*” and “**”, respectively.

Figure 11. Philogenetic tree of Caucasian controls and MS patients

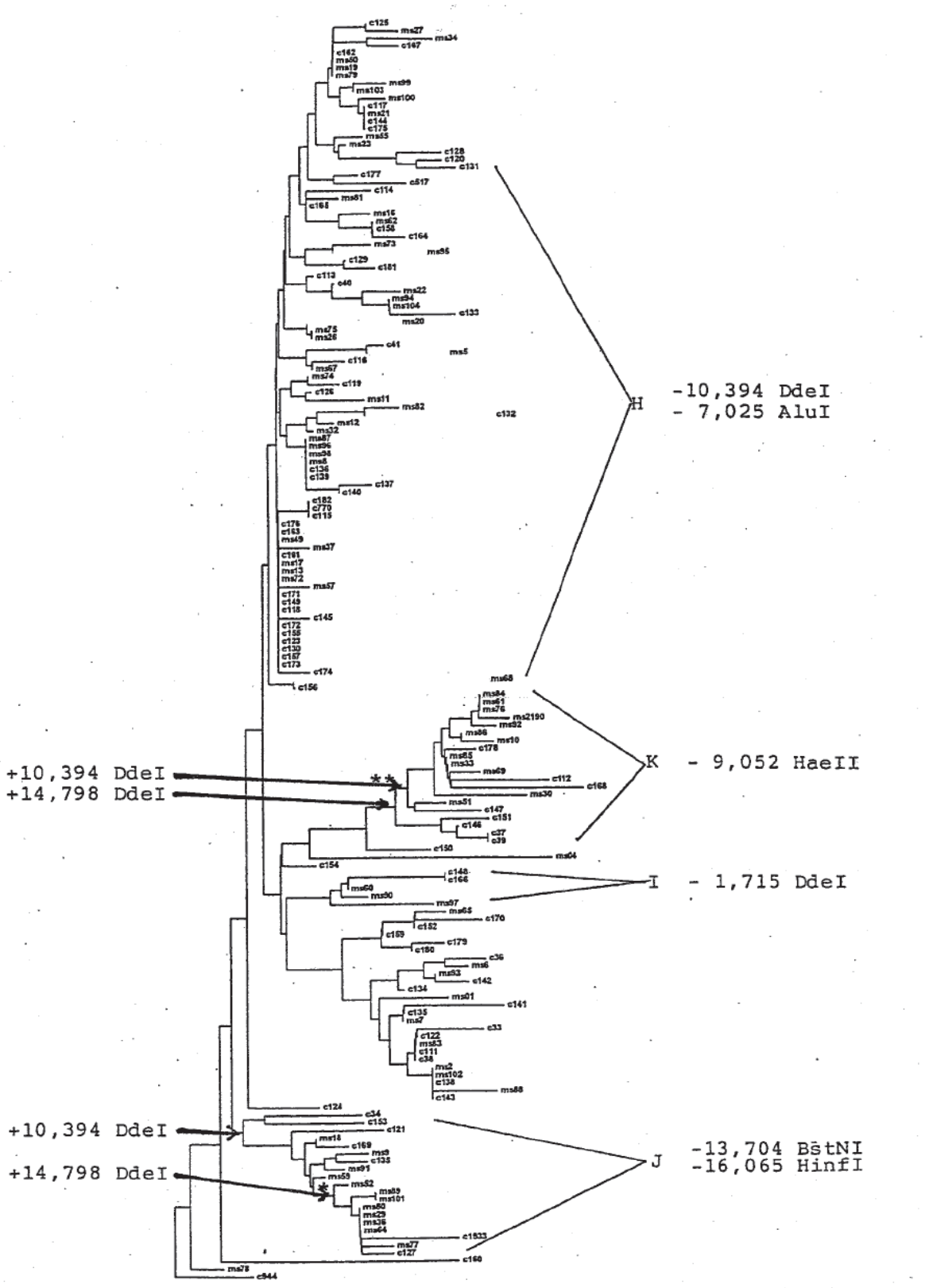

3.3.2 Genetic variants of Complex I in MS (81)

nDNA encoded SNP alleles and genotypes in families

No significant differences in the SNP allele frequencies were observed in the three investigated datasets. Genotype frequencies were calculated for random Caucasian controls in the validation set, and for unrelated parents in each dataset. No deviations from the HWE were noted in either the sporadic cohort or in the 268 unaffected parents in DS101-112.

Transmission of Complex I variants from unaffected parents to affected children

Although the genotyping and pilot analyses were carried out separately in DS101-105, DS106-108 and DS109-112, here we present results from the combined DS101-112, since the subgroups have similar allele and genotype frequencies, ethnic composition, and transmission distortion of markers. As all MS phenotypes were included in DS101-112, we asked in a subanalysis of stratified RR/SP-MS and PP-MS families if phenotypic differences would influence the outcome. Significant p-values were obtained when the numbers of transmitted and non-transmitted SNP alleles were compared by the χ^2 statistics in PDT on chromosomes 1 (NDUFS5X), 11 (NDUFC2E) and 19 (NDUFB7Y, NDUFB7X) in DS101-112 and the RR/SP-MS subgroup (Table 25). Only NDUFB7Y and NDUFB7X are non-synonymous mutations. The PP-MS group alone did not have a sufficient size to draw conclusion regarding allelic transmission distortions. All the moderately significant observations lost relevance to MS after the false discovery rate (242) or the Bonferroni correction for multiple comparisons (Table 25). As none of these marker alleles showed direct association with the disease, we next asked if haplotypes defined by some of the markers have transmission distortion due to a proximity of MS relevant mutations. Setting the threshold of significance to p=/<0.01 in the TRANSMIT analyses of SNP haplotypes in DS101-112, we identified two-marker haplotypes and a three-marker haplotype in chromosomes 1p34.2-p33 (NDUFS5) and 19p13.3, 19p13.2 and 19p13.12-p11 (NDUFS7, NDUFA7 and NDUFB7, respectively) (Table 26).

Table 25. PDT analyses of SNP markers

		Unstratified DS101-112				RR/SP-MS			
		trans	untrans	Z	p-value	trans	untrans	Z	p-value
1p34.2-p33									
NDUFS5X***	Allele G	56	85	-2.268	**0.0233**	50	74	-1.465	0.1428
NDUFS5X***	Allele T	358	329	+2.268	**0.0233**	332	308	+1.465	0.1428
11q13.4									
NDUFC2E**	Allele C	200	229	-2.494	**0.0126**	183	215	-1.964	**0.0495**
NDUFC2E**	Allele T	198	169	+2.494	**0.0126**	193	161	+1.964	**0.0495**
19p13.12-p13.11									
NDUFB7Y*	Allele A	3	20	-2.574	**0.0101**	2	18	-2.988	**0.0028**
NDUFB7Y*	Allele G	403	386	+2.574	**0.0101**	382	366	+2.988	**0.0028**
NDUFB7X*	Allele C	404	391	+2.478	**0.0132**	382	370	+2.602	**0.0093**
NDUFB7X*	Allele G	2	15	-2.478	**0.0132**	2	14	-2.602	**0.0093**

PDT used 178 individual families, 205 trios and 413 discordant sib pairs in DS101-112; 159 individual families, 191 trios and 389 discordant sib pairs in the RR/SP-MS group; and 23 individual families, 12 trios and 14 discordant sib pairs in the PP-MS group. *Nonsynonymous mutations / polymorphisms; **Locus SNP; ***Untranslated region SNP. P-values <0.05 are highlighted. All the above observations become insignificant both after the Benjamini and Hochberg false discovery rate (242) and the Bonferroni correction for multiple comparisons. When testing 53 markers on the same dataset, a p</=0.00097 is required by the latter method to attain an experiment-wide α=0.05.

Table 26. TRANSMIT analysis of two-marker and three-marker haplotypes

Chromosome	DS101-112 TRANSMIT p-value	RR/SP-MS TRANSMIT p-value
1p34.2-p33		
NDUFS5A-NDUFS5X		
Haplotype C G	0.0184	0.0258
Haplotype: C T	0.6533	0.7964
Haplotype: T G	**0.0013**	**0.0057**
Haplotype: T T	**0.0053**	0.0105
NDUFS5X-NDUFS5D		
Haplotype: G G	**0.0055**	**0.0073**
Haplotype: T A	0.9644	0.8117
Haplotype: T G	0.0114	0.0157
NDUFS5A-NDUFS5X-NDUFS5D		
Haplotype C G G	0.0228	0.0292
Haplotype C T G	0.6058	0.7557
Haplotype T T A	0.9589	0.7858
Haplotype T G G	**0.0022**	**0.006**
Haplotype T T G	**0.009**	0.0207
19p13.3		
NDUFS7N-NDUFS7B		
Haplotype A A	0.6409	0.5083
Haplotype A G	0.2669	0.4535
Haplotype G A	0.8281	0.5053
Haplotype G G	**0.0004**	**0.0006**
19p13.2		
NDUFA7X-NDUFA7Y		
Haplotype C C	**0**	**0**
Haplotype C T	**0**	**0**
Haplotype G C	0.1808	0.3529
Haplotype G T	0.7559	0.8362
19p13.12-p13.11		
NDUFB7Y- NDUFB7X		
Haplotype: A C	0.0593	0.0328
Haplotype A G	0.2385	0.2456
Haplotype: G C	0.0122	**0.0049**
Haplotype: G G	0.067	0.0644

Transmission distortion of haplotypes was defined by setting p=/<0.01 for significance threshold. The number of families with transmissions to affected offspring was 209 in DS101-112, 189 in RR/SP-MS and 26 in PP-MS.

Investigation of the preferentially transmitted haplotypes

To test whether or not the observed transmission distortions in Table 26 are specific for MS, we also used the TRANSMIT program to analyze the transmission of haplotypes to unaffected sibs in 72 ASP families (83 transmissions to unaffected offspring) (DS101-104 and DS109-112). Two- and three-marker haplotypes of NDUFS5A-NDUFS5X-NDUFS5D, NDUFS7N-NDUFS7B and NDUFA7X-NDUFA7Y showed no distortion of transmission to unaffected sibs (controls). Thus, the biased transmissions of these marker-haplotypes to affected sibs seem to be relevant to MS (Table 26). However, a three-marker haplotype of NDUFB7Y-NDUFB7X-NDUFB7M did show a moderate distortion of transmission to unaffected sibs (controls) (p=0.0389). A preferential transmission of the G allele of NDUFB7Y and of the C allele of NDUFB7X was seen not only to patients, but also to their unaffected siblings. Also, these preferentially transmitted alleles of NDUFB7Y and NDUFB7X were not the minor alleles (A and G with frequencies of 3.5% and 2.4%, respectively), but the major alleles G and C present in 96.5% and 97.6% of the normal population, respectively. Thus, neither individual alleles nor the haplotype of NDUFB7Y and NDYFB7X markers have true association with MS.

LD distribution in regions of interest

Using the ldmax program, we detected strong pair-wise LD (D'=1) among SNP markers of NDUFS5A, NDUFS5X and NDUFS5D in a 12 kb segment of 1p34.2-p33 (Table 27a). The observed transmission distortion and LD distribution (Table 26, Table 27a) suggest that a MS relevant nucleotide variant may reside near to this extended three-marker haplotype. Further, the TRANSMIT program also detected transmission distortion for two-marker haplotypes in chromosome 19 (Table 27b). Haplotypes of NDUFS7N-NDUFS7B and NDUFA7X-NDUFA7Y encompass segments of 19p13.3 and 19p13.2 with D'>0.98 reflecting strong LD. MS relevant variants are again likely to be located near or within these haplotypes.

Table 27a. LD map of markers located on Chromosome 1

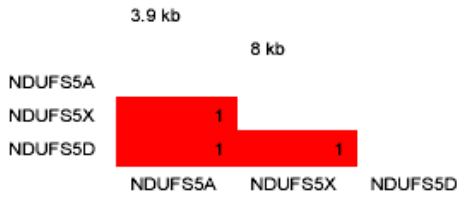

Table 27b. LD map of markers located on Chromosome 19

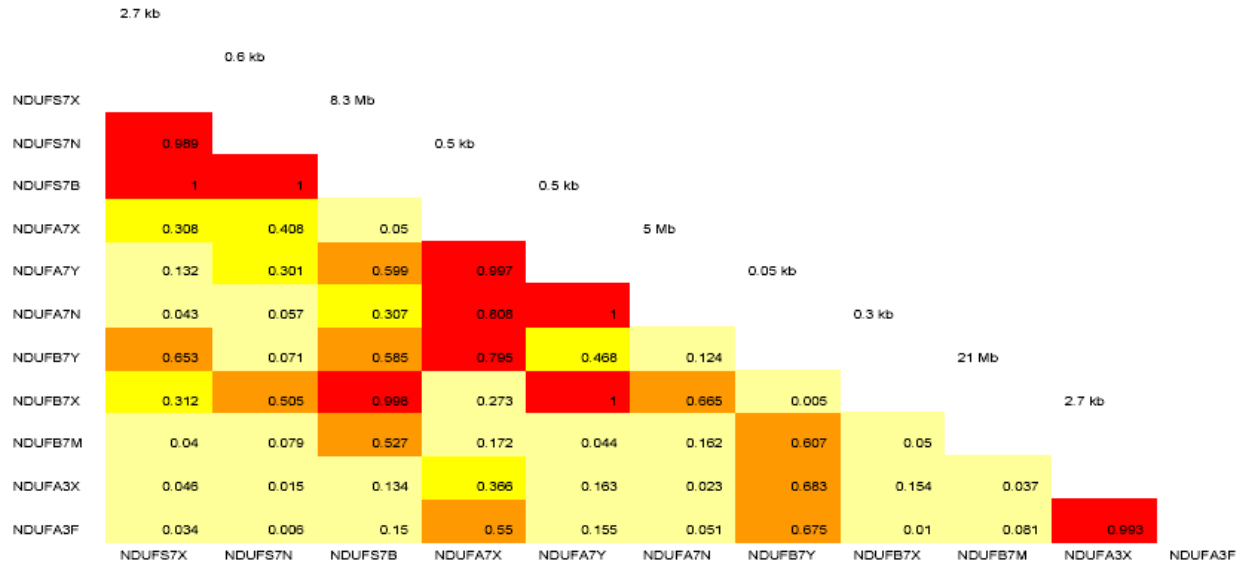

Table 27a and b show the distributions of inter-marker D' values. Red color designates D'>0.70; orange designates D'=/<0.70 and D'>0.50; dark yellow designates D'=/<0.50 and D'>0.30; light yellow designates D'=/<0.30. In Table 27a, pair-wise D' values are shown for NDUFS5A - NDUFS5X and NDUFS5X - NDUFS5D with inter-marker distances of 3.9 kb and 8 kb, respectively. In Table 27b, pair-wise D' values are indicated for NDUFS7X - NDUFS7N, NDUFS7N - NDUFS7B, NDUFS7B - NDUFA7X, NDUFA7X – NDUFA7Y, NDUFA7Y – NDUFA7N, etc… with respective inter-marker distances of 2.7 kb, 0.6 kb, 8.3 Mb, 0.5 kb, 0.5 kb, etc..

mtDNA encoded SNP variants in families

Here we ask if mtDNA variants and haplotypes found to be associated with MS in sporadic cohorts (3.3.1) are overrepresented in unaffected mothers (transmitting mtDNA to children) as compared to that of unaffected fathers (non-transmitting mtDNA) in MS families (145). For this comparison, we selected the biological father and mother of an affected offspring in each family, resulting in 131 parent pairs. Families with only one available biological parent were excluded from this analysis. This pair-wise comparison of the transmitted (maternal) vs. non-transmitted (paternal) mtDNA alleles and haplotypes reveals no difference when tested with the Fisher exact test in DS101-112. Similarly, no difference can be seen when the comparisons are restricted to parents of patients with either RR/SP or PP-MS or to the US derived RR/SP-MS cohort of families (DS101-108). In families with vertical transmission of disease, there are only 4 father - child and 6 mother - child concordances, representing too few mitochondrial lineages for a statistical comparison.

However, further analyses of data reveal that both mothers and fathers in DS101-112 have an increased frequency of mtDNA polymorphisms and haplotypes of interest when compared to those of Caucasian sporadic controls in the case-control study (3.3.1.4, 127,128). Considering that unaffected mothers as well as fathers carry MS relevant (nuclear) susceptibility genes, we asked if the frequency of MS associated mtDNA polymorphisms and haplotypes (J* or K*) are increased among mothers and fathers who carry the MS associated nDNA haplotypes. This investigation reveals that the 46 fathers positive for the MS relevant haplotypes of NDUFS5 have a higher frequency of the MS associated mtDNA haplotype (J* positive 15.2%) when compared to the 88 fathers negative for the MS associated NDUFS5 haplotypes (J* positive 3.4%) (Fisher exact test p=0.01). A similar result is noted in mothers when the MS associated NDUFS5 haplotype and mtDNA variants are correlated. Because of the low number of alleles of interest, we could not perform similar analyses with the MS relevant NDUFS7 and NDUFA7 haplotypes in correlation with the mtDNA haplotypes.

In summary, these analyses of nDNA encoded genes of Complex I reveal haplotypes within NDUFS5, NDUFS7 and NDUFA7 associated with MS in families (81). Parents who carry MS associated NDUFS5 nDNA haplotypes, tend to carry mtDNA polymorphisms (in haplotype J*) previously found to be associated with the disease in sporadic patients.

3.3.3 Oxidative damage to mtDNA, activity of mitochondrial enzymes, somatic mtDNA deletions and expression of apoptosis-related molecules in chronic active plaques (105,136,148-149,228,261)

3.3.3.1 Southern blot analysis of oxidative damage to mtDNA in plaque and NAWM pairs

Tables 28-30 and Figures 12-14 demonstrate that significantly increased oxidative damage to mtDNA develops in association with inflammation in plaques when compared to corresponding NAWM regions of MS brains. Although a tendency for more pronounced oxidative damage in the light strand (LS) (which contains most of the protein coding genes) than in the heavy strand (HS) of mtDNA is observed, statistical analysis reveals no difference. Similarly, no difference can be seen when the damage to purine and pyrimidine nucleotides is compared.

3.3.3.2 Detection of oxidative damage to mtDNA in plaques by immunohistochemistry

Immunohistochemistry with anti-8OH-dG antibody also shows an increased number of positive cells in plaques compared to NAWM. The reaction is usually observed as granular bodies within the cytoplasm (see Figure 15). No staining is found in normal gray matter. Minimal staining can be found in NAWM.

Table 28 and Figure 12. Break frequency s (=-lnP_0) in mtDNA of cerebellar plaques compared to that of corresponding NAWM tissues of 5 MS patients

Probe	NAWM Endo III	Plaque Endo III	NAWM FPG	Plaque FPG
^{32}P-labeled HS mtDNA (damage in the LS)	0.198+/-0.069	0.566+/-0.085[a]	0.036+/-0.092	0.306+/-0.090[c]
^{32}P-labeled LS mtDNA (damage in the HS)	0.122+/-0.081	0.341+/-0.097[b]	0.031+/-0.067	0.186+/-0.059[d]
Biotinylated DS mtDNA (damage in both strands)	0.106+/-0.090	0.416+/-0.116[e]		

[a]p=0.032 [b]p=0.032 [c]p=0.032 [d]p=0.032 [e]p=0.032

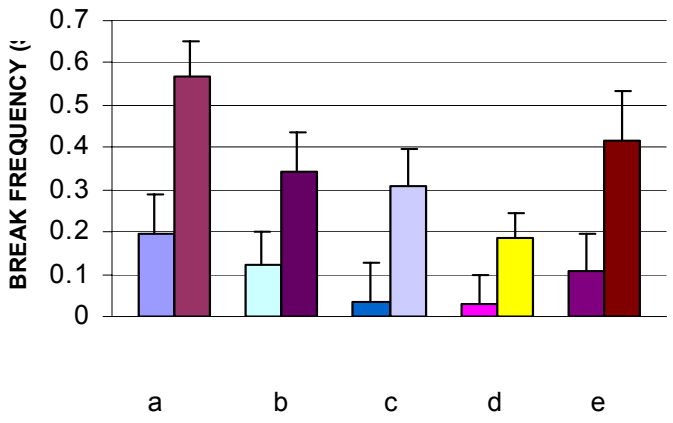

a: Endo III digested DNA from NAWM and plaque hybridized with a HS probe.

b: Endo III digested DNA from NAWM and plaque hybridized with a LS probe.

c: FPG digested DNA from NAWM and plaque hybridized with a HS probe.

d: FPG digested DNA from NAWM and plaque hybridized with a LS probe.

e: Endo III digested DNA from NAWM and plaque hybridized with a DS (double stranded) biotinylated probe.

Legend to Table 28 and Figure 12.

DNA samples were processed as described in the Methods. Mean and standard error of the mean of calculated break frequency values in mtDNA from 5 NAWM and plaque samples are summarized above. The 1-tailed Wilcoxon signed rank test reveals [a-e]p=0.032 in each pairwise (plaque vs. NAWM) comparison. Comparison of oxidative damage at either purine or pyrimidine sites in the light and heavy strands (LS and HS) of mtDNA (2-tailed Wilcoxon signed rank test) reveals no statistical difference.

Table 29 and Figure 13. Break frequency s (=-lnP_0) in mtDNA of hemispheral plaques compared to that of corresponding NAWM tissues of 8 MS patients

Probe	NAWM Endo III	Plaque Endo III	NAWM FPG	Plaque FPG
^{32}P-labeled HS mtDNA (damage in the LS)	0.188+/-0.088	0.298+/-0.083[a]	0.247+/-0.153	0.305+/-0.102[c]
^{32}P-labeled LS mtDNA (damage in the HS)	0.098+/-0.084	0.170+/-0.067[b]	0.004+/-0.016	0.064+/-0.007[d]

[a]p=0.039 [b]p=0.125 [c]p=0.273 [d]p=0.004

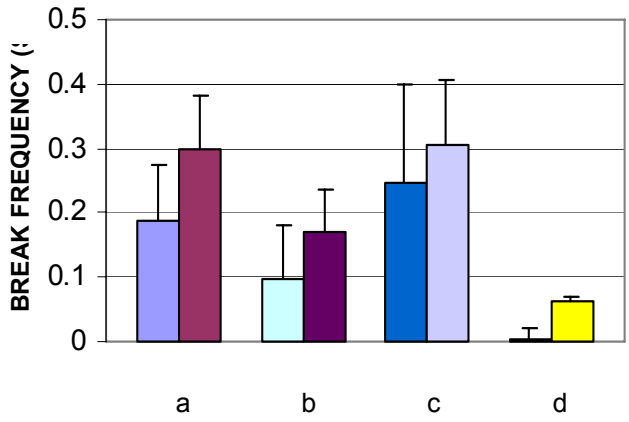

a: Endo III digested DNA from NAWM and plaque hybridized with HS probe.

b: Endo III digested DNA from NAWM and plaque hybridized with LS probe.

c: FPG digested DNA from NAWM and plaque hybridized with HS probe.

d: FPG digested DNA from NAWM and plaque hybridized with LS probe.

Legend to Table 29 and Figure 13.

Mean values and standard error of mean values are indicated. One-tailed p-values were calculated by using the Wilcoxon signed rank test.

Table 30 and Figure 14. Break frequency s (=-lnP_0) in mtDNA of plaques compared to that of corresponding NAWM pairs in cerebellar and hemispheral samples of 13 MS patients.

Probe	NAWM Endo III	Plaque Endo III	NAWM FPG	Plaque FPG
^{32}P-labeled HS mtDNA (damage in the L strand)	0.192+/-0.058	0.401+/-0.070[a]	0.166+/-0.102	0.305+/-0.085[c]
^{32}P-labeled LS mtDNA (damage in the H strand)	0.107+/-0.060	0.236+/-0.058[b]	0.015+/-0.026	0.111+/-0.028[d]

[a]p=0.001 [b]p=0.013 [c]p=0.029 [d]p<0.0005.

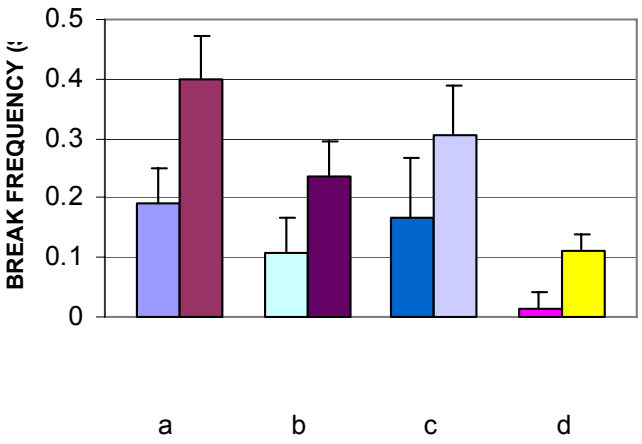

a: Endo III digested DNA from NAWM and plaque hybridized with HS probe.

b: Endo III digested DNA from NAWM and plaque hybridized with LS probe.

c: FPG digested DNA from NAWM and plaque hybridized with HS probe.

d: FPG digested DNA from NAWM and plaque hybridized with LS probe.

Legend to Table 30and Figure 14

Table 30 and Figure 14 combine data from cerebellar and hemispheral sample pairs (presented separately in Tables 28-29, Figures 12-13), and show mean +/- standard error of mean values of oxidative damage. The Wilcoxon signed rank test (1-tailed) reveals a significantly increased oxidative damage to both pyrimidine (Endo III treated DNA) and purine (FPG treated DNA) nucleotides of mtDNA in plaques as compared to that in NAWMs. Although visual comparison of mean values of oxidative damage in the light and heavy strand of mtDNA (detected by a HS and a LS probe, respectively) would suggest that the light strand of mtDNA containing most of the protein coding genes is more susceptible to oxidative damage than the heavy strand, the 2-tailed Wilcoxon signed rank test reveals no statistical difference (p>0.40 for both Endo III and FPG treated samples).

Figure 15. *In situ* detection of oxidative damage to mtDNA and nDNA in plaques

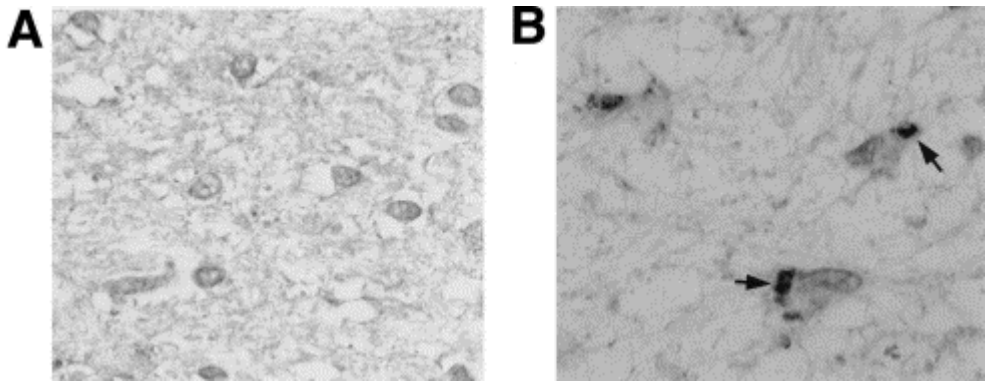

Serial sections were prepared from paraffin embedded NAWM and active plaque containing tissues. The distribution of pathology was verified by Haematoxylin-Eosin staining of sections. Parallel sections were prepared for immunohistochemistry with anti-8OH-dG antibody and counter stained with Haematoxylin. Figure 15A demonstrates a lack of staining with anti-8OH-dG antibody in a normal white matter area of a MS patient. Figure 15B shows cytoplasmic staining with anti-8OH-dG antibody (see arrows) suggesting oxidative damage to mtDNA in an inflamed and demyelinated brain region of the same MS patient.

3.3.3.3 The activity of mitochondrial enzymes in corresponding plaques and NAWM pairs

Six assays of mitochondrial enzymes (NADH DH, Complex I+III, Complex II, Complex II+III, Complex IV and citrate synthase) were performed in 10% w/v homogenates of 10 paired NAWM and plaque tissues. We normalized enzyme activity (umol/min/g wet tissue) values to both protein content and citrate synthase activity. Comparing specific activity values of enzymes (umol/min/g protein) eliminates the potential problem of a differential cellularity (infiltration, astrogliosis, etc...) and protein content in plaques and NAWM. Normalizing values for citrate synthase (exclusively encoded by nDNA) corrects not only for a differential cell density and composition, but also for a potential difference in the mitochondrial gene expression in plaques compared to NAWM. In seven of ten plaques we found a trend for decrease in the activity of NADH dehydrogenase component of Complex I normalized for wet tissue weight and citrase synthase, and an increase in normalized values of complex IV ($p=0.027$ and $p=0.150$, respectively) when compared to those in corresponding NAWM. No differences were found in the activity of other enzyme complexes. These observations suggest an impairment of Complex I in association with inflammation in plaques.

3.3.3.4 Somatic mtDNA deletions in regions of oxidative stress

We postulated that oxidative stress to mtDNA in plaques may contribute to somatic mtDNA deletions in an accelerated manner compared to age matched controls. Such deletions affecting

mtDNA encoded subunits of Complex I could explain the detected decreased activity of Complex I in plaques. For quantifying deleted and full length mtDNA molecules in single neurons and glial cells, we used the method of real-time PCR. While patients and controls up to 60 years of age appeared to have a very low proportion of Cox- relative to Cox+ cells (ranging between 0.008-0.07) irrespective of brain region (NAWM, NAGM, plaque, or WM, GM), the proportion of Cox- cells gradually increased after 60 years of age reaching 0.20 in the oldest NC (80 year old). The ratio of Cox- / Cox + neurons was also high (0.2-0.35) in 2 patients with AD (91 and 94 years of age) and in a patient with PD (81 years of age) (Fig. 15,16A,16B).

Because of the sparse occurrence of Cox- cells in MS patients (all below 60 years of age) and controls matched to patients by age, only cells with strong and weak Cox staining could have been collected in sufficient numbers for the real-time PCR studies in these cohorts. In contrast, from both the normal controls beyond 60 years of age, and OND controls with AD or PD, Cox- cells were available in sufficient numbers for the real-time PCR studies.

Neurons and glial cells sorted by COX staining were isolated by laser dissection for DNA extraction. The proportion of deleted mtDNA molecules was initially quantified in all specimens of the MS “a” and “b” tissue series separately, along with separately isolated cells from matched control tissues (Table 15a,b). Since there was no difference in the corresponding data of “a” and “b” groups, we discuss here the results from the combined (a+b) analyses.

Figure 17a,b summarizes the results of the real-time PCR quatitation of deleted mtDNA molecules in NAGM, NAWM and plaques of MS patients. Figure 17C shows the results of real-time PCR in GM and WM of all controls. No significant differences are observed when data from either the high or from the low Cox positive trios of NAGM, NAWM and plaques are compared with each other, or when similar data from WM and GM of age matched normal controls are compared with each other by using the Wilcoxon signed rank test (intra-individual comparison among NAWM, NAGM and plaque, or between WM and GM). Similarly, no differences are found in the proportion of deleted mtDNA molecules when values in the NAGM and NAWM of MS patients are compared to GM and WM of age matched controls, respectively, using the t-test or ANOVA analyses (intergroup comparisons). Nevertheless, the proportion of deleted mtDNA molecules is higher in the Cox low cells as compared to Cox high cells in all tissue regions of patients (NAGM, NAWM, plaques) and controls (GM, WM), with significant p-values ($p \leq 0.008$, Wilcoxon signed ranks test) in the MS NAWM and control GM and WM (Fig. 17A,B,C). These observations suggest that the proportion of deleted mtDNA molecules is similar in various regions of MS brains (NAGM - NAWM - plaque), and in MS brains and control

brains matched by age (NAWM - WM, NAGM - GM). Cox low positive cells tend to have higher proportion of deleted mtDNA molecules than Cox high positive cells derived from the same tissue specimen.

In contrast, as the proportion of Cox- neurons and glial cells increases with age, the proportion of deleted mtDNA molecules is also increasing beyond 60 years of age in the control cohort (Fig. 17C). Statistical significance is observed when the proportion of deleted mtDNA molecules in Cox- GM (p=0.041, ANOVA) and Cox- WM cells (p=0.000, ANOVA) are compared in the groups below vs. above 60 years of age. No differences are observed in the proportion of mtDNA deletions in Cox+ cells from controls below vs. above 60 years of age. Similarly, Figure 17D shows that Cox- neurons of the three oldest patients with neurodegenerative diseases (AD2985, AD2943 and PD4078) display marked deletions in mtDNA molecules as compared to Cox+ neurons (p=0.0003 [1-tail], p=0.0007 [2-tail] Wilcoxon signed rank test).

Figure 16. COX/SDH histochemistry in brains of patients with MS and AD

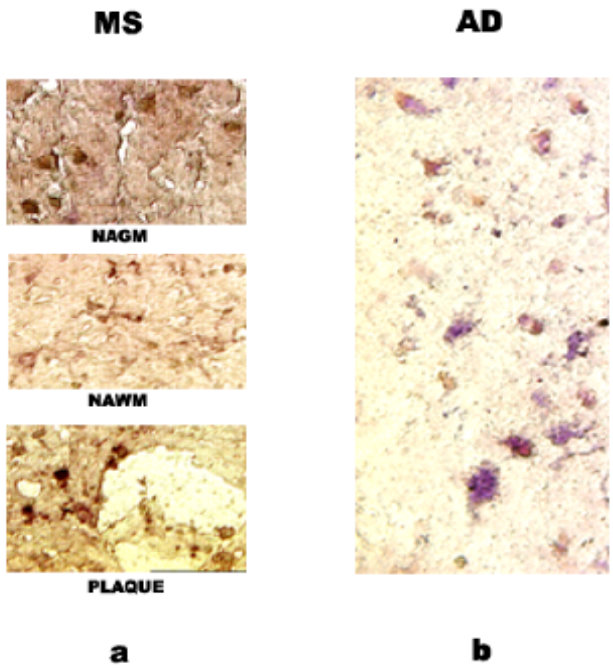

COX/SDH staining of NAGM, NAWM and plaque from a MS brain (a) and cortex from an AD brain. Brown cells are COX+ and purple cells are COX-.

Figure 17a. mtDNA deletion rates in Cox strongly positive cells from NAGM, NAWM and plaques

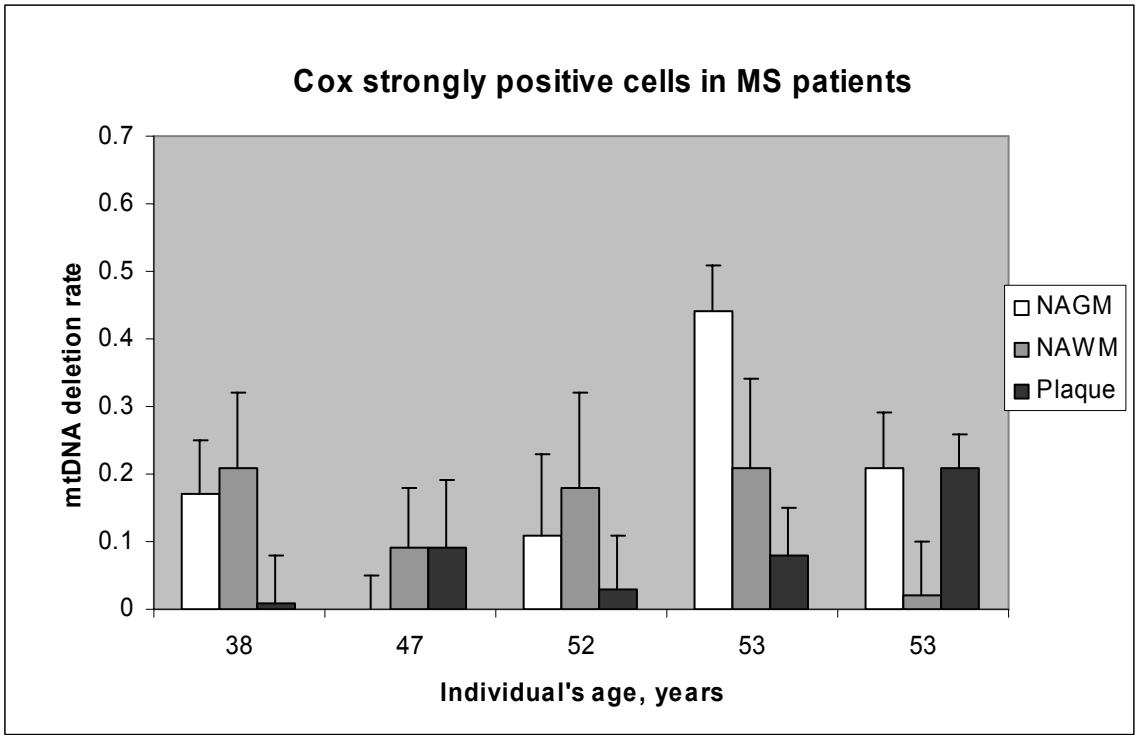

Figure 17b. mtDNA deletion rates in Cox weakly positive cells from NAGM, NAWM and plaques

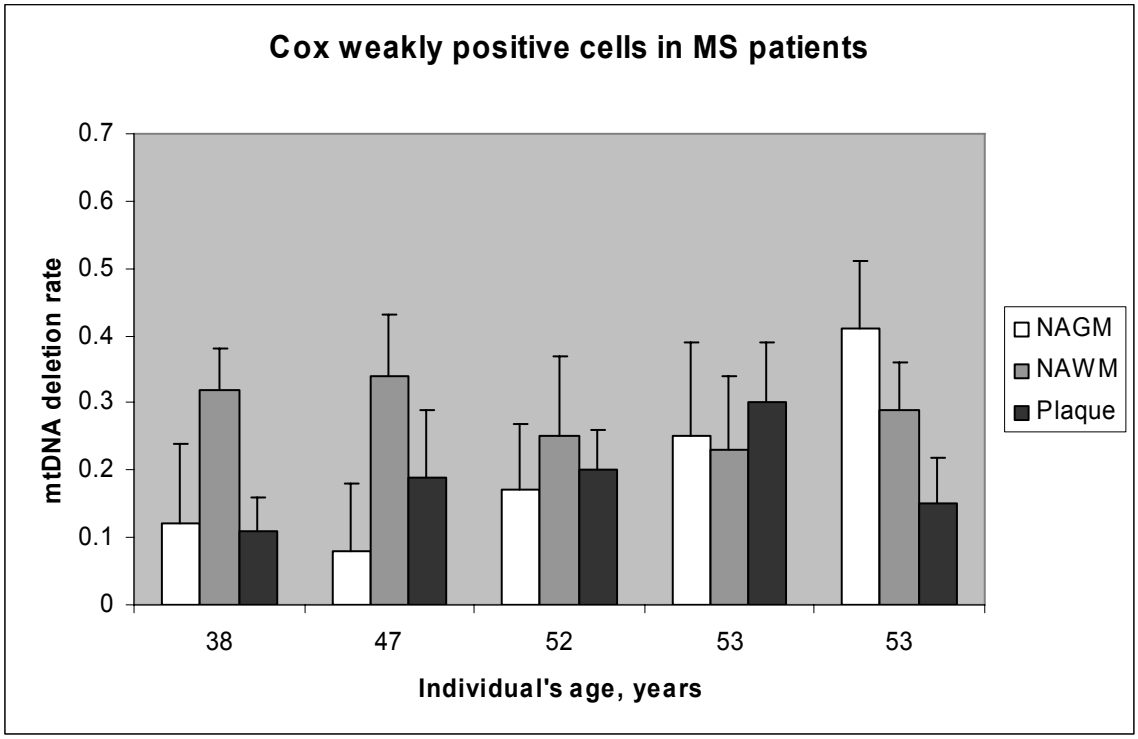

Figure 17c. mtDNA deletion rates in neurons and glial cells from control GM and WM

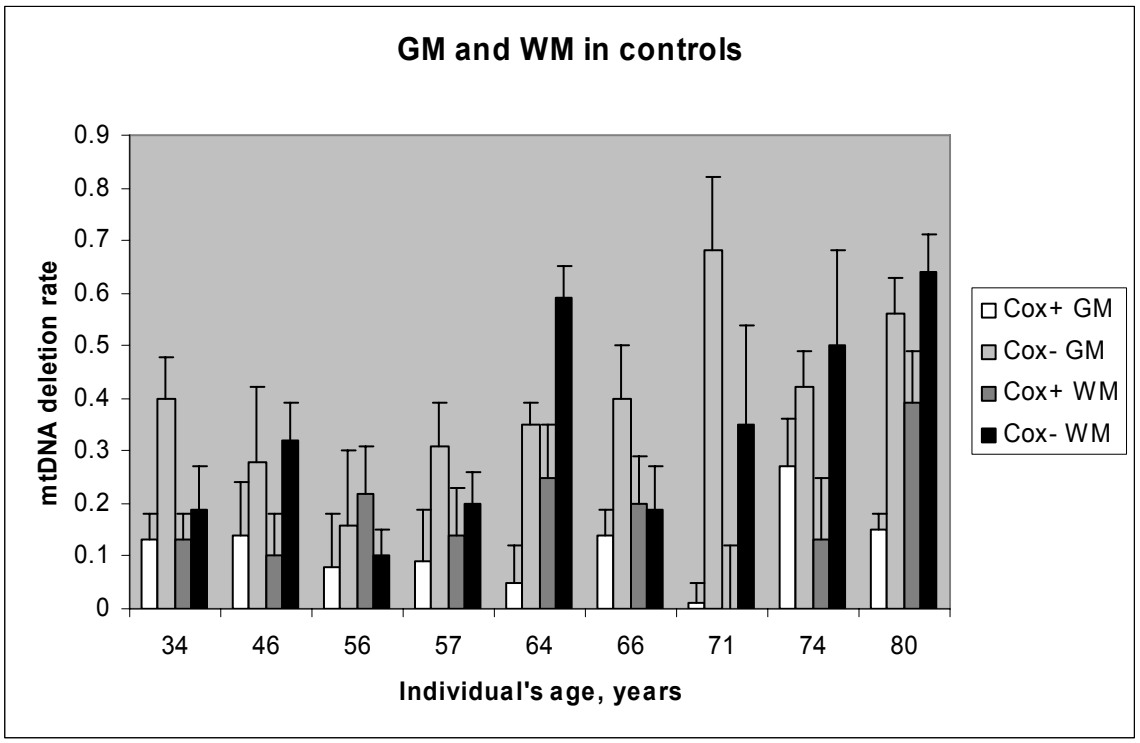

Figure 17d. mtDNA deletion rates in neurons from patients with AD and PD

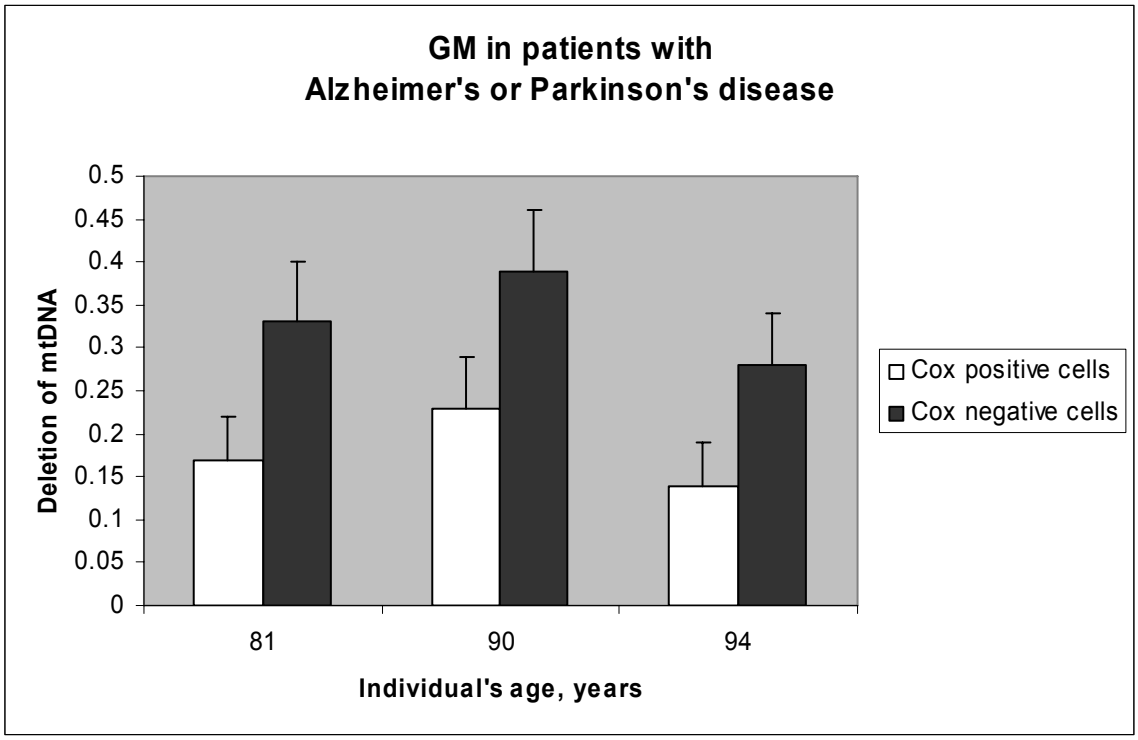

Figure 17 shows the mean+/-SE of deleted mtDNA molecules (defined as 1-ND4/ND1) in strongly COX+ cells of MS NAGM, NAWM and plaques (a), in weakly Cox+ cells of MS NAGM, NAWM and plaques (b), in Cox+ and Cox- neurons and glial cells of non-neurological controls (c) and in Cox + and Cox-neurons of patients with AD and PD (d). From each tissue category, at least 10 Cox+ and 10 Cox- cells were collected for real-time PCR analyses (details in 3.2.3.2). No statistically relevant variations in mtDNA deletions are seen in MS NAGM, NAWM and plaque (a and b), but and age-related increase is noted for both COX- cells and mtDNA deletions in the controls (c). Elderly patients with neurodegenerative diseases also have increased proportion of COX- cells and mtDNA deletions, particularly in COX- neurons (d) (See detailed explanation in the text of 3.3.3.4).

In summary, these studies reveal no accumulation of Cox- cells and somatic mtDNA deletions in association with inflammation, oxidative stress and reduced Complex I activity in chronic active plaques as compared to NAWM and NAGM of MS patients. However, similar to controls, there appears to be an age-related accumulation of Cox- neurons and somatic mtDNA deletions. This process is modest in the first 6 decades of life, but is accelerated and exponencially increases in and after the 7^{th} decade of life.

In consensus with studies by others, we also noted a particularly high accumulation of somatic mtDNA mutations and loss of Cox+ neurons in neurons of patients with neurodegenerative diseases (228-230).

3.3.3.5 mRNA expression for anti-oxidants, pro and anti-apoptotic molecules in plaques

Here we asked in oxidative damage and decreased Complex I activity correlate with the expression of anti-oxidants and molecules involved in apoptosis. Table 31 demonstrates along with signs of increased MHC I (as reflected by an increased β_2-microglobulin-β_2Mg) expression, an increased mRNA expression for both the anti-apoptotic Bcl-2 and pro-apoptotic Bak in NAWM and chronic active plaques compared to the corresponding NAGM regions. The expression level of the anti-apoptotic Bcl-x_L is generally low in the brain, but is increased in plaques compared to NAWMs. We did not detect regional differences in the expression levels of the free radical scavenger GSHS or SOD-1. Figure 18 shows low expression of β_2-microglobulin in the MS NAGM, its increased expression in both the NAWM and plaques in correlation with pro- and anti-apoptotic mRNA molecules.

We did not detect differences in the expression levels of these genes in corresponding WM and GM specimens of normal and Alzheimer disease controls (Wilcoxon Signed Rank Test). However, in correlation with histological signs of inflammation and immune activation, a trend for an increase in all pro and anti-apoptotic mRNA molecules was observed in both the WM and GM regions of the encephalitis controls compared to normal and OND controls or MS specimens (because of the low number of samples, no statistical analysis could be used for these specimens).

In summary, the studies in section 3.3.3 reveal oxidative damage to mtDNA without secondary mtDNA deletions, impaired activity of Complex I and upregulation of pro- and anti-apoptotic members of the Bcl-2 family in association with histological (H&E) and molecular (β_2Mg, CD68) signs of inflammation in chronic active plaques (105,136).

Table 31. Wilcoxon Signed Rank test analysis of mRNA copy numbers for GSHS, Bcl-2, Bak, Bcl-x_L, SOD-1 and β_2Mg in corresponding NAWM, plaque and NAGM specimens

Correlated tissues of MS brains	Z score	P-value
GSHS		
NAWM vs. Plaque	-0.035	0.97
NAGM vs. Plaque	-1.05	0.133
NAGM vs. NAWM	-1.572	0.116
Bcl-2		
NAWM vs. Plaque	-1.223	0.221
NAGM vs. Plaque	-2.51	0.012
NAGM vs. NAWM	-2.903	0.004
Bak		
NAWM vs. Plaque	-0.035	0.972
NAGM vs. Plaque	-2.201	0.028
NAGM vs. NAWM	-2.481	0.013
Bcl-x_L		
NAWM vs. Plaque	-2.197	0.028
NAGM vs. Plaque	-0.314	0.754
NAGM vs. NAWM	-0.622	0.534
SOD-1		
NAWM vs. Plaque	-1.049	0.294
NAGM vs. Plaque	-0.524	0.6
NAGM vs. NAWM	-0.664	0.507
β_2Mg		
NAWM vs. Plaque	-0.245	0.807
NAGM vs. Plaque	-2.97	0.003
NAGM vs. NAWM	-3.04	0.002

The Wilcoxon Signed Rank test reveals a significant increase in the copy numbers of β_2Mg, Bcl-2 and Bak molecules in NAWM and plaque as compared to NAGM regions of MS brains. Bcl-x_L is only increased in plaques relative to NAWMs.

Figure 18. Correlation between the normalized values of Bak, Bcl-2 and Bcl-x_L and β_2-Mg mRNA molecules in NAWM, NAGM and Plaque

A

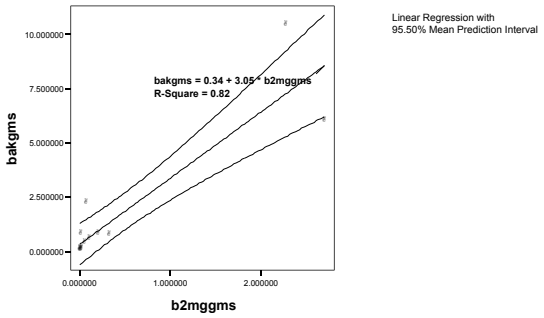

B

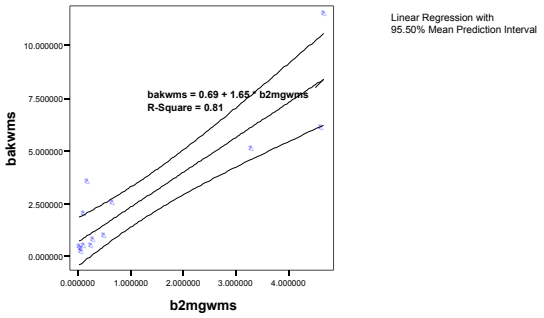

C

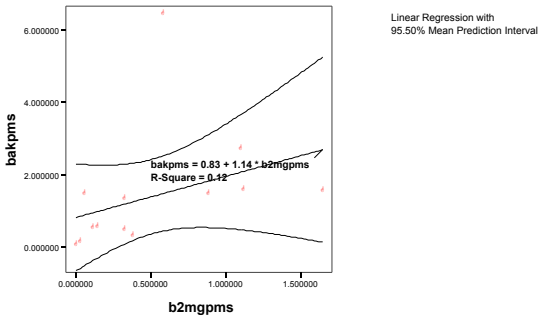

D

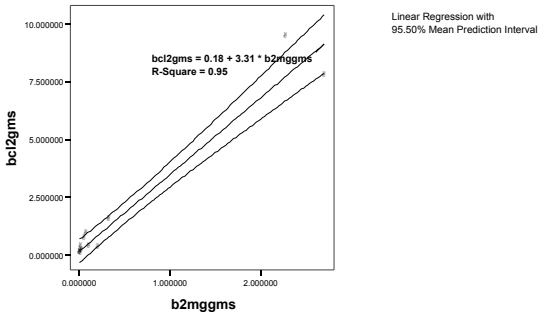

E

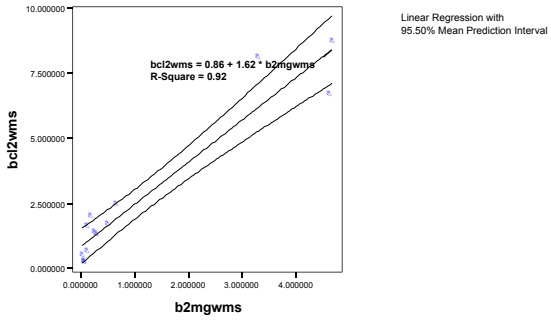

F

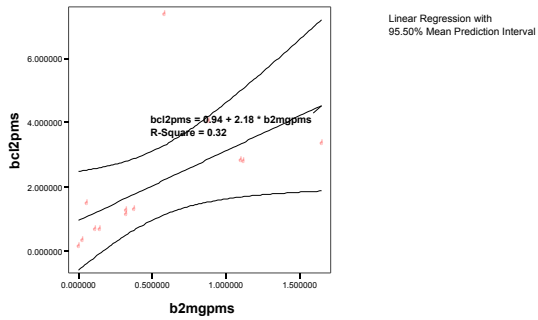

G

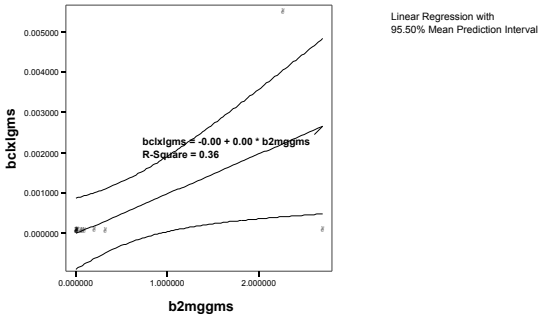

H

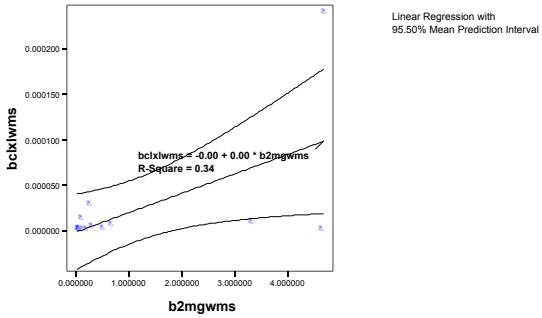

I

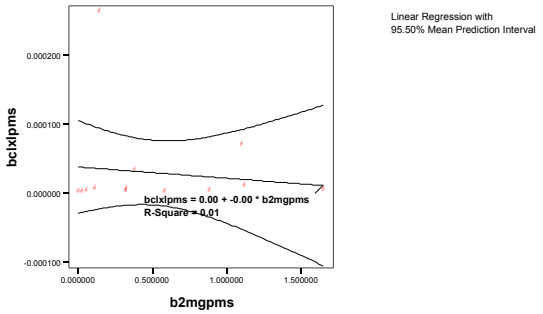

Scatter plots of normalized mRNA copy numbers for Bak, Bcl-2 and Bcl-x_L vs. β_2Mg in NAWM, NAGM and Plaque. Black symbols designate normalized values in NAGM; Blue symbols designate normalized values in NAWM; Red symbols designate normalized values in plaque. A-C: Scatter plots of Bak vs. β_2Mg in NAGM, NAWM and Plaque; D-F: Scatter plots of Bcl-2 vs. β_2Mg in NAGM, NAWM and Plaque; G-I: Scatter plots of Bcl-x_L vs. β_2Mg in NAGM, NAWM and Plaque.

3.4 DISCUSSION: INVOLVEMENT OF MITOCHONDRIAL MOLECULES IN MS

3.4.1 mtDNA mutations, polymorphisms and haplotypes in MS, PON and NMO

3.4.1.1 Screening for mtDNA mutations in MS

In this first explorative study of mtDNA in patients with MS, eight LHON type mutations were investigated by sequencing and restriction endonuclease analyses. In the proximity of LHON mutations, non-LHON mtDNA abnormalities were also searched. None of the primary mutations located in the ND-1 (at nt 3,460 and 4,160), ND-4 (at nt 11,778) or ND-6 (at nt 14,484) genes were detected in 20 randomly selected MS patients. This finding is consistent with the negative conclusion of another study of mutations at nt 11,778 and 3,460 in typical MS (157). We also failed to detect non-LHON type, potentially pathogenic mutations within the sequenced regions of mtDNA in these 20 MS patients. One

of the nucleotide transitions (G to A) at position 14,569 in the ND-6 gene was previously reported in a patient with mitochondrial encephalomyopathy, but considering its homoplasmic and synonymous nature, and the lack of pathological confirmations, it is likely to be a rare polymorphism (243).

Since secondary LHON mutations appeared more frequently than expected by chance in the 20 patients, we extended the screening to a larger group of MS patients and controls (Table 17). In the 74 controls, appearance of all but the 4,917 mutation was similar to that reported previously (Table 17). In the 53 MS patients, an increased incidence (20.8% vs 9.5%, p=0.036) was found for the mutation at nt 4,216 as well as for the associated secondary mutations compared to the controls. Variants at nts 4,216, 4,917 and 13,708 often simultaneously occur in patients with LHON (187), however, in association with primary and sometimes with additional secondary LHON mutations (183,231). In contrast to the primary mutations, secondary mutations are variants which do not contribute to visual loss in LHON. Our study suggests that these mutations do not increase the risk for severe optic nerve involvement or for any optic nerve involvement in MS (Table 18). We also confirm that the mutation at 15,257 (with provisional status in the literature at the time of this study) is not pathogenic (244) as it was present in both a healthy individual and a MS patient with only mild visual problems. Heterogeneity of the phenotypic expression of MS among carriers of secondary LHON mutations indicates that these mutations do not contribute directly to the clinical manifestation of the disease.

In summary, this first analysis of mtDNA reveals the absence (or rarity) of primary LHON mutations but a possible increase of secondary LHON mutations in MS.

3.4.1.2. Screening for mtDNA mutations in PON

As we detected no primary LHON mutations in typical MS, next we asked if such mutations are more likely to be present in patients with PON. In contrast to a report of primary LHON mutations in white and black Americans with PON (139), the present study failed to detect the 11,778, 3,460 or 14,484 mutations in 22 similar patients (Table 13 and 14). Our results suggest that the frequency of these mutations in patients with PON is less than 4.5%, in contrast to the 15% occurrence of the 11,778 and 3,460 mutations in a cohort of clinically similar twenty British patients (157). Both ethnic-genetic differences and referral biases may contribute to the different findings. The outcome of our study is supported by another report demonstrating the lack of the 11,778 mutation in 80 Japanese MS patients, including 18 patients with PON (245).

As we ruled out a mitochondrial genetic etiology (study) and environmental causes (inclusion / exclusion criteria) of optic nerve atrophy in this cohort, PON seems to be the consequence of inflammatory demyelination. Therefore, we asked if the devastating visual loss is part of a severe MS,

or the highly disabling process is restricted to the optic nerves. Based on the clinical documents, the severe visual loss was independent of the course, distribution, duration, progression rate or family history of inflammatory demyelination in these patients with PON.

In summary, LHON-type pathogenic mtDNA mutations do not occur frequently in patients with PON. Instead of a single (mitochondrial) genetic cause, an interaction among several factors may lead to severe visual loss in MS. Existence of local factors or a selective vulnerability of optic nerve fibers to inflammation may explain the severe visual disability in those PON patients in whom no other signs of neurological disability can be observed even after a long duration of the disease with extensive white matter lesions.

3.4.1.3 Comprehensive sequence analyses of mtDNA in MS and NMO

As we established that primary LHON mutations must be rare in typical MS and PON, but secondary LHON mutations may be associated with inflammatory demyelination, next we asked if mtDNA mutation of any kind can be detected in patients with MS and NMO. These studies represent the first full mtDNA sequence analyses in both of these entities. Three unique MS patients (with fulminant MS, PON and distinct mtDNA genetic background) were selected for the study. Partial characterization of their mtDNA in a previous study (Ref 139, Sections 3.3.1.1, 3.3.1.2) suggested that these patients belonged to distinct mtDNA lineages. We also postulated, that the necrotizing nature of NMO pathology may be related to a mitochondrial mechanism or molecular abnormality.

We sequenced the entire mtDNA of these patients to determine all the nucleotide alterations relative to the Cambridge sequence (150). Each mutation detected in the patients was compared to those in a large control population described in the literature (181-183,232-238) (these analyses represented the standard at the time of our studies and preceded the availability of the current Mitomap database). After identifying the synonymous nucleotide alterations, errors of the Cambridge sequence and the common mtDNA polymorphisms among the detected individual variants, eight novel homoplasmic mtDNA variants were selected in the MS patients for further characterization (Table 19, Table 20).

The nucleotide alteration at 1,888 found in patient MS-1NP, is located in a conserved site of the 16S rRNA. It was not detected in our 63 controls or in the large control population in the literature (181-183,212,232-238). Nevertheless, this mutation was also not present in the additional 51 patients, thus its direct relationship with MS is unlikely. Since the two detected tRNA mutations at 10,463 ($tRNA^{Arg}$) and 15,928 ($tRNA^{Thr}$) appeared equally in the MS and control populations, their association with MS can be excluded. No other mtDNA abnormality with potential pathogenic significance was identified in this patient who presented with a fulminant form of PP-MS. This patient, however, carried secondary

LHON mutations at nts 4,216 and 4,917, determinants of a mtDNA lineage which may have relevance to MS (see 3.3.1.4 and 3.4.1.4).

Patient MS-R51 with bilateral blindness from PON had no primary and secondary LHON mutations or other mtDNA abnormalities with suspected pathogenic significance. The homoplasmic mutation detected at nt 14,798 (Table 19, 20) is a known polymorphism often noted in mtDNA haplotypes associated with LHON (181,213,235). Our subsequent comprehensive mtDNA polymorphisms and haplotype analyses (3.3.1.4, 3.4.1.4) also confirmed the role of this variant in MS.

The investigation of mtDNA in patient MS-R4 revealed four new variants. Three variants at nts 980 (12S rRNA), 8,684 (ATP-ase 6) and 9,300 (CO III) were only detected in MS-R4 but not in the additional 51 patients or 63 controls, suggesting that these variants probably define a rare Caucasian mtDNA haplotype. The fourth mutation at 13,966 in the ND-5 gene was present in another MS patient, who did not carry mutations at nts 980, 8,684 or 9,300 (Table 19, 20), indicating that the 13,966 variant appeared in different mtDNA haplotypes. Although this mutation had not been described before, nor was it present in our control group of 63 individuals, its homoplasmic appearance and the non-conserved nature of the altered amino acid suggest that the 13,966 variant is a rare polymorphism (162,180,183). Dystonia in the family of MS-R4 was not related to the maternally inherited LHON-dystonia-MS entity (154), as it occurred without features of LHON and with an autosomal dominant transmission pattern (214). Sequence analyses of mtDNA in MS-R4 also excluded the presence of the 14,459 mutation detected in LHON - dystonia families (246).

Similar to MS, no pathogenic mtDNA mutations were revealed by sequencing in the three NMO patients. After the exclusion of synonymous mutations and common polymorphisms from the detected variants identified by aligning the patients' mtDNA sequences the Cambridge sequence (http://www.gen.emory.edu/mitomap.html 2000,150), only one new variant was identified at T4695C, Phe->Leu in the ND2 gene of NMO-B (Table 19) (no new variant occurred in NMO-A and C). This T4695C mutation was homoplasmic, characteristic of phylogenetically old and biologically neutral mutations. A restriction endonuclease analysis detected this variant in 2 of 80 Caucasian controls and in 1 of 65 Caucasian MS patients, further confirming that this polymorphic mutation has no relevance to inflammatory demyelination. However, we noted in these three NMO patients the presence of mtDNA variants and haplotypes found in association with MS: in patient A: A10,398G, T14,798C (polymorphisms in haplotype K* associated with MS); in patient B: T4,216C, A4,917G (polymorphisms associated with both MS and LHON); and in patient C: T4,216C, T14,798C (polymorphisms in haplotype J* associated with MS) (see 3.3.1.4 and 3.4.1.4, ref 144,145).

In conclusion, these analyses establish that MS, PON and NMO may develop without pathogenic mtDNA mutations of any kind. The novel mtDNA variants identified by sequence analyses in the probands were not found to be associated with MS when a larger group of patients and controls was screened. However, mtDNA polymorphisms (secondary LHON mutations and a variant at 14,798) in five of six patients with MS and NMO suggest that a shared mitochondrial genetic background of the two diseases may exist in Caucasians (see 3.3.1.4 and 3.4.1.4).

3.4.1.4 Restriction site polymorphism and haplotype analyses in MS

The above studies revealed an increased frequency of secondary LHON mutations (at nt 4,216, 4,917 and 13,708) and a putative involvement of two novel mtDNA variants (at nts 14,798 and 13,966) in MS. However, sequence analyses of mtDNA in a number of patients also established that MS can occur without pathogenic mtDNA abnormality of any kind. Screening of patients with MS and PON proved that the presence of primary LHON mutations is infrequent in inflammatory demyelination, despite some case reports suggesting associations (155-161). Therefore, a large scale screening of patients and controls seemed necessary to draw a final conclusion in regard to the involvement of mtDNA mutations, polymorphisms and haplotypes in MS. Such a screening was expected to complement data from previous studies which were limited by selecting only certain sites (e.g. LHON mutations) for screening (Sections 3.3.1.1, 3.3.1.2, 3.4.1.1, 3.4.1.2, ref 139,142,155-161,188,189,245), or by the number of individuals involved in the full mtDNA sequencing (Sections 3.3.1.3, 3.4.1.3, ref 140).

The method of restriction site polymorphism and haplotype analysis was successfully applied to identify new mutations and disease associated haplotypes in neurodegenerative diseases such as LHON, Alzheimer’s and Parkinson’s diseases (162,215). This method revealed that pathogenic LHON mutations occurred multiple times while secondary mutations sequentially accumulated in mtDNA lineages (215). Both the 14,484 and the 11,778 primary LHON mutations seem to cluster in haplogroup J, suggesting that the mitochondrial genetic background confers susceptibility to LHON (191).

The high resolution restriction site polymorphism and haplotype analysis provides information about 25% of the entire mtDNA sequence (190,215). Complementing data from previous mtDNA sequencing in 3 MS patients (3.3.1.3, ref 139,140,147), the screening of patient and control cohorts with this method confirmed the lack of pathogenic mtDNA point mutations in typical forms of MS. The potential association of the mutation at nt 13,966 with MS raised by sequencing and the subsequent screening (3.3.1.3, ref 140) was also excluded unambiguously in this larger population study (Table 21, 24). However, our haplotype analyses revealed interesting findings. Table 24 and the phylogenetic tree (Figure 11) demonstrate two clusters of MS patients with the +10,394*Dde*I / +14,798*Dde*I restriction sites defining haplotypes K* and J* in haplogroups K and J, respectively. These restriction site

polymorphisms correspond to mtDNA variants 10,394 and 14,798, respectively. Haplogroup K is defined by the -9,052*Hae*II site, and haplogroup J is defined by the -13,704*Bst*NI / -16,065*Hinf*I / +4,216*Nla*III restriction sites. Fisher's exact test reveals significant p-values (< 0.05) when the association of MS with either the J* or the K* haplotype is tested. When all MS patients and controls with the +10,394*Dde*I / +14,798*Dde*I haplotypes (K*+J* haplotypes) in the two haplogroups are compared, the Fisher's exact test suggests a p-value = 0.001.

The -13,704*Bst*NI and the +4,216*Nla*III sites correspond to the 13,708 and 4,216 secondary LHON variants in haplotype J*. Haplotype J* is defined by the +10,394*Dde*I / +14,798*Dde*I / +4,216*Nla*III/ -13,704*Bst*NI restriction sites which correspond to the 10,394 / 14,798 / 4,216 / 13,708 nucleotide variants. Patients preferentially carry the J* haplotype, while controls preferentially carry non-J* haplotypes in haplogroup J (p=0.049). Similarly, patients are found predominantly with the K* haplotype, while controls are found predominantly with non-K* haplotypes in haplogroup K. The association of haplotype J* with MS confirms and clarifies the involvement of secondary LHON variants in the disease suggested in our first mtDNA scan (in 3.2.1.1, 3.3.1.1). As primary LHON mutations at 11,778 or 14,484 preferentially occur in haplotype J* in haplogroup J (191), the above data suggest that the observed association between LHON and MS is related to a shared mitochondrial genetic background (haplotype J*) of the two diseases (155-161).

In summary, this study complements and reconciles data from previous reports on mtDNA in MS. There is now sufficient evidence to reject with a high degree of probability the hypothesis of an MS related pathogenic mtDNA mutation. However, certain mtDNA haplotypes (K* and J*) determined by a simultaneous presence of the +10,394*Dde*I / +14,798*Dde*I restriction site polymorphisms and secondary LHON mutations (nts 4,216 and 13,708) show association with MS. Therefore, the previously suggested association between LHON and MS may be, at least in part, related to their overlapping association with the J* haplotype. MS patients with K* and J* haplotypes do not present with specific phenotypes. The biological importance of these haplotypes remains to be established.

3.4.2 Complex I variants in MS

The preceding studies identified MS associated mtDNA haplotypes that are defined by sequence variants in mtDNA encoded subunits of Complex I. The question arises whether these polymorphisms merely designate mtDNA lineages associated with susceptibility to MS in Caucasians, or they interact with each other and probably also with nDNA encoded variants of Complex I at protein level. If the latter hypothesis is true, variants in multiple subunits may influence functional properties of Complex I. The involvement of Complex I genes in MS is supported by the observation that several of its subunits are encoded in chromosomal regions close to or within linkage defined susceptibility loci (41,68,69).

These considerations prompted us to scan nDNA and mtDNA encoded genes of Complex I in MS families. Our nDNA studies reveal associations of MS with two- and three-marker haplotypes within the NDUFS5, NDUFS7 and NDUFA7 subunits of Complex I. As the observations were similar in DS101-112 (all families) and in the RR/SP-MS subgroup, we conclude that the inclusion of 26 PP-MS families did not alter the outcome, and as a subgroup alone did not have enough power to draw conclusion regarding phenotype-specific associations. Our analyses suggest that haplotypes in NDUFS5, NDUFS7 and NDUFA7 are associated with MS. Markers NDUFB7Y and NDUFB7X though with significant p-values, are not relevant to MS. These two markers represent nonsynonymous mutations with their major alleles preferentially transmitted to both unaffected and affected offspring. Similar transmission distortions have been noted in humans and attributed to selection against deleterious mutations, meiotic drive or maternal-fetal incompatibility (248).

This study focused on 20 of 38 nuclear genes of Complex I, representing the most comprehensive scan of this macromolecular complex to date. This is also the first scan of Complex I genes in MS. Fifteen of these genes were selected based on their proximity to regions with positive linkage scores in MS (41,68,69). The additional genes were included assuming that an association based analysis may be capable of revealing disease relevant findings in regions where the conventional linkage approach has reached its resolution limits (79). Contrary to expectations, only one of the MS associated haplotypes, NDUFS5A-NDUFS5X-NDUFS5D (1p34.2-p33) was found in proximity of a previously defined susceptibility locus (1p34.3) (68). It is important to note that we only considered association with MS when a haplotype preferentially transmitted to MS patients was not preferentially transmitted to unaffected sibs. Therefore, the detected moderate genetic associations are unlikely to be by chance findings and the identified haplotypes may carry or be close to variants directly involved in MS.

Relatively sparse information is available for most of the Complex I genes, including the ones identified in this study. NDUFS5 and NDUFS7 are iron-sulfur subunits, while NDUFA7 is part of the hydrophobic fraction (Figure 9). The amino acid and cDNA sequences of NDUFS5, NDUFS7 and NDUFA7 share high degrees of homology with their bovine counterparts (249-251), and their genes are mapped to 1p34.2-p33, 19p13.3 and 19p13.2, respectively (251-253). Subunits of Complex I are ubiquitously expressed, but with varying abundance in different tissues. Using real-time PCR, we did not find regional differences in the β-actin normalized values of NDUFV1, NDUFS4, NDUFS5, NDUFS6 and NDUFS7 mRNA molecules in ten sets of NAWM, NAGM and plaque (data not shown). While pathogenic mutations have not been reported in NDUFS5 and NDUFA7 to date, a Val122Met substitution in the NDUFS7 gene was described in association with Complex I deficiency and Leigh's syndrome (192).

We did not find differences in the frequency of previously defined MS associated mtDNA polymorphisms and haplotypes, when the maternal (transmitted) and paternal (non-transmitted) mtDNA molecules were compared in DS101-112, mostly because the fathers of MS patients in DS101-112 had a higher percentage of mtDNA polymorphisms aligning in haplotype J* than the previously tested normal controls (144,145). The cause of this frequency difference is unknown.

We considered that unaffected fathers and mothers with nuclear MS susceptibility Complex I genes, may also carry mitochondrial susceptibility genes of MS. Indeed, mothers and fathers positive for the NDUFS5axd haplotype (Table 26) turned out to have significantly higher rate of J* mtDNA haplotype than mothers and fathers negative for the NDUFS5axd haplotype. It is, therefore, tempting to postulate that nDNA (e.g. in NDUFS5) and mtDNA encoded MS relevant variants (e.g. secondary LHON mutations) interact with each other at protein level in Complex I. Offspring of mothers with both nuclear and mitochondrial susceptibility genes of MS may receive both nuclear and mtDNA encoded susceptibility variants from their mothers, while offspring of fathers with both nuclear and mitochondrial susceptibility genes of MS would only get nuclear susceptibility variants from their fathers, explaining at least in part a larger maternal genetic contribution to the disease. Due to the pedigree and data structures, the co-occurrence of nDNA and mtDNA encoded susceptibility variants could not be evaluated without biases in affected individuals in the studied families.

In conclusion, we investigated simultaneously mitochondrial and nuclear genes of Complex I in MS families. This is the most comprehensive scan for variants in Complex I genes to date. The identified nDNA SNP haplotypes have modest but specific association with MS, and likely indicate nearby variants involved in lesion development. Our data suggest that an interaction between the MS associated mtDNA and nDNA variants is possible at protein level, a preliminary observation that merit further investigations. The subcellular location and the known function of these subunits indicate that Complex I variants more likely influence bioenergetic and cell survival pathways than act as new antigenic determinants. These genetic data and the biochemical observations below suggest that Complex I may represent a link between the upstream inflammation and the downstream neurodegeneration in MS.

3.4.3. Oxidative damage to mitochondrial macromolecules, Complex I impairment, somatic mtDNA deletions and expression of pro- and anti-apoptotic molecules

3.4.3.1 Oxidative damage to mtDNA, impairment of Complex I and somatic mtDNA deletions in chronic active plaques

While genetic data suggest the involvement of Complex I variants in MS, it remains unknown as to what ways these variants contribute to lesion development: Can sequence variants directly influence

functional properties of Complex I or do the inherited susceptibility determinants only become biologically significant under pathological conditions (e.g. inflammation)? Since neither we nor others have detected differences in Complex I activity related to gene polymorphisms (192,193), we examined the correlation between inflammatory ROS, oxidative damage to mitochondrial macromolecules and the activity of Complex I.

We postulated that inflammation-induced oxidative damage to mitochondrial macromolecules that exceeds the capacity of repair may contribute to impaired energy metabolism and degeneration of CNS cells with the highest degrees of exposure and energy requirement. This hypothesis in MS is supported by studies in neurodegenerative diseases of non-inflammatory origin, in which a relationship between intracellular ROS, oxidative damage to DNA, decreased OXPHOS and neuronal loss has been demonstrated (162,164-165,212,221,254-260).

As a continuation of our preliminary studies on ROS production by inflammatory cells and the associated oxidative damage in the CNS (148,149), here specific features and consequences of oxidative damage to mtDNA were presented. For this study we adapted a molecular method to assess selectively mtDNA in ug amounts of total DNA (217-219), which was not possible in the previous study that needed large DNA amounts for HPLC (our HPLC study not detailed here but reported in 148). As summarized in Tables 28-30 and Figure 12-14, the molecular method revealed a significant increase in oxidative damage at both purine and pyrimidine nucleotides in the light as well as the heavy strands of mtDNA in plaques. Immunohistochemistry confirmed the increased oxidative damage to DNA predominantly in the cytoplasmic (in contrast to the nuclear) compartment of cells in inflamed plaques (Figure 15). The present study extends our previous observation on oxidative damage to DNA, and establishes that it predominantly affects mtDNA in association with chronic inflammation in the CNS.

In pathological conditions including inherited or acquired forms of neurodegeneration, oxidative damage to DNA / mtDNA has been associated with a decline of mitochondrial energy metabolism resulting in structural changes in neurons (162,164-165,212,221,255-260). While the initial abnormality and molecular events are specific to each disease entity, the downstream pathway includes shared biochemical features (oxidative DNA damage, decline in ATP synthesis) converging in a similar end result (neuronal / axonal degeneration). We postulated that a cause and effect relationship also exists between inflammatory ROS, oxidative damage to macromolecules, impaired OXPHOS and degenerative changes in MS lesions. Oxidative damage measured in DNA, likely also affects membrane lipids, proteins or nonheme iron containing prosthetic groups of enzymes (Complex I-III and aconitase) in mitochondria, leading to an impairment of electron transfer in plaques. Alternatively, oxidative damage may lead to somatic mtDNA deletions and reduced expression of mtDNA encoded

subunits of OXPHOS enzymes in active plaques. Comparing the activity of mitochondrial enzyme complexes in NAWM and plaque pairs of 10 MS patients, we indeed found an impaired activity of the NADH-DH component of Complex I, and an increased activity of Complex IV in 70% of plaques. The higher activity of Complex IV in plaques is likely compensatory, since similar reciprocal direction of changes have been noted in mitochondrial disease with decreased activity of Complex I.

To support to the above postulated *in vivo* sequence of events, we induced ROS production and determined the kinetics of oxidative damage to mtDNA in the U87MG human astroglioma cell line (ATCC). After defining and reproducing the conditions which induced the highest degree of damage, a mitochondrial probe (JC1) was introduced to the cells. Both cytofluorometric and microscopic detection demonstrated a shift from red to green color in the JC1 probe, indicating that oxidative damage to mitochondrial macromolecules resulted in a decline of mitochondrial energy metabolism and membrane potential (105). Thus, an exposure to oxidative stress may lead to impairment of OXPHOS followed by tissue degeneration and cell death.

To test if the decreased Complex I activity was related to oxidative damage-induced somatic mtDNA deletions in subunits of Complex I, we measured the proportion of deleted and full length mtDNA molecules in single cells of NAWM, NAGM and plaques. This study demonstrated that while there is an age-related accumulation of Cox- cells as well as somatic mtDNA deletions in MS brains similar to those of control brains, chronic active plaques do not have higher proportion of Cox- cells and deleted mtDNA molecules than NAWM or NAGM (228). In a parallel study we also tested copy numbers of mtDNA molecules in the NAWM, NAGM and plaque regions, but again found no pathology-related alterations (data not detailed here; see in 261). Thus, these studies excluded the possibility of oxidative-stress related somatic mtDNA deletions or copy number alterations as a potential cause of decreased Complex I activity in chronic active plaques. The detected functional impairment of Complex I in chronic active plaques, therefore, is likely related to a direct effect of oxidative damage to the enzyme and its redox sensitive subunits.

Following our mtDNA and OXPHOS studies published mostly in the 1990-ies and early 2000, several groups started to evaluate mitochondrial protein expression levels or mRNA of mitochondrial proteins in brains of MS patients using enzyme histochemistry, immunohistochemistry, in situ hybridization and mRNA microarray methods (262-265). Dutta et al (262) demonstrated a decreased activity of Complex I and III, and a down-regulation of the transcripts for several mitochondrial proteins in MS cortex. Mahad et al (263) demonstrated functionally important defects of Complex IV and down-regulation of its catalytic component (COX-I) in Pattern III but not in Pattern II MS lesions (19). This finding does not conflict with ours, since we did not subclassify pathological lesion types (Pattern I and II are the most

common types likely predominantly present in our specimen selection). Subsequently, Mahad et al (264) also showed that Complex IV activity is reduced despite the presence of mitochondria in demyelinated axons, and this Complex IV reduction appeared in negative correlation with the distribution of macrophages. In contrast, in inactive areas of chronic MS lesions the Complex IV activity and mitochondrial mass were increased within approximately half of large chronically demyelinated axons compared with large myelinated axons in the brain and spinal cord (264). The lack of Complex IV activity in a proportion of Na+/K+ ATPase alpha-1 positive demyelinated axons supported axonal dysfunction as a contributor to neurological impairment and disease progression. In vitro studies also showed that inhibition of Complex IV augmented glutamate-mediated axonal injury.

3.4.3.2 Bcl-2 and its homologues in the brains of patients with MS

We postulated that oxidative damage to mitochondrial macromolecules and impaired activity of OXPHOS may be linked to the activation of an apoptotic pathway. Therefore, we asked if the distribution of inflammation induced oxidative stress correlates with the expression of molecules involved in free radical scavenging and apoptosis in MS. A previous study (266) noted decreased SOD-1 activity in erythrocytes suggesting an impaired free radical scavenging machinery in MS. Although we did not assess the activity of SOD-1 or GSHS, the mRNA expressions for these enzymes were not altered in association with oxidative stress in plaques (105). This regionally uniform expression of SOD-1 and GSHS in MS was similar to that detected in the gray and white matter of normal or Alzheimer disease controls.

In contrast, we noted an up-regulation of pro- and anti-apoptotic molecules in correlation with β_2-microglobulin expression primarily in plaque but also in NAWM compared to corresponding NAGM regions. These changes were related to the inflammatory pathology of MS, as no similar regional differences were observed in the gray – white matter comparisons of normal or Alzheimer disease controls. However, as reported by others (267), our analysis in the encephalitis specimens also suggests that the increased expression levels of pro- and anti-apoptotic molecules are related to the inflammatory process, and not specific for the plaque formation in MS.

In the murine model of MS, an increased expression of Fas – FasL was associated with Bax in CD4 T cells and microglia in correlation with the activity of EAE (268). Low Fas expression was constitutively present on oligodendrocytes and up-regulated during EAE. Bax expression or signs of apoptosis, however, were not seen in oligodendrocytes, probably due to the up-regulation of the anti-apoptotic Bcl-2. Similarly, an increased expression of TNF receptor but lack of apoptosis in oligodendrocytes was described in and around MS lesions (269,270), while infiltrating lymphocytes and activated microglia showed definite signs of apoptosis. Others (19,55,271), however, noted heterogeneity of plaques with

varying numbers of apoptotic oligodendrocytes. These observations suggest that cells expressing pro-apoptotic and anti-apoptotic molecules are composed of residential microglia and infiltrating mononuclear cells in NAWM, NAGM and plaque regions, and may include varying numbers of oligodendrocytes in plaques. Real-time PCR can quantify small differences in specimens, but without defining the cellular substrates of the differentially expressed mRNA molecules. Based on data from immunohistochemistry studies, the increased Bak, Bcl-2, Bcl-x_L and β_2-microglobulin expression in plaque and to lesser degrees in NAWM, likely is related to the activation of microglia, infiltrating mononuclear cells and oligodendrocytes.

Altogether, our study suggests that histological (H & E, CD68, β_2Mg) and molecular (β_2Mg mRNA) signs of immune activation and inflammation correlate with the expression of pro- and anti-apoptotic molecules in MS brains. The lack of a compensatory upregulation of the free radical scavenging machinery in regions affected by oxidative stress indicates that inflammation may exert its harm not only via inducing death receptor-ligand interactions in the CNS but also via a sequence of events that includes unprotected oxidative damage to mitochondrial macromolececules, impairment of Complex I, induction of apoptosis-related molecules and a direct (toxic) mitochondrial mechanism of cell death.

4. CONCLUSIONS: THE ROLE OF MITOCHONDRIA IN NEURODEGENERATION DEVELOPING SECONDARY TO INFLAMMATION IN MS

4.1 Mitochondria

Mitochondria are located in the cytoplasm and play central roles in the maintenance and function of all tissue types. The mitochondrion has a double membrane surrounding a distinct molecular machinery including mtDNA and proteins. The inner mitochondrial membrane (IMM) forms cristae emanating into the matrix and provide a surface for many enzymatic reactions (e.g. lipid metabolism, citric acid cycle, oxidative phosphorylation). Oxidation of substrates generates electrons which pass through enzyme Complexes I to V and leads to ATP synthesis (Figure 8).

The mitochondrial control of energy metabolism is closely linked to cell survival and death. Permeabilization of the IMM and outer mitochondrial membrane (OMM) precedes the signs of caspase activation leading to apoptosis or necrosis (20,21,271-272). The permeability transition pore (PTP) complex between the IMM and OMM is formed by several proteins including pro- and anti-apoptotic homologs of Bcl-2. The opening and closing of PTP is controlled by the actual MTMP, concentration of divalent cations, matrix pH, oxidation / reduction of nucleotides, and the expression of pro- and anti-apoptotic members of the Bcl-2 family (Figure 19) (20,21,271-272). A complete opening of PTP leads to uncoupling of the respiratory chain, arrest of ATP synthesis, drop of the MTMP, Ca^{2+} outflow from the matrix, generation of free radicals and a release of pro-apoptotic molecules (cytochrome c, Smac /

DIABLO and apoptosis inducing factor) from the inter-membranous space and matrix to the cytoplasm (20,21,165,221,271-272).

Cytochrome c in the cytosol binds to the apoptotic protease-activating factor 1 (Apaf-1) that leads to the activation of the caspase cascade of apoptosis in the presence of ATP. Without sufficient ATP, the apoptosome cannot be formed and the cell dies by necrosis. Both inherited (e.g. primary LHON mutations) and acquired OXPHOS defects (e.g. oxidative damage) are pore openers leading to the above outlined self-amplifying process and cell death (Figure 19). Activated calcium-dependent cysteine proteases and caspases also can impair cytoskeletal structures, causing suspension of axonal transport and axonal degeneration (Figure 20).

Figure 19. The role of mitochondria in apoptosis and necrosis

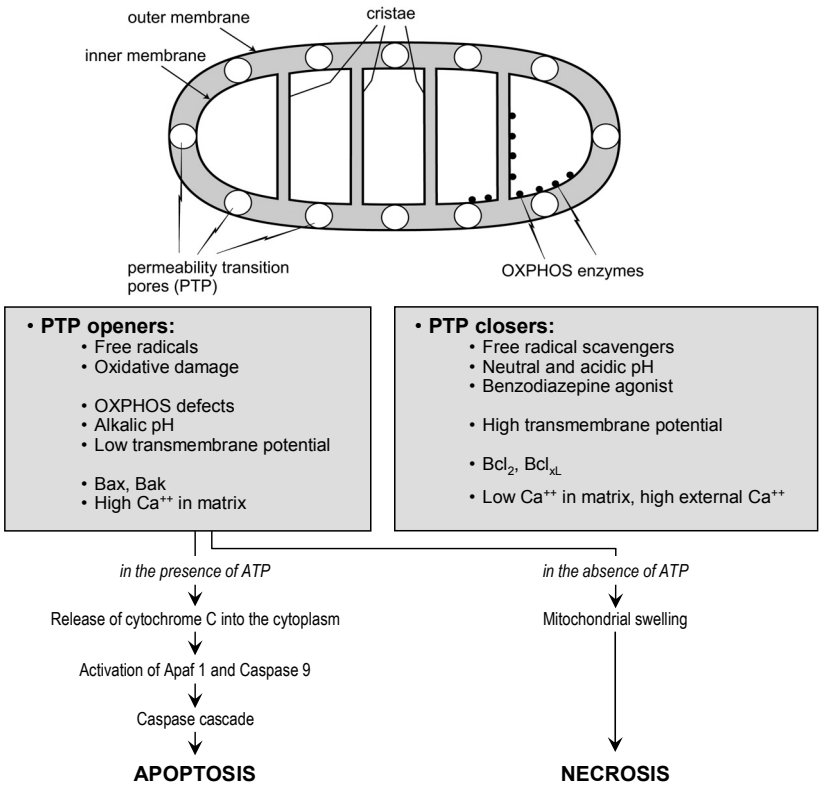

In the presence of ATP, the opening of PTP leads to the release of cytochrome c into the cytoplasm, activation of the caspase cascade and apoptosis. In the absence of ATP, PTP opening is followed by mitochondrial swelling and necrosis. PTP openers and closers are listed in the gray windows. Pro-apoptotic members of the Bcl-2 family (Bax, Bak) cause PTP opening, while anti-apoptotic members (Bcl-2, Bcl-x_L) are involved in PTP closing.

Figure 20. A proposed mechanism of inflammation induced neurodegeneration in MS

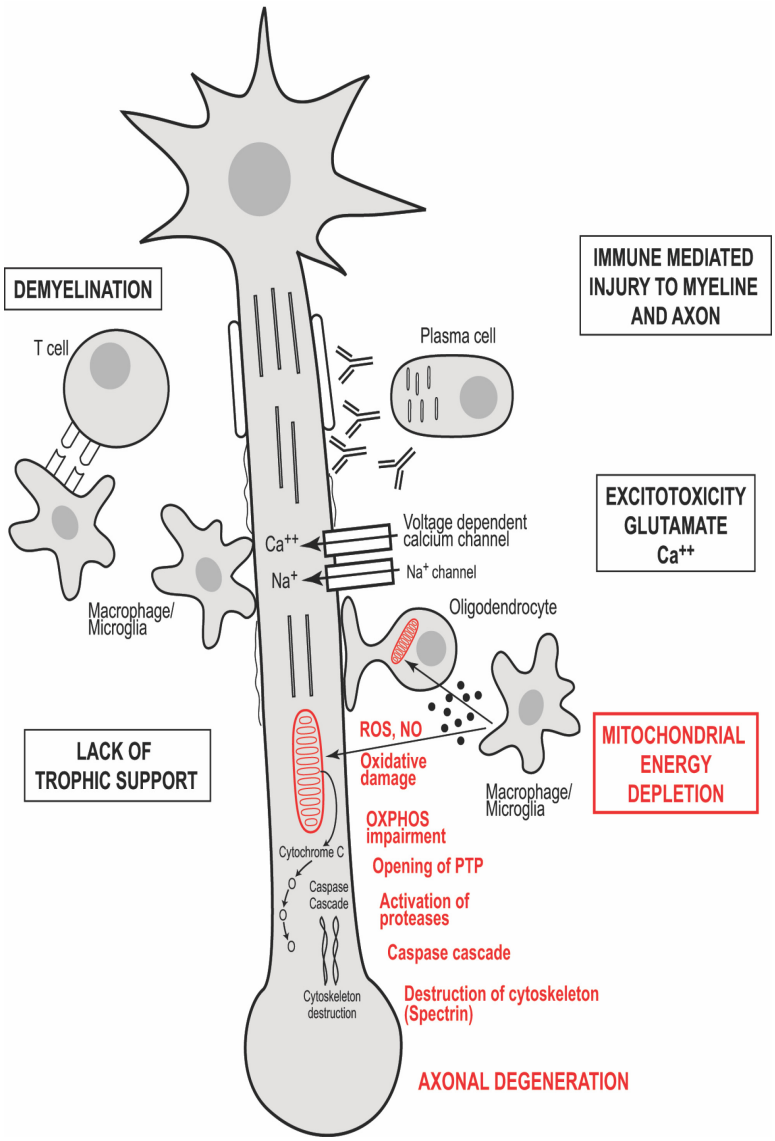

Axonal degeneration in inflammatory demyelination has been related to lack of trophic support (glial cells, growth factors), the loss of protective myelin sheaths, a direct effect of immunoglobulins and cytokines, and excitotoxicity mediated by glutamate and Ca^{2+}. We propose that mitochondria are also involved in the down-stream pathway of neurodegeneration initiated by inflammatory ROS and NO. Oxidative damage to mitochondrial macromolecules may cause OXPHOS impairment, opening of PTP, activation of caspases and apoptosis or other forms of cell death. The activation of caspases and other proteases can also cause a destruction of cytoskeletal proteins.

4.2 A proposed role of mitochondria in inflammation induced neurodegeneration

Based on our observations we propose that inflammation ignites a mitochondrion-driven mechanism that contributes to the observed apoptotic and non-apoptotic oligodendroglial loss and neuroaxonal degeneration in MS (Figure 19,20). Immune mediated forms of oligodendroglial and neuronal apoptosis have been comprehensively studied in MS (55,56,58,59,207,273). A MHC dependent cytotoxicity mediated by CD8 or CD4 T lymphocytes has been debated, since *in vivo* data do not show significant expression of MHC Class I molecules by oligodendrocytes and neurons, and Class II is not expressed by these cells at all. Nevertheless, CD8 T cells curiously line up along demyelinated axons (63). However, a by-stander mechanism caused by the engagement of antigen specific T cell receptors with the appropriate MHC molecules on antigen-presenting cells can cause oligodendrocytopathy or neuronal damage (63). CD95-ligand (L) positive T cells also induce apoptosis of CD95 positive oligodendrocytes in a non-MHC-dependent manner (59), while activated CD95 positive T lymphocytes are eliminated by CD95L positive residential cells from evolving plaques (274-275). Further, activated macrophages and microglia cause cell damage in the CNS by multiple mechanisms including antibody- and complement-dependent cytotoxicity, cytokine ligand - receptor or adhesion molecule - receptor mediated cytotoxicity (204).

A mitochondrion-driven component of neurodegeneration in inflammatory demyelination had not been described prior to our studies. We propose that this pathway is initiated by inflammation in MS. Activated monocytes and microglia in MS express iNOS and produce increased amounts of NO (203,279), which damages proteins by generating nitration adducts (e.g. nitrotyrosine). NO can also react with O_2^- (a component of ROS) resulting in a toxic intermediate called peroxinitrite. ROS are produced in increased amounts by activated MNCs in MS (149) and released by macrophages giving a ring like appearance on MRI in acute plaques (211). ROS cause oxidative damage to macromolecules in the site of inflammation. While evidence suggest that scavengers of NO and physiologic anti-oxidants can provide significant therapeutical effects in EAE (276-278), we did not detect an upregulation of such molecules in lesions of MS. In contrast, we consistently detected a significant accumulation of oxidative damage to DNA in association with inflammation in plaques, by using High Pressure Liquid Chromatography (148), immunohistochemistry and endonucleases (FPG and Endo III) which introduce single strand breaks at oxidized purine and pyrimidine nucleotides, respectively (105). Assaying mitochondrial enzyme complexes, we found a decreased activity of NADH-DH component of Complex I in 70% of active plaques (105). Despite the accumulated oxidative damage in mtDNA, this decreased Complex I activity was not related to an accelerated accumulation of somatic mtDNA deletions. Therefore, a direct effect of oxidative stress on the enzyme complex per se may need to be further evaluated. In correlation with markers of immune activation, inflammation, oxidative damage and OXPHOS impairment, we detected an upregulation of mRNAs for molecules regulating cell survival and

death (136). The temporal and spatial correlations suggest that these events align in a biological sequence and contribute to a mitochondrial regulation of cell survival and death in lesions of MS. While our data had supported alone this concept for years, recent histological analyses with new molecular markers revealed further evidence for an oxidative stress related mitochondrial mechanism of neurodegeneration in MS (279,280). In these studies, an increased expression and nuclear translocation of hypoxia inducible factor (HIF)-1α was detected in plaques characterized by distal oligodendrocytopathy, apoptotic death of oligodendrocytes and signs of hypoxic tissue injury (19,279,280). The authors proposed that this condition resulted from oxidative stress and mitochondrial dysfunction, best defined in large acute, histological type III plaques and Balo's type of concentric lesions, but also present in some chronic active lesions. Subsequent observations on altered mRNA and protein expressions of mitochondrial molecules in MS cortex and white matter lesions can be reconciled with our conclusion and underscore the role of mitochondria in inflammatory demyelination (262-265). However, in addition to inflammation leading to neurodegeneration via a mitochondrial pathway, demyelination may also contribute to a mitochondrial mechanism faciliating axonal loss. This mechanism results from the increased expression and redistribution of the voltage-gaited Na-channels from the node of Ranvier to the entire length of demyelinated axons. The higher numbers of Na-channels are associated with higher energy demand, but at a time when the Na+/K+ ATPase molecules are compromised by inflammation. This deficiency of the Na+/K+ ATPase leads to an excessive axoplasmic Ca2+ accumulation via the Na+/Ca++ exchanger. Thus, the chronically depolarized demyelinated axons ultimately suffer from energy depletion, altered Ca2+ homeostasis, and impaired structural integrity (263-265). In addition, both the energy depleted axons and oligodendrocytes are highly sensitive to the toxic effects of glutamate mediated by distinct glutamate receptors (265). The recent identification of a KIF1B SNP as susceptibility marker for MS (116), brings the kinesin family of transport proteins also in the picture. These molecules are responsible for the axoplasmic transport of mitochondria and neurotransmitters, and thus, may also contribute to an inflammation induced, mitochondrion-mediated neurodegenerative process. These data underscore the complexity of mitochondrial involvement in the final pathway of neurodegeneration in MS. Our works represents the first introduction of a concept that links inflammation via a mitochondrial mechanism to CNS tissue loss.

4.3 The involvement of Complex I in MS

A possible involvement of Complex I in inflammatory demyelination and neurodegeneration was suggested by previous clinical and genetic observations, including 1) the occurrence of inflammatory demyelination in pedigrees with LHON; 2) the detection of primary LHON mutations in mtDNA encoded subunits of Complex I in some patients with MS; 2) the increased frequency of secondary LHON mutations in mtDNA encoded subunits of Complex I in patients with MS; and 3) the co-localization of several nDNA encoded subunits of Complex I with linkage defined susceptibility loci of MS. These

observations prompted us to perform the most comprehensive analyses of mtDNA to date, and to define variants and haplotypes of nDNA encoded genes of Complex I in MS.

The mtDNA studies were comprehensive in two ways: 1) Screening 25% of the entire mtDNA sequence in populations of patients and controls, and 2) Determining the full sequence of mtDNA in a few patients with MS, PON and NMO. Our studies establish that primary LHON mutations rarely occur, and the involvement of other pathogenic mtDNA mutations also can be excluded in MS, PON and NMO. However, there is an increased frequency of secondary LHON mutations that align in two MS associated (designated as K* and J*) mtDNA haplotypes in Caucasians. Since primary LHON mutations predominantly occur in haplotype J*, the observed association between LHON and MS may be related to the overlapping mitochondrial genetic background of the two diseases.

Although the functional significance of secondary LHON mutations remains to be determined, it is notable that these missense variants are all located within mtDNA encoded subunits of Complex I. Since mtDNA and nDNA encoded subunits of Complex I are assembled in a single protein complex, the small effects of variants in different subunits may become additive or synergistic and influence the overall function of the enzyme complex.

We observed that haplotypes within the NDUFS5, NDUFS7 and NDUFA7 nDNA encoded subunits of Complex I are associated with MS in families. Fathers as well as mothers who carry the MS associated NDUFS5 haplotypes have an increased frequency of the J* mtDNA haplotype including secondary LHON mtDNA variants. This observation suggests an epistatic interaction among nDNA and mtDNA encoded subunits. However, our unpublished observations suggest that the sequence variants don't directly influence the activity of the enzyme under normal conditions (data not shown). We postulate that the genetic variants only exert very subtle effects on the enzyme's physical properties, however, these small effects may become additive to or synergistic with the effects of biochemical modifiers (e.g. inflammatory molecules, oxidative stress) in a pathological environment.

4.4 Summary of conclusions

The limited effectiveness of currently available medications in progressive forms of MS has reemphasized the importance of neurodegeneration developing in association with inflammation. Loss of oligodendrocytes and failure of their regeneration from precursors is the cause of an irreversible demyelination. A functionally most significant correlate of disability is the neuroaxonal loss, which progresses from the onset of the disease. Direct inflammatory injury contributes to focal loss of axons, neurons and oligodendrocytes within circumscribed lesions, while subtle degenerative processes are likely more instrumental in the diffuse loss of these tissue elements outside of plaques. We propose a

concept of neurodegeneration in MS as a process linked to inflammation via an acquired mitochondrial dysfunction and to its consequences including apoptotic and non-apoptotic cell death. Individual differences in the tissue response to inflammation show great variations and may depend on genetic polymorphisms in molecules defining the mitochondrial regulation of energy metabolism, cell survival and death. Earlier MS genetic studies identified several susceptibility loci in chromosomal regions where subunits of OXPHOS enzymes are encoded. Our early studies revealed an association between mtDNA variants in subunits of Complex I, cytochrome b and MS. The subsequent studies on nuclear genes of Complex I demonstrate that nucleotide variants and haplotypes within the genes of NDUFS5, NDUFS7 and NDUFA7 subunits are associated with the disease in families, and that an interaction between mtDNA and nDNA variants of Complex I may occur at protein level. Our biochemical and histological data suggest that Complex I may be affected by oxidative stress and contribute to the degenerative process downstream to chronic inflammation in the CNS. While targeting inflammatory mediators (e.g. CCL-CCR molecules) shortly after the onset or early during the course of the disease is necessary to prevent the development of a downstream pathology (demyelination, oligodendrocytopathy, neuroaxonal loss), new strategies (e.g. neuroprotection preserving mitochondrial function) are needed to minimize neurodegeneration in both early and established forms of the disease. Identification of genetic markers rendering individuals susceptible to autoimmunity and neurodegeneration associated with inflammation may facilitate the development of an early combined therapy personnaly designed for the treatment of multiple sclerosis.

Acknowledgments:

I am greatly indebted to Drs. Andras Guseo, Gyozo Petranyi and Peter Halasz for the exceptional professional and personal support they provided early during my studies in neurology, MS and immunogenetics, which allowed me to develop interest in research. I am also very grateful to Dr. Samuel Komoly for his collaboration and continuing support in building bridges with the Medical University of Pecs.

I am very grateful to Dr. George C. Ebers and Dr. Jorge Oksenberg for allowing us obtaining DNA specimens for the family based genetic studies from the Collection of the Canadian MS Collaborative Group, London, ON, and from the Multiple Sclerosis DNA Bank, UCSF, San Francisco, CA, respectively. Dr. Gary Birnbaum also contributed specimens of PP-MS families from the Multiple Sclerosis Treatment and Research Center, Minneapolis, MN. Specimens from sporadic patients with MS and controls were collected with the help of Dr. Fred D. Lublin, at the Multiple Sclerosis Center, Thomas Jefferson University, Philadelphia, PA.

Peers who contributed to my studies (in chronological order):
Michael D. Brown, Ph.D. discussed mitochondrial genetics of LHON.
Hansjuerg Alder, Ph.D. consulted technical issues in the mtDNA studies.
Fred D. Lublin, M.D. invited me for a one year fellowship in the USA, and contributed specimens to my studies.
Raul N. Mandler, M.D. contributed specimens to the studies on Devic's disease.
George C. Ebers, M.D. generously allowed me to learn about linkage analysis during my sabbatical at the Wellcome Trust Center, Oxford University.

Yin Yao Shugart, Ph.D., a genetic statistician, consulted some aspects of data analyses.
Mary Selak, Ph.D. was involved in the assessment of Complex I activity.
Dr. Saud Sadiq generously offered space for moving my lab from Philadelphia to the Roosevelt Hospital, Columbia University, New York, NY and helped us with his patients' specimens.

Postdoctoral fellows, associates and technicians trained in my lab and involved in my projects:
Shulan Li, Ph.D, Mary R. Vohl, Ursula Bosch, M.D, Jose L. Rodriguez, M.D., Alan Cahill, Ph.D., Fengmin Lu, M.D., Ph.D., Linda Shawver, John O'Connor, Ph.D., Olga Vladimirova, Ph.D., Devjani Chatterjee, Ph.D. and Zheng Kee, M.D., Ph.D. were involved in the laboratory procedures or in running the computer programs used in the mitochondrial DNA and biochemical studies. Tamara Vyshkina, Ph.D. ran the computer programs in the family based association studies. Ileana Banisor carried out the laboratory procedures in the real-time PCR studies. Andrei Blokhin and was involved in the somatic mtDNA deletion studies as a postdoc in my lab.

At last, but not least, I will never be able to say enough thanks to my parents who unconditionally and with so much love supported my personal and academic progress from the earliest age to date.

The studies presented here, including all salaries, laboratory equipments, contract and consultation fees, laboratory supplies and overhead fees, were supported by competitive external grants to the author (as principal investigator) of this thesis from the following agencies:

1. Characterization of the mitochondrial DNA in multiple sclerosis. RG2770A2/2 National Multiple Sclerosis Society. $ 321,379. 1996-2000.
2. Analysis of subcellular pathology in the brain of MS patients. PP0501
National Multiple Sclerosis Society. $24,681 1996-1997.
3. Mitochondrial DNA variants in Devic's disease.
National Multiple Sclerosis Society, PP0765 $27,500. 2000-2002.
4. Traveling Grant. The Burroughs Wellcome Fund. $12,344. 2000-2001.
5. Nuclear and mitochondrial candidate genes in multiple sclerosis. RG3334-A-4/T
National Multiple Sclerosis Society, $405,594. 2002-2005.
6. Candidate genes in primary progressive multiple sclerosis.
Wadsworth Foundation $330,000. 2002-2005.
7. The role of genetic variations in β-chemokines in defining the disease modifying effect of Rebif in MS. Serono $120,000. 2003-2005.
8. Variants of beta-chemokines within chromosome 17q11 in MS. RG35212-A-6
National Multiple Sclerosis Society $632,251. 2004-2006.
9. Mitochondrial DNA deletions in MS brains. NMSS. PP1334 $44,000, 11.01.2006-10.31.2008.

Abbreviations:

BBB: blood-brain barrier

β_2Mg (b2mg): β_2-microglobulin

CCL: CC chemokine ligand

cM: centi-morgan

CCR: CC chemokine receptor

CMSCG: Canadian Multiple Sclerosis Collaborative Group

CNS: central nervous system

D-loop: displacement loop

DS: data set

EAE: experimental autoimmune encephalomyelitis

EDSS: extended disability status scale

FBAT: family based association test

GSHS: glutathione synthetase

HBAT: haplotype based association test

HBSFRC: Human Brain and Spinal Fluid Resource Center

HIF1α: Hypoxia inducible factor-1α

HIPAA: Health Insurance Portability and Accountability Act

HLA: human leukocyte antigen

HPLC: high pressure liquid chromatography

HS: heavy strand (of mtDNA)

HWE: Hardy-Weinberg equilibrium

IDDM: insulin dependent diabetes mellitus

IMM: inner mitochondrial membrane

IRB: internal review board

LD: linkage disequilibrium

LHON: Leber's Hereditary Optic Neuropathy

LS: light strand (of mtDNA)

MBP: myelin basic protein

MHC: major histocompatibility complex

MMP: matrix-metallo-protease

MNC: mononuclear cell

mRNA: messenger RNA

mtDNA: mitochondrial DNA

MRI: magnetic resonance imaging

MRS: magnetic resonance spectroscopy

MTR / MTI: magnetization transfer ratio / imaging

NAA: N-acethyl-aspartate

NAGM: normal appearing gray matter

NAWM: normal appearing white matter

NCBI: National Center for Biotechnology Information

nDNA: nuclear DNA

NMO: neuromyelitis optica

NO: nitric oxide

OMM: outer mitochondrial membrane

ON: optic neuritis

OND: other neurological disease

OXPHOS: oxidative phosphorylation

PBL: peripheral blood lymphocyte

PCR: polymerase chain reaction

PDT: pedigree disequilibrium test

PON: prominent optic neuritis

PP-MS: primary progressive MS

PR-MS: progressive-relapsing MS

PTP: permeability transition pore

QTL: quantitative trait locus

RA: rheumatoid arthritis

RMMSBB: Rocky Mountain Multiple Sclerosis Brain Bank

rRNA: ribosomal RNA

ROS: reactive oxygen species

RR-MS: relapsing-remitting MS

RP-MS: relapsing-progressive MS

SLE: systemic lupus erythematosus

SNP: single nucleotide polymorphism

SOD-1: superoxide dismutase-1

SP-MS: secondary progressive MS

TCR: T cell receptor

TDT: transmission disequilibrium test

TH1 / TH2: T helper-1 / T helper-2

tRNA: transfer RNA

UCSF MSDB: University of California, San Francisco, Multiple Sclerosis DNA Bank

VEP: visual evoked potential

VCAM1: vascular cell adhesion molecule-1

VLA4: very late antigen-4

WM: white matter

References:

1. Kalman B, Lublin FD. The genetics of multiple sclerosis. A review. Biomed Pharmacother 1999;53:358-370.
2. Kurtzke JF, Beebe GW, Norman JE, Jr. Epidemiology of multiple sclerosis in U.S. veterans: 1. Race, sex, and geographic distribution. Neurology 1979;29:1228-1235.
3. Pratt RTC, Compston ND, McAlpine D. The familial incidence of multiple sclerosis and its significance. Brain 1951;74:191-232.
4. Bulman DE, Ebers GC. The geography of multiple sclerosis reflects genetic susceptibility. J Trop and Geograph Neurol 1992:66-72.
5. Ebers GC, Bulman DE, Sadovnick AD, Paty DW, Warren S, Hader W, Murray TJ, Seland TP, Duquette P, Grey T, et al. A population-based study of multiple sclerosis in twins. New Engl J Med 1986;315:1638-1642.
6. Ebers GC, Sadovnick AD, Risch NJ. A genetic basis for familial aggregation in multiple sclerosis. Canadian Collaborative Study Group. Nature 1995;377:150-151.
7. Ebers GC, Yee IM, Sadovnick AD, Duquette P. Conjugal multiple sclerosis: population-based prevalence and recurrence risks in offspring. Canadian Collaborative Study Group. Ann Neurol 2000;48:927-931.
8. Sadovnick AD, Baird PA, Ward RH. Multiple sclerosis: updated risks for relatives. Am J Med Genet 1988;29:533-541.
9. Sadovnick AD, Armstrong H, Rice GP, Bulman D, Hashimoto L, Paty DW, Hashimoto SA, Warren S, Hader W, Murray TJ, et al. A population-based study of multiple sclerosis in twins: update. Ann Neurol 1993;33:281-285.
10. Sadovnick AD, Bulman D, Ebers GC. Parent-child concordance in multiple sclerosis. Ann Neurol 1991;29:252-255.
11. Heltberg A, Holm NV. Concordance in twins and recurrence in sibship in multiple sclerosis. Lancet 1982;i:1068.
12. Bobowick AR, Kurtzke JF, Brody JA, Hrubec Z, Gillespie M. Twin study of multiple sclerosis: an epidemiologic inquiry. Neurology 1978;28:978-987.
13. Kinnunen E, Juntunen J, Ketonen L, Koskimies S, Konttinen YT, Salmi T, Koskenvuo M, Kaprio J. Genetic susceptibility to multiple sclerosis. A co-twin study of a nationwide series. Archives of Neurology 1988;45:1108-1111.
14. Mumford CJ, Wood NW, Kellar-Wood H, Thorpe JW, Miller DH, Compston DA. The British Isles survey of multiple sclerosis in twins. Neurology 1994;44:11-15.
15. Kalman B, Lublin FD. Spectrum and classification of inflammatory demyelinating diseases of the central nervous system. Curr Neurol Neurosci Rep 2001;1:249-256.
16. Kalman B, Albert RH, Leist TP. Genetics of multiple sclerosis: determinants of autoimmunity and neurodegeneration. Autoimmunity 2002;35:225-234.
17. Kalman B, Leist TP. A mitochondrial component of neurodegeneration in multiple sclerosis. Neuromol Med 2003;3:147-158.
18. Becker KG, Simon RM, Bailey-Wilson JE, Freidlin B, Biddison WE, McFarland HF, Trent JM. Clustering of non-major histocompatibility complex susceptibility candidate loci in human autoimmune diseases. Proc Natl Acad Sci USA 1998;95:9979-9984.
19. Lucchinetti C, Bruck W, Parisi J, Scheithauer B, Rodriguez M, Lassmann H. Heterogeneity of multiple sclerosis lesions: implications for the pathogenesis of demyelination. Ann Neurol 2000;47:707-717.
20. Kalman B: Role of Mitochondria in MS. In: Current Neurology and Neuroscience Report. Section: Demyelinating Disorders. Invited paper. 2006;6:244-252.
21. Kalman B, Laitinen K, Komoly S: The involvement of mitochondria in the pathogenesis of multiple sclerosis. J. Neuroimmunol. 2007;188 (1-2):1-12.
22. Herz J, Zipp F, Siffrin V. Neurodegeneration in autoimmune CNS inflammation. Exp Neurol. 2009 Dec 1. [Epub ahead of print]
23. Lublin FD, Reingold SC. Defining the clinical course of multiple sclerosis: results of an international survey. National Multiple Sclerosis Society (USA) Advisory Committee on Clinical Trials of New Agents in Multiple Sclerosis. Neurology 1996;46:907-911.
24. Cottrell DA, Kremenchutzky M, Rice GP, Koopman WJ, Hader W, Baskerville J, Ebers GC. The natural history of multiple sclerosis: a geographically based study. 5. The clinical features and natural history of primary progressive multiple sclerosis. Brain 1999;122 (Pt 4):625-639.
25. Confavreux C, Vukusic S, Moreau T, Adeleine P. Relapses and progression of disability in multiple sclerosis. N Engl J Med 2000;343:1430-1438.

26. Ebers GC. Natural history of primary progressive multiple sclerosis. Mult Scler 2004;10 Suppl 1:S8-13; discussion S13-15.
27. Kremenchutzky M, Cottrell D, Rice G, Hader W, Baskerville J, Koopman W, Ebers GC. The natural history of multiple sclerosis: a geographically based study. 7. Progressive-relapsing and relapsing-progressive multiple sclerosis: a re-evaluation. Brain 1999;122 (Pt 10):1941-1950.
28. Poser CM, Paty DW, Scheinberg L, McDonald WI, Davis FA, Ebers GC, Johnson KP, Sibley WA, Silberberg DH, Tourtellotte WW. New diagnostic criteria for multiple sclerosis: guidelines for research protocols. Ann Neurol 1983;13:227-231.
29. McDonald WI, Compston A, Edan G, Goodkin D, Hartung HP, Lublin FD, McFarland HF, Paty DW, Polman CH, Reingold SC, Sandberg-Wollheim M, Sibley W, Thompson A, van den Noort S, Weinshenker BY, Wolinsky JS. Recommended diagnostic criteria for multiple sclerosis: guidelines from the International Panel on the diagnosis of multiple sclerosis. Ann Neurol 2001;50:121-127.
30. Thompson AJ, Montalban X, Barkhof F, Brochet B, Filippi M, Miller DH, Polman CH, Stevenson VL, McDonald WI. Diagnostic criteria for primary progressive multiple sclerosis: a position paper. Ann Neurol 2000;47:831-835.
31. Broadley SA, Deans J, Sawcer SJ, Clayton D, Compston DA. Autoimmune disease in first-degree relatives of patients with multiple sclerosis. A UK survey. Brain 2000;123 (Pt 6):1102-1111.
32. Heward J, Gough SC. Genetic susceptibility to the development of autoimmune disease (Editorial). Clin Sci (Colch) 1997;93:479-491.
33. Heinzlef O, Alamowitch S, Sazdovitch V, Chillet P, Joutel A, Tournier-Lasserve E, Roullet E. Autoimmune diseases in families of French patients with multiple sclerosis. Acta Neurol Scand 2000;101:36-40.
34. McCombe PA, Chalk JB, Pender MP. Familial occurrence of multiple sclerosis with thyroid disease and systemic lupus erythematosus. J Neurol Sci 1990;97:163-171.
35. Reveille JD, Wilson RW, Provost TT, Bias WB, Arnett FC. Primary Sjogren's syndrome and other autoimmune diseases in families. Prevalence and immunogenetic studies in six kindreds. Ann Int Med 1984;101:748-756.
36. Sadovnick AD, Paty DW, Yannakoulias G. Concurrence of multiple sclerosis and inflammatory bowel disease. New Eng J Med 1989;321:762-763.
37. Kalman B, Takacs K, Gyodi E, Kramer J, Fust G, Tauszik T, Guseo A, Kuntar L, Komoly S, Nagy C, Petranyi G. Sclerosis multiplex in gypsies. Acta Neurol Scand 1991;84:181-185.
38. Kira J, Kanai T, Nishimura Y, Yamasaki K, Matsushita S, Kawano Y, Hasuo K, Tobimatsu S, Kobayashi T. Western versus Asian types of multiple sclerosis: immunogenetically and clinically distinct disorders. Ann Neurol 1996;40:569-574.
39. Mirsattari SM, Johnston JB, McKenna R, Del Bigio MR, Orr P, Ross RT, Power C. Aboriginals with multiple sclerosis. HLA types and predominance of neuromyelitis optica. Neurology 2001;56:317-323.
40. Wingerchuk DM, Hogancamp WF, O'Brien PC, Weinshenker BG. The clinical course of neuromyelitis optica (Devic's syndrome). Neurology 1999;53:1107-1114.
41. Sawcer S, Jones HB, Feakes R, Gray J, Smaldon N, Chataway J, Robertson N, Clayton D, Goodfellow PN, Compston A. A genome screen in multiple sclerosis reveals susceptibility loci on chromosome 6p21 and 17q22. Nat Genet 1996;13:464-468.
42. Merriman TR, Cordell HJ, Eaves IA, Danoy PA, Coraddu F, Barber R, Cucca F, Broadley S, Sawcer S, Compston A, Wordsworth P, Shatford J, Laval S, Jirholt J, Holmdahl R, Theofilopoulos AN, Kono DH, Tuomilehto J, Tuomilehto-Wolf E, Buzzetti R, Marrosu MG, Undlien DE, Ronningen KS, Ionesco-Tirgoviste C, Shield JP, Pociot F, Nerup J, Jacob CO, Polychronakos C, Bain SC, Todd JA. Suggestive evidence for association of human chromosome 18q12-q21 and its orthologue on rat and mouse chromosome 18 with several autoimmune diseases. Diabetes 2001;50:184-194.
43. Jawaheer D, Seldin MF, Amos CI, Chen WV, Shigeta R, Monteiro J, Kern M, Criswell LA, Albani S, Nelson JL, Clegg DO, Pope R, Schroeder HW Jr, Bridges SL Jr, Pisetsky DS, Ward R, Kastner DL, Wilder RL, Pincus T, Callahan LF, Flemming D, Wener MH, Gregersen PK. A genomewide screen in multiplex rheumatoid arthritis families suggests genetic overlap with other autoimmune diseases. Am J Hum Genet 2001;68:927-936.
44. Criswell LA, Pfeiffer KA, Lum RF, Gonzales B, Novitzke J, Kern M, Moser KL, Begovich AB, Carlton VE, Li W, Lee AT, Ortmann W, Behrens TW, Gregersen PK. Analysis of Families in the Multiple Autoimmune Disease Genetics Consortium (MADGC) Collection: the PTPN22 620W Allele Associates with Multiple Autoimmune Phenotypes. Am J Hum Genet 2005;76:561-571.
45. Johansson CM, Zunec R, Garcia MA, Scherbarth HR, Tate GA, Paira S, Navarro SM, Perandones CE, Gamron S, Alvarellos A, Graf CE, Manni J, Berbotto GA, Palatnik SA, Catoggio LJ, Battagliotti CG, Sebastiani GD, Migliaresi S, Galeazzi M, Pons-Estel BA, Alarcon-Riquelme ME; Collaborative Group on

the Genetics of SLE; Argentine Collaborative Group. Chromosome 17p12-q11 harbors susceptibility loci for systemic lupus erythematosus. Hum Genet 2004;115:230-238.
46. Vyshkina T, Sylvester A, Sadiq S, Bonita E, Perl A, Kalman B: CCL genes in multiple sclerosis and lupus erythematosus. J Neuroimmunol 2008;200:145-152.
47. Bruck W, Bitsch A, Kolenda H, Bruck Y, Stiefel M, Lassmann H. Inflammatory central nervous system demyelination: correlation of magnetic resonance imaging findings with lesion pathology. Ann Neurol 1997;42:783-793.
48. Leist TP, Gobbini MI, Frank JA, McFarland HF. Enhancing magnetic resonance imaging lesions and cerebral atrophy in patients with relapsing multiple sclerosis. Arch Neurol 2001;58:57-60.
49. Silver NC, Lai M, Symms MR, Barker GJ, McDonald WI, Miller DH. Serial magnetization transfer imaging to characterize the early evolution of new MS lesions. Neurology 1998;51:758-764.
50. Filippi M, Rocca MA, Martino G, Horsfield MA, Comi G. Magnetization transfer changes in the normal appearing white matter precede the appearance of enhancing lesions in patients with multiple sclerosis. Ann Neurol 1998;43:809-814.
51. Richert ND, Ostuni JL, Bash CN, Leist TP, McFarland HF, Frank JA. Interferon beta-1b and intravenous methylprednisolone promote lesion recovery in multiple sclerosis. Mult Scler 2001;7:49-58.
52. Bjartmar C, Trapp BD. Axonal and neuronal degeneration in multiple sclerosis: mechanisms and functional consequences. Curr Opin Neurol 2001;14:271-278.
53. De Stefano N, Matthews PM, Antel JP, Preul M, Francis G, Arnold DL. Chemical pathology of acute demyelinating lesions and its correlation with disability. Ann Neurol 1995;38:901-909.
54. Narayana PA, Doyle TJ, Lai D, Wolinsky JS. Serial proton magnetic resonance spectroscopic imaging, contrast-enhanced magnetic resonance imaging, and quantitative lesion volumetry in multiple sclerosis. Ann Neurol 1998;43:56-71.
55. Henderson AP, Barnett MH, Parratt JD, Prineas JW. Multiple sclerosis: distribution of inflammatory cells in newly forming lesions. Ann Neurol. 2009;66:739-753.
56. Trapp BD, Peterson J, Ransohoff RM, Rudick R, Mork S, Bo L. Axonal transection in the lesions of multiple sclerosis. N Engl J Med 1998;338:278-285.
57. Bitsch A, Schuchard J, Bunkowski S, Kuhlmann T, Bruck W. Acute axonal injury in multiple sclerosis. Correlation with demyelination and inflammation. Brain 2000;123:1174-1183.
58. Ozawa K, Suchanek G, Breitschopf H, Bruck W, Budka H, Jellinger K, Lassmann H. Patterns of oligodendroglia pathology in multiple sclerosis. Brain 1994;117:1311-1322.
59. Sabelko-Downes KA, Russell JH, Cross AH. Role of Fas-FasL interactions in the pathogenesis and regulation of autoimmune demyelinating disease. J Neuroimmunol 1999;100:42-52.
60. Vyshkina T, Kalman B: Autoantibodies and neurodegeneration in multiple sclerosis. Lab Invest 2008;88:796-807.
61. Nataf S. Neuroinflammation responses and neurodegeneration in multiple sclerosis. Rev Neurol. 2009;165:1023-8.
62. Banisor I,Leist TP, Kalman B. Involvement of β-chemokines in the development of inflammatory demyelination. J Neuroinflammation 2005;2:7. epub
63. Bennett JL, Stüve O. Update on inflammation, neurodegeneration, and immunoregulation in multiple sclerosis: therapeutic implications. Clin Neuropharmacol. 2009;32:121-32.
64. Vyshkina T, Leist TP, Shugart YY, Kalman B. CD45 (PTPRC) as a candidate gene in multiple sclerosis. Mult Scler. 2004;10:614-617.
65. Hillert J. Human leukocyte antigen studies in multiple sclerosis. Ann Neurol 1994;36 Suppl:S15-17.
66. Takacs K, Kalman B, Gyodi E, Tauszik T, Palffy G, Kuntar L, Guseo A, Nagy C, Petranyi G: Association between the lack of HLA-DQw6 and low incidence of multiple sclerosis in Hungarian Gypsies. Immunogenetics 1990;31:383-385.
67. Kalman B and Brannagan TH III (Eds): Neuroimmunology in Clinical Practice. Blackwell, 2007;29-35.
68. Ebers GC, Kukay K, Bulman DE, Sadovnick AD, Rice G, Anderson C, Armstrong H, Cousin K, Bell RB, Hader W, Paty DW, Hashimoto S, Oger J, Duquette P, Warren S, Gray T, O'Connor P, Nath A, Auty A, Metz L, Francis G, Paulseth JE, Murray TJ, Pryse-Phillips W, Risch N, et al. A full genome search in multiple sclerosis. Nat Genet 1996;13:472-476.
69. The Multiple Sclerosis Genetics Group. A complete genomic screen for multiple sclerosis underscores a role for the major histocompatibility complex. Nat Genet 1996;13:469-471.
70. Kuokkanen S, Gschwend M, Rioux JD, Daly MJ, Terwilliger JD, Tienari PJ, Wikstrom J, Palo J, Stein LD, Hudson TJ, Lander ES, Peltonen L. Genomewide scan of multiple sclerosis in Finnish multiplex families. Am J Hum Genet 1997;61:1379-1387.
71. Green AJ, Barcellos LF, Rimmler JB, Garcia ME, Caillier S, Lincoln RR, Bucher P, Pericak-Vance MA, Haines JL, Hauser SL, Oksenberg JR; Multiple Sclerosis Genetics Group. Sequence variation in the

transforming growth factor-beta1 (TGFB1) gene and multiple sclerosis susceptibility. J Neuroimmunol 2001;116:116-124.
72. Dyment DA, Sadovnick AD, Willer CJ, Armstrong H, Cader ZM, Wiltshire S, Kalman B, Risch N, Ebers GC; Canadian Collaborative Study Group. An extended genome scan in 442 Canadian multiple sclerosis-affected sibships: a report from the Canadian Collaborative Study Group. Hum Mol Genet 2004;13:1005-1015.
73. The Transatlantic Multiple Sclerosis Genetics Cooperative Group. A meta-analysis of genomic screens in multiple sclerosis. Mult Scler 2001;7:3-11.
74. Schmidt S, Barcellos LF, DeSombre K, Rimmler JB, Lincoln RR, Bucher P, Saunders AM, Lai E, Martin ER, Vance JM, Oksenberg JR, Hauser SL, Pericak-Vance MA, Haines JL; Multiple Sclerosis Genetics Group. Association of polymorphisms in the apolipoprotein E region with susceptibility to and progression of multiple sclerosis. Am J Hum Genet 2002;70:708-717.
75. Saarela J, Schoenberg Fejzo M, Chen D, Finnila S, Parkkonen M, Kuokkanen S, Sobel E, Tienari PJ, Sumelahti ML, Wikstrom J, Elovaara I, Koivisto K, Pirttila T, Reunanen M, Palotie A, Peltonen L. Fine mapping of a multiple sclerosis locus to 2.5 Mb on chromosome 17q22-q24. Hum Mol Genet 2002;11:2257-2267.
76. Barton A, Woolmore JA, Ward D, Eyre S, Hinks A, Ollier WE, Strange RC, Fryer AA, John S, Hawkins CP, Worthington J. Association of protein kinase C alpha (PRKCA) gene with multiple sclerosis in a UK population. Brain 2004;127(Pt 8):1717-1722.
77. Haines JL, Terwedow HA, Burgess K, Pericak-Vance MA, Rimmler JB, Martin ER, Oksenberg JR, Lincoln R, Zhang DY, Banatao DR, Gatto N, Goodkin DE, Hauser SL. Linkage of the MHC to familial multiple sclerosis suggests genetic heterogeneity. Hum Mol Genet 1998;7:1229-1234.
78. Ligers A, Dyment DA, Willer CJ, Sadovnick AD, Ebers G, Risch N, Hillert J; Canadian Collaborative Study Groups. Evidence of linkage with HLA-DR in DRB1*15-negative families with multiple sclerosis. Am J Hum Genet 2001;69:900-903.
79. Risch N, Merikangas K. The future of genetic studies of complex human diseases. Science 1996;273:1516-1517.
80. Gabriel SB, Schaffner SF, Nguyen H, Moore JM, Roy J, Blumenstiel B, Higgins J, DeFelice M, Lochner A, Faggart M, Liu-Cordero SN, Rotimi C, Adeyemo A, Cooper R, Ward R, Lander ES, Daly MJ, Altshuler D. The structure of haplotype blocks in the human genome. Science 2002;296:2225-2229.
81. Vyshkina T, Banisor I, Shugart YY, Leist TP, Kalman B. Genetic variants of Complex I in multiple sclerosis. J Neurol Sci 2005;228:55-64.
82. Vyshkina T, Shugart YY, Birnbaum G, Leist TP, Kalman B. Association of haplotypes in the beta-chemokine locus with multiple sclerosis. Eur J Hum Genet 2005;13:240-247.
83. Vyshkina T, Kalman B: Haplotypes within genes of β-chemokines are associated with multiple sclerosis: a second phase study. Hum Genet 2005;118:67-75.
84. Vyshkina T, Kalman B: Analyses of a MS-associated haplotype encompassing the CCL3 gene. J Neuroimmunol 2006;176:216-218.
85. Zlotnik A, Yoshie O. Chemokines: a new classification system and their role in immunity. Immunity 2000;12:121-127.
86. Maurer M, von Stebut E. Macrophage inflammatory protein-1. Int J Biochem Cell Biol 2004;36:1882-1886.
87. Karpus WJ, Ransohoff RM. Chemokine regulation of experimental autoimmune encephalomyelitis: temporal and spatial expression patterns govern disease pathogenesis. J Immunol 1998;161:2667-2671.
88. Alt C, Laschinger M, Engelhardt B. Functional expression of the lymphoid chemokines CCL19 (ELC) and CCL 21 (SLC) at the blood-brain barrier suggests their involvement in G-protein-dependent lymphocyte recruitment into the central nervous system during experimental autoimmune encephalomyelitis. Eur J Immunol 2002;32:2133-2144.
89. Mahad DJ, Ransohoff RM. The role of MCP-1 (CCL2) and CCR2 in multiple sclerosis and experimental autoimmune encephalomyelitis (EAE). Semin Immunol 2003;15:23-32.
90. Teuscher C, Butterfield RJ, Ma RZ, Zachary JF, Doerge RW, Blankenhorn EP. Sequence polymorphisms in the chemokines Scya1 (TCA-3), Scya2 (monocyte chemoattractant protein (MCP)-1), and Scya12 (MCP-5) are candidates for eae7, a locus controlling susceptibility to monophasic remitting/nonrelapsing experimental allergic encephalomyelitis. J Immunol 1999;163:2262-2266.
91. Jagodic M, Becanovic K, Sheng JR, Wu X, Backdahl L, Lorentzen JC, Wallstrom E, Olsson T. An advanced intercross line resolves Eae18 into two narrow quantitative trait loci syntenic to multiple sclerosis candidate loci. J Immunol 2004;173:1366-1373.
92. Abecasis GR, Cherny SS, Cookson WO, Cardon LR. Merlin--rapid analysis of dense genetic maps using sparse gene flow trees. Nat Genet 2002;30:97-101.

93. Knapp M. A note on power approximations for the transmission/disequilibrium test. Am J Hum Genet 1999;64:1177-1185.
94. McGinnis R. General equations for Pt, Ps, and the power of the TDT and the affected-sib-pair test. Am J Hum Genet 2000;67:1340-1347.
95. Spielman RS, McGinnis RE, Ewens WJ. Transmission test for linkage disequilibrium: the insulin gene region and insulin-dependent diabetes mellitus (IDDM). Am J Hum Genet 1993;52:506-516.
96. Martin ER, Monks SA, Warren LL, Kaplan NL. A test for linkage and association in general pedigrees: the pedigree disequilibrium test. Am J Hum Genet 2000;67:146-154.
97. Clayton D. A generalization of the transmission/disequilibrium test for uncertain-haplotype transmission. Am J Hum Genet 1999;65:1170-1177.
98. Dempster AP, Laird NM, Rubin DB. Maximum-likelihood with incomplete data via the EM algorithm. J Royal Stat Soc Serier B 1977;39:1-38.
99. Slatkin M. Excoffier L. Testing for linkage disequilibrium in genotypic data using the Expectation-Maximization algorithm. Heredity 1996;76:377-383.
100. Hill WG, Robertson A. Linkage disequilibrium in finite populations. Theor Appl Genet 1968;38:226-231.
101. Rabinowitz D, Laird NM. A unified approach to adjusting association tests for population admixture with arbitrary pedigree structure and arbitrary missing marker information. Hum Hered 2000;50:211-223.
102. Laird NM, Horvath S, Xu X. Implementing a unified approach to family-based tests of association. Genet Epi 2000;19(suppl 1):S36-S42.
103. Nyholt DR. A simple correction for multiple testing for single-nucleotide polymorphisms in linkage disequilibrium with each other. Am J Hum Genet 2004;74:765-769.
104. Sidak Z. On multivariate normal probabilities of rectangles: their dependence on correlation. Ann Math Statist 1968;39:1425-1434.
105. Lu F, Selak M, O'Connor J, Croul S, Lorenzana C, Butunoi C, Kalman B. Oxidative damage to mitochondrial DNA and activity of mitochondrial enzymes in chronic active lesions of multiple sclerosis. J Neurol Sci 2000;177:95-103.
106. Croutcher PJP, Mascheretti S, Hampe J, Huse K, Frenzel H, Stoll M, Lu T, Nikolaus S, Yang SK, Krawczak M, Kim WH, Schreiber S. Haplotype structure and association to Crohn's disease of CARD15 mutations in two ethnically divergent populations. Eur J Hum Genet 2003;11:6-16.
107. Clark VJ, Dean M. Haplotype structure and linkage disequilibrium in chemokine and chemokine receptor genes. Hum Genomics 2004;1:255-273.
108. Modi WS . CCL3L1 and CCL4L1 chemokine genes are located in a segmental duplication at chromosome 17q12. Genomics 2004;83:735-738.
109. Hinds DA, Stuve LL, Nilsen GB, Halperin E, Eskin E, Ballinger DG, Frazer KA, Cox DR. Whole-genome patterns of common DNA variation in three human populations. Science 2005;307:1072-1079.
110. Chen DC, Saarela J, Clark RA, Miettinen T, Chi A, Eichler EE, Peltonen L, Palotie A. Segmental duplications flank the multiple sclerosis locus on chromosome 17q. Genome Res 2004;14:1483-1492.
111. International Multiple Sclerosis Genetics Consortium, Hafler DA, Compston A, Sawcer S, Lander ES, Daly MJ, De Jager PL, de Bakker PI, Gabriel SB, Mirel DB, Ivinson AJ, Pericak-Vance MA, Gregory SG, Rioux JD, McCauley JL, Haines JL, Barcellos LF, Cree B, Oksenberg JR, Hauser SLRisk alleles for multiple sclerosis identified by a genomewide study. N Engl J Med. 2007;357:851-862.
112. Lundmark F, Duvefelt K, Iacobaeus E, Kockum I, Wallström E, Khademi M, Oturai A, Ryder LP, Saarela J, Harbo HF, Celius EG, Salter H, Olsson T, Hillert J. Variation in interleukin 7 receptor alpha chain (IL7R) influences risk of multiple sclerosis. Nat Genet. 2007;39:1108-1113.
113. Gregory SG, Schmidt S, Seth P, Oksenberg JR, Hart J, Prokop A, Caillier SJ, Ban M, Goris A, Barcellos LF, Lincoln R, McCauley JL, Sawcer SJ, Compston DA, Dubois B, Hauser SL, Garcia-Blanco MA, Pericak-Vance MA, Haines JL; for the Multiple Sclerosis Genetics Group. Interleukin 7 receptor alpha chain (IL7R) shows allelic and functional association with multiple sclerosis. Nat Genet. 2007;39:1083-1091.
114. De Jager PL, Jia X, Wang J, de Bakker PI, Ottoboni L, Aggarwal NT, Piccio L, Raychaudhuri S, Tran D, Aubin C, Briskin R, Romano S; International MS Genetics Consortium, Baranzini SE, McCauley JL, Pericak-Vance MA, Haines JL, Gibson RA, Naeglin Y, Uitdehaag B, Matthews PM, Kappos L, Polman C, McArdle WL, Strachan DP, Evans D, Cross AH, Daly MJ, Compston A, Sawcer SJ, Weiner HL, Hauser SL, Hafler DA, Oksenberg JR. Meta-analysis of genome scans and replication identify CD6, IRF8 and TNFRSF1A as new multiple sclerosis susceptibility loci. Nat Genet. 2009;41:776-782.
115. De Jager PL, Baecher-Allan C, Maier LM, Arthur AT, Ottoboni L, Barcellos L, McCauley JL, Sawcer S, Goris A, Saarela J, Yelensky R, Price A, Leppa V, Patterson N, de Bakker PI, Tran D, Aubin C, Pobywajlo S, Rossin E, Hu X, Ashley CW, Choy E, Rioux JD, Pericak-Vance MA, Ivinson A, Booth DR,

Stewart GJ, Palotie A, Peltonen L, Dubois B, Haines JL, Weiner HL, Compston A, Hauser SL, Daly MJ, Reich D, Oksenberg JR, Hafler DA. The role of the CD58 locus in multiple sclerosis. Proc Natl Acad Sci U S A. 2009;31;106:5264-5269.
116. Aulchenko YS, Hoppenbrouwers IA, Ramagopalan SV, Broer L, Jafari N, Hillert J, Link J, Lundström W, Greiner E, Dessa Sadovnick A, Goossens D, Van Broeckhoven C, Del-Favero J, Ebers GC, Oostra BA, van Duijn CM, Hintzen RQ. Genetic variation in the KIF1B locus influences susceptibility to multiple sclerosis. Nat Genet. 2008;40:1402-1403.
117. Kalman B and Vitale E: Chromosomal structural variations in neurological disorders. The Neurologist 2009;15:245-53.
118. Trebst C, Sorensen TL, Kivisakk P, Cathcart MK, Hesselgesser J, Horuk R, Sellebjerg F, Lassmann H, Ransohoff RM. CCR1+/CCR5+ mononuclear phagocytes accumulate in the central nervous system of patients with multiple sclerosis. Am J Pathol 2001;159:1701-1711.
119. Nakajima H, Fukuda K, Doi Y, Sugino M, Kimura F, Hanafusa T, Ikemoto T, Shimizu A. Expression of TH1/TH2-related chemokine receptors on peripheral T cells and correlation with clinical disease activity in patients with multiple sclerosis. Eur Neurol 2004;52:162-168.
120. Miyagishi R, Kikuchi S, Fukazawa T, Tashiro K: Macrophage inflammatory protein-1 alpha in the cerebrospinal fluid of patients with multiple sclerosis and other inflammatory neurological diseases. J Neurol Sci 1995;129:223-227.
121. Bartosik-Psujek H, Stelmasiak Z. The levels of chemokines CXCL8, CCL2 and CCL5 in multiple sclerosis patients are linked to the activity of the disease. Eur J Neurol 2005;12:49-54.
122. Ransohoff RM, Hamilton TA, Tani M, Stoler MH, Shick HE, Major JA, Estes ML, Thomas DM, Tuohy VK. Astrocyte expression of mRNA encoding cytokines IP-10 and JE/MCP-1 in experimental autoimmune encephalomyelitis. Faseb J 1993;7:592-600.
123. Kennedy KJ, Strieter RM, Kunkel SL, Lukacs NW, Karpus WJ. Acute and relapsing experimental autoimmune encephalomyelitis are regulated by differential expression of the CC chemokines macrophage inflammatory protein-1alpha and monocyte chemotactic protein-1. J Neuroimmunol 1998;92:98-108.
124. Juedes AE, Hjelmstrom P, Bergman CM, Neild AL, Ruddle NH: Kinetics and cellular origin of cytokines in the central nervous system: insight into mechanisms of myelin oligodendrocyte glycoprotein-induced experimental autoimmune encephalomyelitis. J Immunol 2000;164:419-426.
125. Elhofy A, Wang J, Tani M, Fife BT, Kennedy KJ, Bennett J, Huang D, Ransohoff RM, Karpus WJ. Transgenic expression of CCL2 in the central nervous system prevents experimental autoimmune encephalomyelitis. J Leukoc Biol 2005;77:229-237.
126. Huang DR, Wang J, Kivisakk P, Rollins BJ, Ransohoff RM. Absence of monocyte chemoattractant protein 1 in mice leads to decreased local macrophage recruitment and antigen-specific T helper cell type 1 immune response in experimental autoimmune encephalomyelitis. J Exp Med 2001;193:713-726.
127. Fife BT, Huffnagle GB, Kuziel WA, Karpus WJ. CC chemokine receptor 2 is critical for induction of experimental autoimmune encephalomyelitis. J Exp Med 2000;192:899-905.
128. Mahad DJ, Howell SJ, Woodroofe MN. Expression of chemokines in the CSF and correlation with clinical disease activity in patients with multiple sclerosis. J Neurol Neurosurg Psychiatry 2002;72:498-502.
129. Sorensen TL, Tani M, Jensen J, Pierce V, Lucchinetti C, Folcik VA, Qin S, Rottman J, Sellebjerg F, Strieter RM, Frederiksen JL, Ransohoff RM. Expression of specific chemokines and chemokine receptors in the central nervous system of multiple sclerosis patients. J Clin Invest 1999;103:807-815.
130. Sorensen TL, Sellebjerg F, Jensen CV, Strieter RM, Ransohoff RM. Chemokines CXCL10 and CCL2: differential involvement in intrathecal inflammation in multiple sclerosis. Eur J Neurol 2001;8:665-672.
131. McManus C, Berman JW, Brett FM, Staunton H, Farrell M, Brosnan CF. MCP-1, MCP-2 and MCP-3 expression in multiple sclerosis lesions: an immunohistochemical and in situ hybridization study. J Neuroimmunol 1998;86:20-29.
132. Simpson JE, Newcombe J, Cuzner ML, Woodroofe MN. Expression of monocyte chemoattractant protein-1 and other beta-chemokines by resident glia and inflammatory cells in multiple sclerosis lesions. J Neuroimmunol 1998;84:238-249.
133. Woodroofe N, Cross AK, Harkness K, Simpson JE. The role of chemokines in the pathogenesis of multiple sclerosis. Adv Exp Med Biol 1999;468:135-150.
134. Boven LA, Montagne L, Nottet HS, De Groot CJ. Macrophage inflammatory protein-1alpha (MIP-1alpha), MIP-1beta, and RANTES mRNA semiquantification and protein expression in active demyelinating multiple sclerosis (MS) lesions. Clin Exp Immunol 2000;122:257-263.

135. Hvas J, McLean C, Justesen J, Kannourakis G, Steinman L, Oksenberg JR, Bernard CC. Perivascular T cells express the pro-inflammatory chemokine RANTES mRNA in multiple sclerosis lesions. Scand J Immunol 1997;46:195-203.
136. Banisor I, Kalman B. Bcl-2 and its homologues in the brain of patients with multiple sclerosis. Mult Scler 2004;10:176-181.
137. Trebst C, Ransohoff RM. Investigating chemokines and chemokine receptors in patients with multiple sclerosis: opportunities and challenges. Arch Neurol 2001;58:1975-1980.
138. Mahad DJ, Trebst C, Kivisakk P, Staugaitis SM, Tucky B, Wei T, Lucchinetti CF, Lassmann H, Ransohoff RM. Expression of chemokine receptors CCR1 and CCR5 reflects differential activation of mononuclear phagocytes in pattern II and pattern III multiple sclerosis lesions. J Neuropathol Exp Neurol 2004;63:262-273.
139. Kalman B, Lublin FD, Alder H. Mitochondrial DNA mutations in multiple sclerosis. Mult Scler 1995;1:32-36.
140. Kalman B, Lublin FD, Alder H. Characterization of the mitochondrial DNA in patients with multiple sclerosis. J Neurol Sci 1996;140:75-84.
141. Kalman B, Alder H, Bosch UF, Lublin FD, Chatterjee D. The evolutionary relationship among Caucasian MS patients and controls. Mult Scler 1996;1:288-295.
142. Kalman B, Rodriguez-Valdez JL, Bosch U, Lublin FD. Screening for Leber's hereditary optic neuropathy associated mitochondrial DNA mutations in patients with prominent optic neuritis. Mult Scler 1997;2:279-282.
143. Kalman B, Lublin FD, Alder H. Impairment of central and peripheral myelin in mitochondrial diseases. Mult Scler 1997;2:267-278.
144. Kalman B, Alder H. Is the mitochondrial DNA involved in determining susceptibility to multiple sclerosis? Acta Neurol Scand 1998;98:232-237.
145. Kalman B, Li S, Chatterjee D, O'Connor J, Voehl MR, Brown MD, Alder H. Large scale screening of the mitochondrial DNA reveals no pathogenic mutations but a haplotype associated with multiple sclerosis in Caucasians. Acta Neurol Scand 1999;99:16-25.
146. Vyshkina T, Sylvester A, Sadiq S, Bonilla E, Canter JA, Perl A, Kalman B. Association of common mitochondrial DNA variants with multiple sclerosis and systemic lupus erythematosus. Clin Immunol. 2008;129:31-35.
147. Kalman B, Mandler RN. Studies of mitochondrial DNA in Devic's disease revealed no pathogenic mutations, but polymorphisms also found in association with multiple sclerosis. Ann Neurol 2002;51:661-662.
148. Vladimirova O, O'Connor J, Cahill A, Alder H, Butunoi C, Kalman B. Oxidative damage to DNA in plaques of MS brains. Mult Scler 1998;4:413-418.
149. Vladimirova O, Lu FM, Shawver L, Kalman B. The activation of protein kinase C induces higher production of reactive oxygen species by mononuclear cells in patients with multiple sclerosis than in controls. Inflamm Res 1999;48:412-416.
150. Anderson S, Bankier AT, Barrell BG, de Bruijn MH, Coulson AR, Drouin J, Eperon IC, Nierlich DP, Roe BA, Sanger F, Schreier PH, Smith AJ, Staden R, Young IG. Sequence and organization of the human mitochondrial genome. Nature 1981;290:457-465.
151. Mauksch H. Ein beitrag zur Kenntsnis der familiar-hereditared Sehnervenatrophie. Augenheilk 1925; 55:196-198.
152. Lundsgaard RLsd, 21: 300-306. A genealogic, genetic and clinical study of 101 cases of retrobulbar optic neuritis in 20 Danish families. Acta Ophthalmol (Suppl.) 1944;21:300-306.
153. Lees F, MacDonald AM, Aldren Turner JW. Leber’s disease with symptoms resembling disseminated sclerosis. J Neurol Neurosurg Psychiatry 1964;27:415-421.
154. Bruyn GW, Went LN. A sex-linked heredo-degenerative neurological disorder, associated with Leber's optic atrophy. Part I Clinical studies. J Neurol Sci 1964;1:59-80.
155. Harding AE, Sweeney MG, Miller DH, Mumford CJ, Kellar-Wood H, Menard D, McDonald WI, Compston DA. Occurrence of a multiple sclerosis-like illness in women who have a Leber's hereditary optic neuropathy mitochondrial DNA mutation. Brain 1992;115:979-989.
156. Flanigan KM, Johns DR. Association of the 11778 mitochondrial DNA mutation and demyelinating disease. Neurology 1993;43:2720-2722.
157. Kellar-Wood H, Robertson N, Govan GG, Compston DA, Harding AE. Leber's hereditary optic neuropathy mitochondrial DNA mutations in multiple sclerosis. Ann Neurol 1994;36:109-112.
158. Olsen NK, Hansen AW, Norby S, Edal AL, Jorgensen JR, Rosenberg T. Leber's hereditary optic neuropathy associated with a disorder indistinguishable from multiple sclerosis in a male harbouring the mitochondrial DNA 11778 mutation. Acta Neurol Scand 1995;91:326-329.

159. Jansen PH, vad der Knaap MS, de Coo IF. Leber's hereditary optic neuropathy with the 11778 mtDNA mutation and white matter disease resembling multiple sclerosis: clinical, MRI and MRS findings. J Neurol Sci 1996;135:176-180.
160. De Vries DD, Went LN, Bruyn GW, Scholte HR, Hofstra RM, Bolhuis PA, van Oost BA. Genetic and biochemical impairment of mitochondrial Complex I activity in a family with Leber hereditary optic neuropathy and hereditary spastic dystonia. Am J Hum Genet 1996;58:703-711.
161. Riordan-Eva P, Sanders MD, Govan GG, Sweeney MG, Da Costa J, Harding AE. The clinical features of Leber's hereditary optic neuropathy defined by the presence of a pathogenic mitochondrial DNA mutation. Brain 1995;118:319-337.
162. Shoffner JM, Brown MD, Torroni A, Lott MT, Cabell MF, Mirra SS, Beal MF, Yang CC, Gearing M, Salvo R, et al. Mitochondrial DNA variants observed in Alzheimer disease and Parkinson disease patients. Genomics 1993;17:171-184.
163. Loveland B, Wang CR, Yonekawa H, Hermel E, Lindahl KF. Maternally transmitted histocompatibility antigen of mice: a hydrophobic peptide of a mitochondrially encoded protein. Cell 1990;60:971-980.
164. Schapira AH, Cooper JM, Manneschi L, Vital C, Morgan-Hughes JA, Clark JB. A mitochondrial encephalomyopathy with specific deficiencies of two respiratory chain polypeptides and a circulating autoantibody to a mitochondrial matrix protein. Brain 1990;113:419-432.
165. Schapira AHV, Cooper JM, Dexter D, Clark JB, Jenner P, Marsden CD. Mitochondrial Complex I deficiency in Parkinson's disease. J Neurochem 1990;54:823-827.
166. Perkin GD, Rose FC. Optic neuritis and its differential diagnosis. Oxford, England: Oxford University Press, 1979;192-200.
167. Beck RW, Cleary PA, Anderson MM Jr, Keltner JL, Shults WT, Kaufman DI, Buckley EG, Corbett JJ, Kupersmith MJ, Miller NR, et al. A randomized, controlled trial of corticosteroids in the treatment of acute optic neuritis. The Optic Neuritis Study Group. N Engl J Med. 1992;326:581-588.
168. Beck RW, Cleary PA, Trobe JD, Kaufman DI, Kupersmith MJ, Paty DW, Brown CH. The effect of corticosteroids for acute optic neuritis on the subsequent development of multiple sclerosis. The Optic Neuritis Study Group. N Engl J Med. 1993;329:1764-1769.
169. Optic Neuritis Study Group. The 5-year risk of MS after optic neuritis. Experience of the Optic Neuritis Treatment Trial. Neurology 1997;49:1404-1413.
170. Mandler RN, Davis LE, Jeffery DR, Kornfeld M. Devic's neuromyelitis optica: a clinicopathological study of 8 patients. Ann Neurol 1993;34:162-168.
171. Wingerchuk DM, Weinshenker BG. Neuromyelitis optica: clinical predictors of a relapsing course and survival. Neurology 2003;60:848-853.
172. Lucchinetti CF, Mandler RN, McGavern D, Bruck W, Gleich G, Ransohoff RM, Trebst C, Weinshenker B, Wingerchuk D, Parisi JE, Lassmann H. A role for humoral mechanisms in the pathogenesis of Devic's neuromyelitis optica. Brain. 2002;125:1450-1461.
173. Kalman B and Brannagan TH. Neuroimmunology in Clinical Practice. Bralckwell 2007;83-88.
174. Weinshenker BG, Wingerchuk DM, Lucchinetti CF, Lennon VA. A marker autoantibody discriminates neuromyelitis optica from MS. Neurology 2003;A520.
175. Leber T. Ueber hereditare und congenital-angelegte Sehnervenleiden. Graefes Arch Ophthalmol 1871;17:249-291.
176. Adams H, Blackwood W, Wilson J. Further clinical and pathological observations on Leber's optic atrophy. Brain 1966; 89:15-26.
177. Nikoskelainen EK, Marttila RJ, Huoponen K, Juvonen V, Lamminen T, Sonninen P, Savontaus ML. Leber's "plus": neurological abnormalities in patients with Leber's hereditary optic neuropathy. J Neurol Neurosurg Psychiatry 1995;59:160-164.
178. Ferguson FR, Critchley M. Leber's optic atrophy and its relation to the heredo-familial ataxias. J Neurol Psychol 1928;9:120-132.
179. Went LJ. Leber disease and variants. in: Handbook of Clinical Neurology. Vol.13. Neuroretinal Degenerations. Eds. Vinken PJ and Bruyn GW, North-Holland Publishing Company, Amsterdam, and American Elsevier Publishing Co., Inc., New York 1972;94-110.
180. Wallace DC, Singh G, Lott MT, Hodge JA, Schurr TG, Lezza AM, Elsas LJ 2nd, Nikoskelainen EK. Mitochondrial DNA mutation associated with Leber's hereditary optic neuropathy. Science 1988;242:1427-1430.
181. Mackey D, Howell N. A variant of Leber hereditary optic neuropathy characterized by recovery of vision and by an unusual mitochondrial genetic etiology. Am J Hum Genet 1992;51:1218-1228.
182. Johns DR, Neufeld MJ, Park RD. An ND-6 mitochondrial DNA mutation associated with Leber hereditary optic neuropathy. Biochem Biophys Res Comm 1992;187:1551-1557.

183. Brown MD, Voljavec AS, Lott MT, MacDonald I, Wallace DC. Leber's hereditary optic neuropathy: a model for mitochondrial neurodegenerative diseases. FASEB J 1992;6:2791-2799.
184. Horvath R, Abicht A, Shoubridge EA, Karcagi V, Rozsa C, Komoly S, Lochmuller H. Leber's hereditary optic neuropathy presenting as multiple sclerosis-like disease of the CNS. J Neurol 2000;247:65-67.
185. Kovacs GG, Hoftberger R, Majtenyi K, Horvath R, Barsi P, Komoly S, Lassmann H, Budka H, Jakab G. Neuropathology of white matter disease in Leber's hereditary optic neuropathy. Brain 2005;128:35-41.
186. Cock H, Mandler R, Ahmed W, Schapira AH. Neuromyelitis optica (Devic's syndrome): No association with the primary mitochondrial DNA mutations found in Leber hereditary optic neuropathy. J Neurol Neurosurg Psychiatry 1997;62:85-87.
187. Johns DR, Hurko O, Attardi G, Griffin JW. Molecular basis of a new mitochondrial disease: Acute optic neuropathy and myopathy. Ann Neurol 1991;230:234.
188. Hanefeld FA, Ernst BP, Wilichowski E, Christen HJ. Leber's hereditary optic neuropathy mitochondrial DNA mutations in childhood multiple sclerosis. Neuropediatrics 1994;25:331.
189. Mayr-Wohlfart U, Paulus C, Henneberg A, Rodel G. Mitochondrial DNA mutations in multiple sclerosis patients with severe optic involvement. Acta Neurol Scand 1996; 94:167-171.
190. Torroni A, Lott MT, Cabell MF, Chen Y-S, Lavergne L, Wallace DC. MtDNA and the origin of Caucasians: Identification of ancient Caucasian-specific haplogroups, one of which is prone to a recurrent somatic duplication in the D-loop region. Am J Hum Genet 1994; 55:760-776.
191. Brown MD, Sun F, Wallace DC. Clustering of Caucasian Leber hereditary optic neuropathy patients containing the 11,778 or 14,484 mutations on an mtDNA lineage. Am J Hum Genet 1997;60:381-387.
192. Smeitink J, van den Heuvel L. Human mitochondrial complex I in health and disease. Am J Hum Genet 1999;64:1505-1510.
193. Triepels RH, Van Den Heuvel LP, Trijbels JM, Smeitink JA. Respiratory chain complex I deficiency. Am J Med Genet 2001;106:37-45.
194. DiMauro S, Schon EA. Mitochondrial respiratory-chain diseases. N Engl J Med 2003;348:2656-2668.
195. Qi X, Lewin AS, Hauswirth WW, Guy J. Suppression of complex I gene expression induces optic neuropathy. Ann Neurol 2003;53:198-205.
196. Williams MD, van Remmen H, Conrad CC, Huang TT, Epstein CJ, Richardson A. Increased oxidative damage is correlated to altered mitochondrial function in heterozygous manganese superoxide dismutase knockout mice. J Biol Chem 1998;43:28510-28515.
197. Baker D, Rosenwasser OA, O'Neill JK, Turk JL. Genetic analysis of experimental allergic encephalomyelitis in mice. J Immunol 1995;155:4046-4051.
198. Coffeen CM, McKenna CE, Koeppen AH, Plaster NM, Maragakis N, Mihalopoulos J, Schwankhaus JD, Flanigan KM, Gregg RG, Ptácek LJ, Fu YH. Genetic localization of an autosomal dominant leukodystrophy mimicking chronic progressive multiple sclerosis to chromosome 5q31. Hum Mol Genet. 2000;9:787-793.
199. Windhagen A, Newcombe J, Dangond F, Strand C, Woodroofe MN, Cuzner ML, Hafler DA. Expression of costimulatory molecules B7-1 (CD80), B7-2 (CD86), and interleukin 12 cytokine in multiple sclerosis lesions. J Exp Med 1995;182:1985-1996.
200. Chofflon M, Juillard C, Juillard P, Gauthier G, Grau GE. Tumor necrosis factor alpha production as a possible predictor of relapse in patients with multiple sclerosis. Eur Cytokine Netw 1992;3:523-531.
201. Selmaj KW, Raine CS. Tumor necrosis factor mediates myelin and oligodendrocyte damage in vitro. Ann Neurol 1988;23:339-346.
202. Bo L, Dawson TM, Wesselingh S, Mork S, Choi S, Kong PA, Hanley D, Trapp BD. Induction of nitric oxide synthase in demyelinating regions of multiple sclerosis brains. Ann Neurol 1994;36:778-786.
203. Bagasra O, Michaels FH, Zheng YM, Bobroski LE, Spitsin SV, Fu ZF, Tawadros R, Koprowski H. Activation of the inducible form of nitric oxide synthase in the brains of patients with multiple sclerosis. Proc Natl Acad Sci USA 1995;92:12041-12045.
204. Merrill JE, Scolding NJ. Mechanisms of damage to myelin and oligodendrocytes and their relevance to disease. Neuropathol Appl Neurobiol 1999;25:435-458.
205. Konat GW. H2O2-induced higher order chromatin degradation: a novel mechanism of oxidative genotoxicity. J Biosci 2003;28:57-60.
206. Cross AH, Manning PT, Stern MK, Misko TP. Evidence for the production of peroxynitrite in inflammatory CNS demyelination. J Neuroimmunol 1997;80:121-30.
207. Trapp BD, Bo L, Mork S, Chang A. Pathogenesis of tissue injury in MS lesions. J Neuroimmunol 1999;98:49-56.

208. Husted CA, Goodin DS, Hugg JW, Maudsley AA, Tsuruda JS, de Bie SH, Fein G, Matson GB, Weiner MW. Biochemical alterations in multiple sclerosis lesions and normal-appearing white matter detected by in vivo 31P and 1H spectroscopic imaging. Ann Neurol 1994;36:157-165.
209. Clark JB. N-acetyl aspartate: a marker for neuronal loss or mitochondrial dysfunction. Dev Neurosci 1998;20:271-276.
210. Allen IV, McKeown SR. A histological, histochemical and biochemical study of the macroscopically normal white matter in multiple sclerosis. J Neurol Sci 1979;41:81-91.
211. Powell T, Sussman JG, Davies-Jones GA. MR imaging in acute multiple sclerosis: ringlike appearance in plaques suggesting the presence of paramagnetic free radicals. Am J Neurorad 1992;13:1544-1546.
212. Mecocci P, MacGarvey U, Kaufman AE, Koontz D, Shoffner JM, Wallace DC, Beal MF. Oxidative damage to mitochondrial DNA shows marked age-dependent increases in human brain. Ann Neurol 1993;34:609-616.
213. Howell N, McCullough DA, Kubacka I, Halvorson S, Mackey D. The sequence of human mtDNA: the question of errors versus polymorphisms. Am J Hum Genet 1992;50:1333-1340.
214. Bressman SB, de Leon D, Brin MF, Risch N, Burke RE, Greene PE, Shale H, Fahn S. Idiopathic dystonia among Ashkenazi Jews: evidence for autosomal dominant inheritance. Ann Neurol 1989;26:612-620.
215. Brown MD, Torroni A, Reckord CL, Wallace DC. Phylogenetic analysis of Leber's hereditary optic neuropathy mitochondrial DNA's indicates multiple independent occurrences of the common mutations. Hum Mutat 1995;6:311-325.
216. Kumar S, Tamura K, Nei M. MEGA: Molecular Evolutionary Genetics Analysis. Version 1.01. The Pennsylvania State University, University Park, PA 16802. 1993.
217. Pfeifer GP, Drouin R, Riggs AD, Holmquist GP. In vivo mapping of a DNA adduct at nucleotide resolution: Detection of pyrimidine (6-4) pyridone photoproducts by ligation-mediated polymerase chain reaction. Proc Natl Acad Sci 1991;88:1374-1378.
218. Pfeifer GP, Drouin R, Holmquist GP. Detection of DNA adducts at the DNA sequence level by ligation-mediated PCR. Mutation Res 1993;288:39-46.
219. Driggers WJ, Holmquist GP, LeDoux SP, Wilson GL. Mapping frequencies of endogenous oxidative damage and the kinetic response to oxidative stress in a region of rat mtDNA. Nucleic Acid Res 1997;25:4362-4369.
220. Yarborough A, Zhang YJ, Hsu TM, Santelli RM. Immunoperoxidase detection of 8-hydroxydeoxyguanosine in Aflatoxin B1-treated rat liver and human oral mucosal cells. Cancer Res 1996;56:683-688.
221. Schapira AHV, Mann VM, Cooper JM, Dexter D, Daniel SE, Clark JB, Marsden CD. Anatomic and disease specificity of NADH CoQ1 reductase (Complex I) deficiency in Parkinson's disease. J Neurochem 1990;55:2142-2145.
222. Singer TP. Determination of the activity of succinate, NADH, choline and α-glycerophosphate dehydrogenase. Methods Biochem Analysis 1974;22:123-175.
223. Moreadith RW, Batshaw ML, Ohnishi T, Kerr D, Knox B, Jackson D, Hruban R, Olson J, Reynsafarje B, Lehninger AL. Deficiency of the iron-sulfur clusters of mitochondrial reduced nicotinamide adenine dinucleotide-ubiquinone oxidoreductase (complex I) in an infant with congenital lactic acidosis. J Clin Invest 1984;74:685-697.
224. Lee CP, Martens ME, Tsang SH. Small-scale preparation of skeletal muscle mitochondria and its application in the study of human disease. Methods of Toxicology 1993;2:70-83.
225. Birch-Machin MA, Brigg HL, Saborido AA, Bindoff LA, Turnbull DM. An evaluation of the measurement of the activities of complexes I-IV in the respiratory chain of human skeletal muscle mitochondria. Biochem Medicine Metabolic Biol 1994;51:35-42.
226. Martens ME, Peterson PL, Lee CP. In vitro effects of glucocorticoids on mitochondrial energy metabolism. Biochim Biophys Acta 1991;11058:152-160.
227. Robinson JB Jr, Inman L, Sumegi B, Srere PA. Further characterization of the Krebs tricarboxylic acid cycle metabolon. J Biol Chem. 1987;262:1786-1790.
228. Blokhin A, Vyshkina T, Komoly S, Kalman B: Lack of mitochondrial DNA deletions in lesion of multiple sclerosis. NeuroMolecular Medicine. 2008;10:187-94.
229. Bender A., Krishnan K.J., Morris C.M., Taylor G.A., Reeve A.K., Perry R.H., Jaros E., Hersheson J.S., Betts J., Klopstock T., Taylor R.W., Turnbull D.M. High levels of mitochondrial DNA deletions in substantia nigra neurons in aging and Parkinson disease. Nat Genet 2006;38:507-508.

230. Kraytsberg Y., Kudryavtseva E., McKee A.C., Geula C., Kowall N.W., Khrapko K. Mitochondrial DNA deletions are abundant and cause functional impairment in aged human substantia nigra neurons. Nat Genet 2006;38:507-508.
231. Newman NJ. Leber's hereditary optic neuropathy. New genetic considerations. Arch Neurol 1993;50:540-548.
232. Marzuki S, Letrit P, Noer AS, Kapsa RMI, Sudoyo H, Byrne E, Thyagarajan D. Reply to Howell et al: the need for a joint effort in the construction of a reference data base for normal sequence variants of human mtDNA. Am J Hum Genet 1992;50:1337-1340.
233. Marzuki S, Noer AS, Lertrit P, Thyagarajan D, Kapsa R, Utthanaphol P, Byrne E. Normal variants of human mitochondrial DNA and translation products: the building of a reference data base. Hum Genet 1991;88:139-145.
234. Obayashi T, Hattori K, Sugiyama S, Tanaka M, Tanaka T, Itoyama S, Kawamura K, Koga Y, Toshima H, Takeda N, Nagano M, Ito T, Ozawa T. Point mutations in mitochondrial DNA in patients with hypertrophic cardiomyopathy. Am Heart J 1992;124:1263-1269.
235. Howell N, Kubacka I, Xu M, McCullough DA. Leber hereditary optic neuropathy: involvement of the mitochondrial ND1 gene and evidence for an intragenic suppressor mutation. Am J Hum Genet 1991;48:935-942.
236. Wallace DC, Lott MT, Torroni A, Brown MD, Shoffner JM. Report of the committee on human mitochondrial DNA. Hum Gene Mapping 1993:813-845.
237. Prezant TR, Agapian JV, Bohlman MC, Bu X, Oztas S, Qiu WQ, Arnos KS, Coropassi GA, Jaber L, Rotter JI, Shohnat M, Fischel-Ghodsian N. Mitochondrial ribosomal RNA mutation associated with both antibiotic-induced and non-syndromic deafness. Nat Genet 1993;4:289-294.
238. Houshmand M, Larsson NG, Holme E, Oldfors A, Tulinius MH, Andersen O. Automatic sequencing of mitochondrial tRNA genes in patients with mitochondrial encephalomyopathy. Biochimica et Biophysica Acta 1994;1226:49-55.
239. Anderson S, de Bruijn MH, Coulson AR, Eperon IC, Sanger F, Young IG. Complete sequence of bovine mitochondrial DNA. Conserved features of the mammalian mitochondrial genome. J Mol Biol 1982;156:683-717.
240. Bibb MJ, Van Etten RA, Wright CT, Walberg MW, Clayton DA. Sequence and gene organization of mouse mitochondrial DNA. Cell 1981;26:167-180.
241. Clary DO, Wolstenholme DR. The mitochondrial DNA molecular of Drosophila yakuba: nucleotide sequence, gene organization, and genetic code. J Mol Evol 1985;22:252-271.
242. Benjamini Y, Hochberg Y. Controlling the false discovery rate: a practical and powerful approach to multiple testing. J Roy Stat Soc B 1995;57:289-300.
243. Ozawa T, Tanaka M, Ino H, Ohno K, Sano T, Wada Y, yoneda M, Tanno Y, Miyatake T, Tanaka T, Itoyama S, Ikebe S, Hattori N, Mizuno Y. Distinct clustering of point mutations in mitochondrial DNA among patients with mitochondrial encephalomyeopathies and Parkinson's disease. Biochem Biophys Res Comm 1991;176:938-946.
244. Oostra RJ, Bolhuis PA, Zorn-Ende I, de Kok-Nazaruk MM, Bleeker-Wagemakers EM. Leber's hereditary optic neuropathy: no significant evidence for primary or secondary pathogenicity of the 15257 mutation. Hum Genet. 1994;94:265-270.
245. Nishimura M, Obayashi H, Ohta M, Uchiyama T, Hao Q, Saida T. No association of the 11778 mitochondrial DNA mutation and multiple sclerosis in Japan. Neurology 1995;45:1333-1334.
246. Jun AS, Brown MD, Wallace DC. A mitochondrial DNA mutation at nucleotide pair 14459 of the NADH dehydrogenase subunit 6 gene associated with maternally inherited Leber hereditary optic neuropathy and dystonia. Proc Nat Acad Sci USA 1994;91:6206-6210.
247. Chalmers RM, Robertson N, Kellar-Wood H, Compston DA, Harding AE. Sequence of the human homologue of a mitochondrially encoded murine transplantation antigen in patients with multiple sclerosis. J Neurol 1995;242:332-334.
248. Zollner S, Wen X, Hanchard NA, Herbert MA, Ober C, Pritchard JK. Evidence for extensive transmission distortion in the human genome. Am J Hum Genet 2004;74:62-72.
249. Loeffen J, Smeets R, Smeitink J, Triepels R, Sengers R, Trijbels F, van den Heuvel L. The human NADH: ubiquinone oxidoreductase NDUFS5 (15 kDa) subunit: cDNA cloning, chromosomal localization, tissue distribution and the absence of mutations in isolated complex I-deficient patients. J Inherit Metab Dis 1999;22:19-28.
250. Loeffen JL, Triepels RH, van den Heuvel LP, Schuelke M, Buskens CA, Smeets RJ, Trijbels JM, Smeitink JA. cDNA of eight nuclear encoded subunits of NADH:ubiquinone oxidoreductase: human complex I cDNA characterization completed. Biochem Biophys Res Commun 1998;253:415-422.

251. Hyslop SJ, Duncan AMV, Pitkanen S, Robinson BH. Assignment of the PSST subunit gene of human mitochondrial complex I to chromosome 19p13. Genomics 1996;37:375-380.
252. Emahazion T, Beskow A, Gyllensten U, Brookes AJ. Intron based radiation hybrid mapping of 15 complex I genes of the human electron transport chain. Cytogenet Cell Genet 1998;82:115-119.
253. Emahazion T, Brookes AJ. Mapping of the NDUFA2, NDUFA6, NDUFA7, NDUFB8, and NDUFS8 electron transport chain genes by intron based radiation hybrid mapping. Cytogenet Cell Genet 1998;82:114.
254. Davie CA, Barker GJ, Thompson AJ, Tofts PS, McDonald WI, Miller DH. 1H magnetic resonance spectroscopy of chronic cerebral white matter lesions and normal appearing white matter in multiple sclerosis. J Neurol Neurosurg Psychiatry 1997;63:736-742.
255. Mecocci P, MacGarvey U, Beal F. Oxidative damage to mitochondrial DNA is increased in Alzheimer's disease. Ann Neurol 1994;36:747-751.
256. Browe SE, Bowling AC, MacGarvey U, Baik MJ, Berger SC, Muqit MMK, Bird ED, Beal MF. Oxidative damage and metabolic dysfunction in Huntington's disease: selective vulnerability of the basal ganglia. Ann Neurol 1997;41:646-653.
257. Tu P, Gurney M, Julien JP, Lee VMY, Trojanowski JQ. Review article: Oxidative stress, mutant SOD1, and neurofilament pathology in transgenic mouse models of human motoneuron disease. Lab Invest 1997;76:441-456.
258. Mutisya EM, Bowling AC, Beal MF. Cortical cytochrome oxidase activity is reduced in Alzheimer's disease. J Neurochem 1994;63:2179-2184.
259. Sanches-Ramos JR, Overvik E, Amos BN. A marker of oxy-radical mediated DNA damage (8-hydroxy-2' deoxyguanosine) is increased in nigro-striatum of Parkinson's brain. Neurodegeneration 1994;3:197-204.
260. Beal FM. Aging, energy and oxidative stress in neurodegenerative diseases. Ann Neurol 1995;38:357-366.
261. Blokhin A, Vyshkina T, Komoly S, Kalman B: Variations in mitochondrial DNA copy numbers in MS brains. Journal of Molecular Neuroscience. 2008;35:283-287
262. Dutta R, McDonough J, Yin X, Peterson J, Chang A, Torres T, Gudz T, Macklin WB, Lewis DA, Fox RJ, Rudick R, Mirnics K, Trapp BD. Mitochondrial dysfunction as a cause of axonal degeneration in multiple sclerosis patients. Ann Neurol. 2006;59:478-89.
263. Mahad D, Ziabreva I, Lassmann H, Turnbull D.Mitochondrial defects in acute multiple sclerosis lesions. Brain. 2008 Jul;131(Pt 7):1722-35.
264. Mahad DJ, Ziabreva I, Campbell G, Lax N, White K, Hanson PS, Lassmann H, Turnbull DM. Mitochondrial changes within axons in multiple sclerosis. Brain. 2009 May;132(Pt 5):1161-74.
265. Trapp BD, Stys PK. Virtual hypoxia and chronic necrosis of demyelinated axons in multiple sclerosis. Review. Lancet Neurology 2009;8:280-291.
266. Zagorski T, Dudek I, Berkan L, Mazurek M, Kedziora J, Chmielewski H. [Superoxide dismutase (SOD-1) activity in erythrocytes of patients with multiple sclerosis]. Neurologia I Neurochirurgia Polska 1991;25:725-730.
267. DeBiasi RL, Kleinschmidt-deMasters BK, Richardson-Burns S, Tyler KL. Central nervous system apoptosis in human Herpes Simplex Virus and Cytomegalovirus encephalitis. J Inf Dis 2002;186:1547-1557.
268. Bonetti B, Pohl J, Gao YL, Raine CS. Cell death during autoimmune demyelination: effector but not target cells are eliminated by apoptosis. J Immunol 1997;159: 5733-5741.
269. Raine CS, Bonetti B, Cannella B. Multiple Sclerosis: expression of molecules of the tumor necrosis factor ligand and receptor families in relationship to the demyelinated plaque. Rev Neurol 1998;154:577-585.
270. Kuhlmann T, Lucchinetti C, Zettl UK, Bitsch A, Lassmann H, Bruck W. Bcl-2-expressing oligodendrocytes in Multiple Sclerosis. GLIA 1999;28:34-39.
271. Zamzami N, Kroemer G. The mitochondrion in apoptosis: how Pandora's box opens. Nat Rev Mol Cell Biol 2001;2:67-71.
272. Martinou JC, Green DR. Breaking the mitochondrial barrier. Nat Rev Mol Cell Biol 2001;2:63-67.
273. Bruck W, Schmied M, Suchanek G, Bruck Y, Breitschopf H, Poser S, Piddlesden S, Lassmann H. Oligodendrocytes in the early course of multiple sclerosis. Ann Neurol 1994;35:65-73.
274. Zipp F, Faber E, Sommer N, Muller C, Dichgans J, Krammer PH, Martin R, Weller M. CD95 expression and CD95-mediated apoptosis of T cells in multiple sclerosis. No differences from normal individuals and no relation to HLA-DR2. J Neuroimmunol 1998;81,168-172.
275. Pender MP, Rist MJ. Apoptosis of inflammatory cells in immune control of the nervous system: role of glia. Glia 2001;36:137-144.

276. Hooper DC, Bagasra O, Marini JC, Zborek A, Ohnishi ST, Kean R, Champion JM, Sarker AB, Bobroski L, Farber JL, Akaike T, Maeda H, Koprowski H. Prevention of experimental allergic encephalomyelitis by targeting nitric oxide and peroxinitrite: implications for the treatment of multiple sclerosis. Proc Natl Acad Sci 1997;94:2528-2533.
277. Baranano DE, Rao M, Ferris CD, Snyder SH. Biliverdin reductase: a major physiologic cytoprotectant. Proc Natl Acad Sci USA 2002;99:16093-16098.
278. Liu Y. Zhu B. Wang X. Luo L. Li P. Paty DW. Cynader MS. Bilirubin as a potent antioxidant suppresses experimental autoimmune encephalomyelitis: implications for the role of oxidative stress in the development of multiple sclerosis. J Neuroimmunol 2003;139:27-35.
279. Aboul-Enein F, Lassmann H. Mitochondrial damage and hypoxic hypoxia: a pathway of tissue injury in inflammatory brain disease? Acta Neuropathologica 2005;109:49-55.
280. Stadelmann C, Ludwin S, Tabira T, Guseo A, Lucchinetti CF, Leel-Ossy L, Ordinario AT, Bruck W, Lassmann H. Tissue preconditioning may explain concentric lesions in Balo's type of multiple sclerosis. Brain. 2005;128:979-987.